RESEARCH

Keeping Utah Moving

Utah Department of Transportation - Research Division
4501 South 2700 West - P.O. Box 148410 - SLC,UT 84114-8410

Report No. UT-18.02

DEVELOPING A METHOD TO IDENTIFY HORIZONTAL CURVE SEGMENTS WITH HIGH CRASH OCCURRENCES USING THE HAF ALGORITHM

Prepared For:

Utah Department of Transportation
Research Division

Submitted By:

Brigham Young University
Department of Civil and Environmental Engineering

Authored By:

Mitsuru Saito, Ph.D., P.E.
Joseph Browning, EIT
Grant G. Schultz, Ph.D., P.E., PTOE

Draft Final Report
April 2018

DISCLAIMER

The authors alone are responsible for the preparation and accuracy of the information, data, analysis, discussions, recommendations, and conclusions presented herein. The contents do not necessarily reflect the views, opinions, endorsements, or policies of the Utah Department of Transportation or the U.S. Department of Transportation. The Utah Department of Transportation makes no representation or warranty of any kind, and assumes no liability therefore.

ACKNOWLEDGMENTS

The authors acknowledge the Utah Department of Transportation (UDOT) for funding this research, and the following individuals from UDOT on the Technical Advisory Committee for helping to guide the research:

- Scott Jones, Safety Programs Engineer
- Jason Richins, Research Project Manager
- Travis Jensen, Research Project Manager (Consultant)
- Clancy Black, Traffic & Safety Support (Consultant)
- Linda Massie, HPMS Coordinator & LRS Manager
- Anne Ogden, Region 4 Traffic Engineer
- Ryan Ferrin, Region 2 Traffic Engineer
- Kelly Jones, Region 2 Traffic Engineer

TECHNICAL REPORT ABSTRACT

1. Report No. UT-18.02	2. Government Accession No. N/A	3. Recipient's Catalog No. N/A
4. Title and Subtitle DEVELOPING A METHOD TO IDENTIFY HORIZONTAL CURVE SEGMENTS WITH HIGH CRASH OCCURRENCES USING THE HAF ALGORITHM		5. Report Date April 2018
		6. Performing Organization Code
7. Author(s) Mitsuru Saito, Ph.D., P.E., Joseph Browning, Grant G. Schultz, Ph.D., P.E., PTOE		8. Performing Organization Report No.
9. Performing Organization Name and Address Brigham Young University Department of Civil and Environmental Engineering Provo, UT 84602		10. Work Unit No. 5H07841H
		11. Contract or Grant No. 17-8512
12. Sponsoring Agency Name and Address Utah Department of Transportation 4501 South 2700 West P.O. Box 148410 Salt Lake City, UT 84114-8410		13. Type of Report & Period Covered Final Dec 2016 to April 2018
		14. Sponsoring Agency Code PIC No. UT16.302

15. Supplementary Notes

Prepared in cooperation with the Utah Department of Transportation and the U.S. Department of Transportation, Federal Highway Administration

16. Abstract

Crashes occur every day on Utah's highways. Curves can be particularly dangerous as they require driver focus due to potentially unseen hazards. Often, crashes occur on curves due to poor curve geometry, a lack of warning signs, or poor surface conditions. This can create conditions in which vehicles are more prone to leave the roadway, and possibly roll over. These types of crashes are responsible for many severe injuries and a few fatalities each year, which could be prevented to a large degree. This highlights a need for identification of curves with high crash occurrences.

The Horizontal Alignment Finder (HAF) Algorithm created by a BYU team in 2014 was improved to achieve 87-100 percent accuracy in finding curved segments of UDOT's highways, depending on highway type. A tool was then developed through Microsoft Excel Visual Basic (VBA) to sort through curve and crash data to determine the number of severe and total crashes that occurred along each curve. The tool displays a list of curves with high crash occurrences. The user can sort curves by several different parameters, including various rates and numbers of crashes. Many curves with high crash rates have already been identified, some of which will be shown in this report. This tool will help UDOT determine which highway curves warrant improvement projects.

17. Key Words Crashes, safety, modeling, prediction, horizontal alignment, curve		18. Distribution Statement Not restricted. Available through: UDOT Research Division 4501 South 2700 West P.O. Box 148410 Salt Lake City, UT 84114-8410 www.udot.utah.gov/go/research		23. Registrant's Seal N/A
19. Security Classification (of this report) Unclassified	20. Security Classification (of this page) Unclassified	21. No. of Pages 118	22. Price N/A	

TABLE OF CONTENTS

LIST OF TABLES

LIST OF FIGURES

LIST OF ACRONYMS

AADT	Annual Average Daily Traffic
AASHTO	American Association of State Highway and Transportation Officials
AGRC	Automated Geographic Reference Center
BYU	Brigham Young University
CARS	Curve Advisory Reporting Service
DBBI	Digital Ball-Bank Indicator
DUI	Driving Under the Influence
FHWA	Federal Highway Administration
GIS	Geographic Information System
GPS	Global Positioning System
HAF	Horizontal Alignment Finder
LiDAR	Light Detection and Ranging
MP	Milepost
MVMT	Million Vehicle-Miles Travelled
PC	Point of Curvature
PT	Point of Tangency
TLTW	Two-Lane Two-Way
UCPM	Utah Crash Prediction Model
UCSM	Utah Crash Severity Model
UDOT	Utah Department of Transportation
VBA	Visual Basic for Applications
VMT	Vehicle-Miles Travelled

EXECUTIVE SUMMARY

The purposes of this research can be summarized in three main objectives, including testing an algorithm designed to identify curves on rural two-lane, two-way highways for its accuracy on other highway types, improving the overall accuracy of the algorithm, and writing a new algorithm to combine curve data with crash data in order to generate lists of curves with their respective crash histories.

In the testing phase, the current algorithm was found to correctly identify highway curves with 71-96 percent accuracy, depending on highway type. Calibration was done by comparing the algorithm's results with measurements obtained from drawing curves in AutoCAD across satellite imagery. Additionally, the algorithm was able to calculate curve length with 91-96 percent accuracy. From these results, it was determined that the core concept of the algorithm did not need to be modified in order to accommodate different highway types.

The improvements to the algorithm involved targeting six specific errors. These improvements were found to increase the accuracy of curve identification to 87-100 percent, depending on highway type. Curve length calculation accuracy was improved to 97-98 percent. In addition, the algorithm was modified in order to run newer data that it could not accept previously due to changes in the data's formatting from 2014 to 2015. Three of the six errors were effectively reduced or eliminated through the improvements outlined in this report.

Finally, a new program was developed to combine curve, roadway, and crash data in order to prepare the way for future analysis. The roadway data included annual average daily traffic, functional class, speed limit, urban code, and lane parameters. These parameters were applied to each curve to determine which of them had an effect on crash rates. Total and severe crashes, as well as their corresponding crash rates, were calculated for each curve segment. Through this process, highway curves with high crash occurrences were identified. This list is intended for further crash prediction and modeling analysis.

1.0 INTRODUCTION

1.1 Problem Statement

As part of the previous research funded by UDOT, an algorithm called the Horizontal Alignment Finder (HAF) was developed to identify horizontal curves along with their points of curvature (PC), points of tangency (PT), and radii (Cook et al. 2015). This algorithm takes advantage of the horizontal alignment data provided by UDOT's light detection and ranging (LiDAR)-based asset management program. The raw LiDAR data were highly segmented and were not ready to be used for crash prediction modeling. The HAF Algorithm was created as a means of identifying horizontal curves based on post-processing of the LiDAR data. Properly locating the PC, PT, and radius is important for crash prediction modeling and curve segment hot spot identification.

For the past several years, BYU researchers have developed Bayesian-based crash prediction models, including the Utah Crash Prediction Model (UCPM) and Utah Crash Severity Model (UCSM). These advanced statistical models account for the uncertainty inherent with random crash events and help safety engineers identify and prioritize hot spots. Prior to the HAF Algorithm research, there was no automated or semi-automated method to identify whether hot spots identified by the models were part of curve segments. The HAF Algorithm can help safety engineers identify horizontal curve segments with high crash histories on state highways.

The HAF Algorithm was originally developed for rural two-lane, two-way (TLTW) highways. Hence, it was necessary to test its robustness for other highway types in both rural and urban areas. The accuracy of the original HAF Algorithm was approximately 85 percent. An error value of 15 percent is an issue when applied to the entire state highway system. The original HAF Algorithm requires human intervention to make sure it correctly identified the horizontal curve segments.

The purposes of the research described in this paper were to improve accuracy of the original HAF Algorithm, test its application to types of roadways other than rural TLTW, and create a new tool for combining curve and crash data to produce a list of curves with high crash occurrences.

1.2 Objectives

The study objectives were to:

- Test if the current HAF Algorithm, developed to analyze horizontal curves on rural TLTW highways, can be used for all other types of highways owned by UDOT
- Modify the current HAF Algorithm to make it useable for other types of highways owned by UDOT
- Improve the HAF Algorithm from its current level of 85 percent accuracy
- Develop a methodology to identify curved segments of state highways with high crash occurrences using the improved HAF Algorithm
- List horizontal curve segments of state highways with high crash occurrences and identify any pertinent physical features such as curve radius, curve length, superelevation, and annual average daily traffic (AADT).

1.3 Scope

This project can be broken down into three primary tasks:

- Calibrating the current HAF Algorithm to test whether or not it works for all highway types
- Improving accuracy of the original HAF Algorithm
- Combining the final curve, roadway, and to generate a list of curve segments with high crash occurrences.

1.4 Outline of Report

This report begins in Chapter 2 with a comprehensive summary of previous research done on the topic of identifying highway curves. This summary includes methods of data collection most appropriate for accurately covering a large road network. It also includes a review of different methods of identifying curves and determining relevant curve parameters. An overview of the methodology used for this research is presented in Chapter 3.

Summaries of the calibration process and results follow in Chapter 4 and 5, respectively. Chapter 4 details how the HAF Algorithm results were compared with measured results from satellite imagery side-by-side. It also describes how curves from different highway types were analyzed separately. Accuracy and error results are then discussed in Chapter 5. Chapter 6 then presents the reasoning for a determination that the core concept of the HAF Algorithm does not require modifications to accommodate other highway types.

The report then covers the sources of error and the improvements made to the HAF Algorithm in Chapter 7. Six types of error are discussed that provided a basis for making changes to the algorithm. This discussion also includes error sources and the fixes made. The results of the improvements are presented in Chapter 8, with a comparison of the accuracy of the original algorithm to the enhanced one.

Finally, an outline of the process that was used to combine curve, roadway and crash data is presented in Chapter 9, along with an examination of a few particular curve segments of interest. This chapter contains information about the VBA program that was created to combine the data, as well as a few lists of curves with high crash occurrences. This chapter concludes with a summary of the information gained from the lists.

2.0 LITERATURE REVIEW

2.1 Overview

Several studies have been done on identifying highway curvature through a variety of methods. This review is divided into three separate subjects, including data collection, curve identification methods, and determination of other curve parameters.

2.2 Data Collection

Various methods have been used in data collection to map road networks. The most common of these is the use of a vehicle-mounted global positioning system (GPS) sensor, but other approaches are viable as well, including data collection by LiDAR, visual methods that include mapping from satellite imagery and still photos, and inertial measurement devices.

2.2.1 GPS

GPS sensors are widely-used in collecting horizontal alignment data, which makes them useful in determining geometric parameters. Many road databases already exist created from GPS data for use in GIS software, especially in Europe (Svenson et al. 2016, Garach et al. 2014, Andrášik et al. 2013). An example of the road database in Sweden is shown in Figure 2.1. As can be seen, mapping horizontal alignment data relies on a series of data points, or points where data were collected, as shown on the right of Figure 2.1.

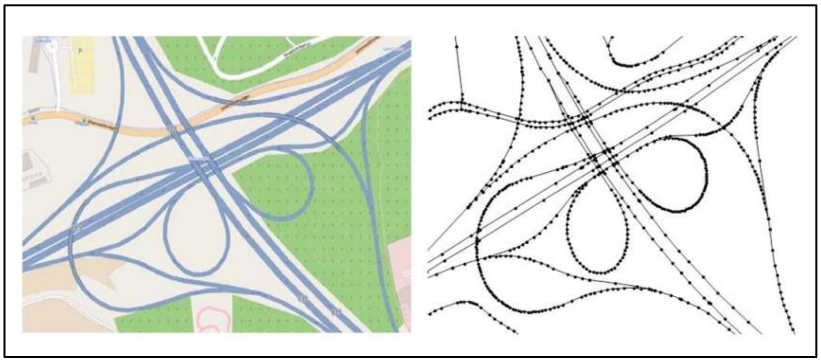

Figure 2.1 Swedish Road Database (Svenson et al. 2016)

Collecting GPS data also works well due to its low cost and widespread application. Carlson et al. (2005) performed a study that compared eight different methods of mapping horizontal alignments including using inertial measurement devices and traditional surveying. The study found that using a GPS would be most beneficial to researchers due to the fact that it is relatively inexpensive and that it works well over a large network of roads. It is also fairly accurate, and the results that were obtained came close to data taken from plan sheets. GPS data collection can also be safe in comparison to traditional surveying methods as work crews are not required to put themselves in harm's way when a GPS device is mounted on a moving vehicle (Williams and Hawkins 2011).

One disadvantage to using GPS data is that the data points follow the path of the data collection vehicle rather than the road itself, although some studies have been done to determine what paths drivers take (Imran et al. 2006). This means that the calculated alignment is subject to change depending on whether or not the driver kept to the center of the lane or whether lane changes were forced due to passing maneuvers, road construction, or other hazards (Osei-Asamoah 2015). Another disadvantage is that GPS data are often inconsistent, especially in the vertical direction (Svenson et al. 2016, Williams and Hawkins 2011, Jiménez et al. 2009). This makes it difficult to measure vertical curve parameters and means that multiple runs must be taken in order for the results to be very accurate.

Overall, GPS data collection works well compared to traditional surveying methods because of its low cost, accessibility, and ease of use. Traditional methods require a lot of time and effort when applied to large-scale road networks, while GPS typically requires the use of a single vehicle driving across a large area. In addition, GPS data can be used to map horizontal alignments on rail networks (Tong et al. 2010).

2.2.2 LiDAR

LiDAR data collection is the method used in this study. A point cloud image from UDOT is shown in Figure 2.2. Collection is done through driving a vehicle across a road or road network just as it is in GPS-based data collection, which means it works well for large-scale studies. LiDAR technology is fairly new in transportation research, and its potential has not yet been fully explored (Cook et al. 2015).

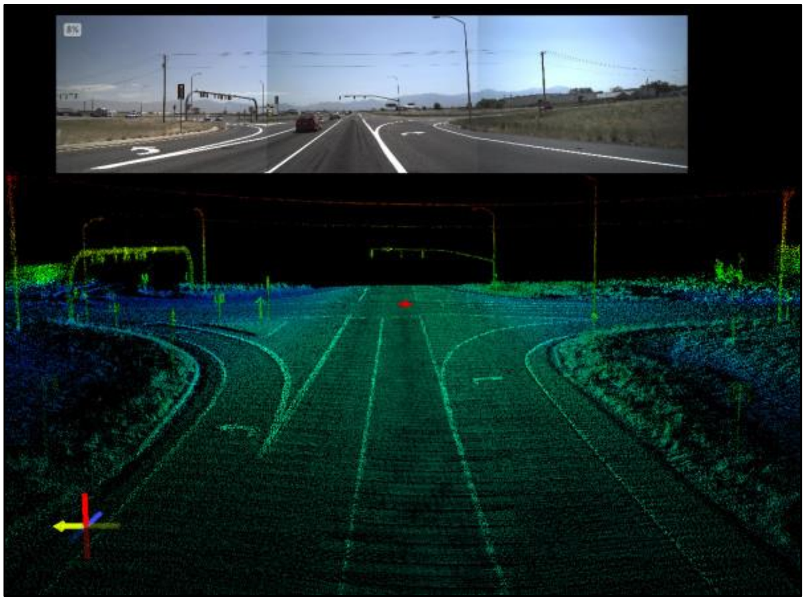

Figure 2.2 LiDAR Point Cloud Image (Ellsworth, P. 2013)

One advantage that LiDAR data have over GPS data is that they represent the path of the road itself rather than the path taken by a single driver. This allows for increased accuracy in determining horizontal curve parameters. Kim et al. (2008) determined in a study in South Korea that terrestrial laser scanning, which is similar to LiDAR, is more accurate than most other available methods.

Mapping roadways from LiDAR data is done through edge detection. Painted lines on the road are identified and used to approximate a centerline that can be imported into geographic information system (GIS) software. From this centerline, an algorithm can be applied to separate curves from tangents and determine curve parameters such as curvature, radius, and curve length. LiDAR data can also be used to map vertical curves (Svenson et al. 2016).

The primary disadvantage to using LiDAR data in terms of accuracy is that painted lane boundaries are not always parallel to the centerline of a road (Cook et al 2015). This is complicated further due to the fact that lanes and shoulders may taper. Additionally, while it may work well to find true road geometry, it does not reflect the path that drivers actually take. However, despite these disadvantages, LiDAR remains a viable option for use in safety studies as it works accurately over a large area unlike some other methods of data collection.

2.2.3 Visual

Visual means of data collection cover a wide variety of sources, including satellite imagery, photos, and videos. Roads are typically mapped through edge detection, similar to the process used in LiDAR. The primary advantage of these methods is the extremely low cost of the equipment used.

Satellite imagery has been used previously to determine horizontal curve parameters. As it is inexpensive and widely available, multiple studies have been done to determine whether or not it could be used. Unlike other methods of data collection, it does not require driving across large road networks or surveying. Dong et al. (2007) performed a study to map horizontal alignments using satellite imagery and an edge detection algorithm. It found that mapping was semi-automated, or that it required human input. The algorithm cannot detect roadways, and it requires the user to specify a starting point after which the road shape can be followed (Easa et al. 2007). An illustration of the road extraction process is shown in Figure 2.3, where an image-based program extracts areas with road-like features to approximate a road system. An additional challenge is that trees and other objects often obscure the edge of the pavement, further complicating the process (Zhao et al. 2002). While it works well for small road segments, this method should not be applied across a large road network.

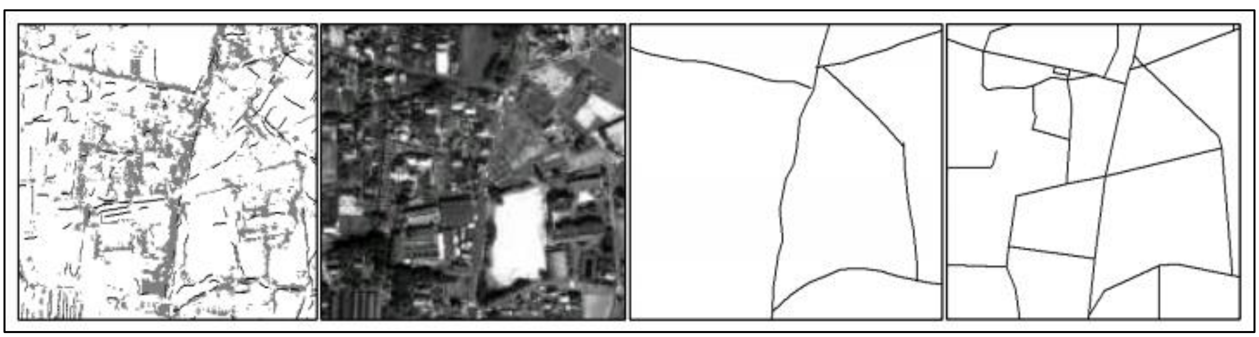

Figure 2.3 Satellite Image Road Extraction (Zhao et al. 2002)

Other studies have been done to map horizontal alignments using still photography. This typically involves photos being taken from a moving vehicle. One advantage to it is that it is very inexpensive and can be done using a simple digital camera without any complicated equipment (Tsai et al. 2010). It works using an edge detection program similar to those used in extracting curve geometry from satellite imagery. However, it cannot be used efficiently to cover a large road network.

Smartphones have also been used as a means to map horizontal alignments. Higuera de Frutos and Castro (2014) performed a study to determine the effectiveness of smartphones as a low-cost mapping tool. The study found that they were a viable option for larger road networks. Besides the fact that smartphones are so widely used, they also contain a lot of equipment including video recording capability, GPS sensors, and accelerometers. This enables them to map roads similarly to GPS and inertial measurement devices. Its primary disadvantage, however, is its accuracy. The study found that horizontal alignments could be mapped with an average error of 2.2 meters in either direction, which pales in comparison to other, more accurate methods of data collection.

2.2.4 Inertial Measurement Devices

Inertial measurement devices, such as ball-bank indicators and accelerometers, are able to map horizontal alignments by collecting data from lateral acceleration. This method works well for short segments on low-speed roads, but cumulative error becomes too great after driving for a distance of about 1500 meters for it to be used properly. When performed on roads with a higher speed limit, the acceptable distance for measurement after which the error becomes too great is reduced significantly (Jiménez 2011).

Ball-bank indicators, which are a type of inertial measurement device, are widely used in the United States. A study performed by Green et al. (2017), using a digital ball-bank indicator (DBBI), found that they provided valuable information for determining advisory speeds on horizontal curves, but that they provided more accurate information when used in conjunction with a GPS sensor. This system that used an inertial measurement device in conjunction with a GPS sensor is called the Curve Advisory Reporting Service (CARS), and a comparison of curve advisory speeds calculated with both methods is shown in Figure 2.4. As can be seen, the calculated advisory speeds differed by as much as 10-15 miles per hour. Jiménez et al. (2009) confirmed that a combination of the two methods might be better by stating that inertial measurement data combined with GPS information have the potential to be very accurate.

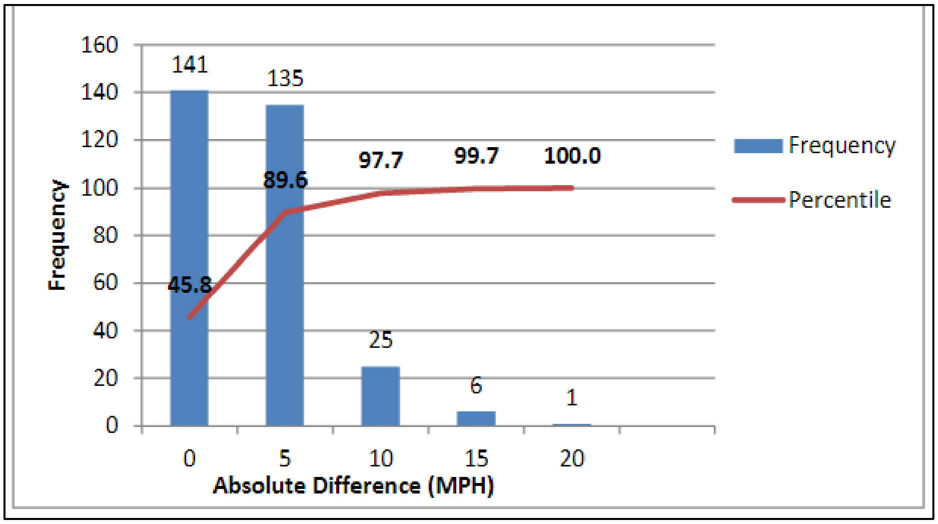

Figure 2.4 Absolute Differences in Advisory Speeds Determined with and without GPS Sensor (Green et al. 2017)

2.3 Methods of Curve Identification

Once the data points have been collected and run through a mapping program, the next step is to run a program to separate curve segments from tangent segments. The three dominant methods to do this include curve identification through change in heading, development of a spline approximation, and identification of a curve through geometric parameters such as radius or length.

2.3.1 Heading Change

Several algorithms differentiate curves from tangents by analyzing direction change beyond a certain threshold, an example of which is shown in Figure 2.5. Camacho-Torregrosa et al. (2015) compared different methods of identifying horizontal curvature along highway segments and found that the heading change method was the most accurate among the tested methods, did not require smoothing, and was less susceptible to measurement errors. While the radius values extracted from this method were found to be consistent with those calculated by other methods, the curve length was significantly more accurate, as shown in Figure 2.6.

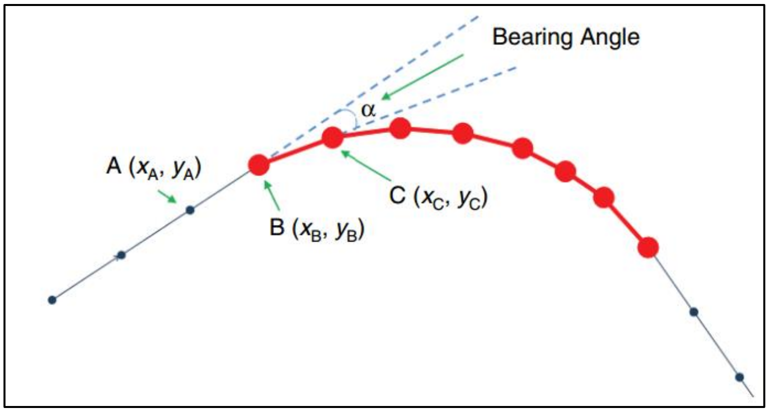

Figure 2.5: Curve Identification via Heading Change (Li et al. 2015)

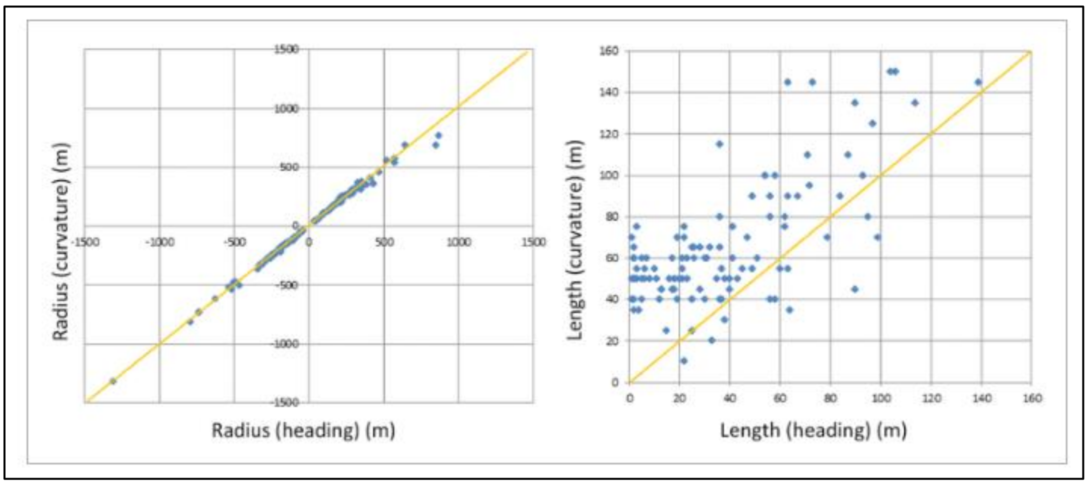

Figure 2.6 Heading Change v. Curvature Method (Camacho-Torregrosa et al. 2015)

A study done by Li et al. (2012) developed an algorithm that was able to identify curves and tangent segments (not their parameters) with 97 percent accuracy. The disadvantage to this method, however, is that direction changes are frequent in tangent sections, which means that additional care must be taken in order to distinguish curves from tangents (Xu and Wei 2016). However, if this issue can be overcome, the heading change method has the potential to identify curves accurately over a large network (Li et al. 2015).

2.3.2 Spline Approximation

Spline approximation differs from other methods in that it does not identify curves themselves, but rather aids in mapping them. Splines are mathematical functions that provide a smooth, fluid connection between different points. This method works well in matching a road centerline between two directions of travel and in creating a smooth, continuous curve (Castro et al. 2006, Ben-Arieh et al. 2004). Two illustrations of this compared with an actual road design are shown in Figure 2.7 and Figure 2.8, with a vertical and horizontal alignment, respectively.

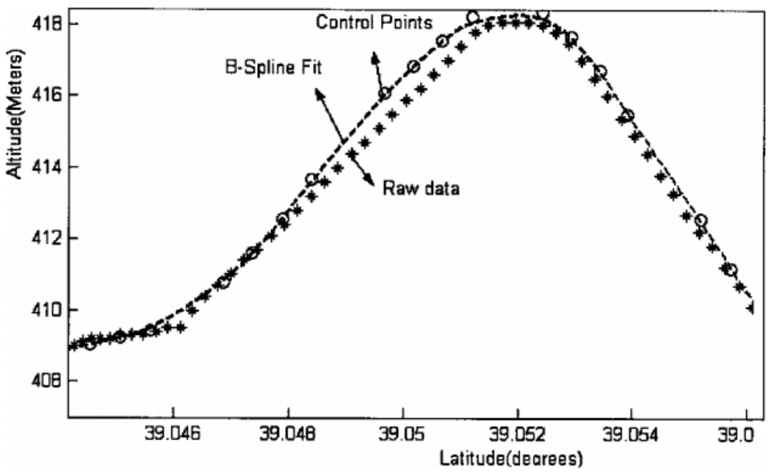

Figure 2.7 Comparison of Spline with Existing Vertical Alignment (Ben-Arieh et al. 2004)

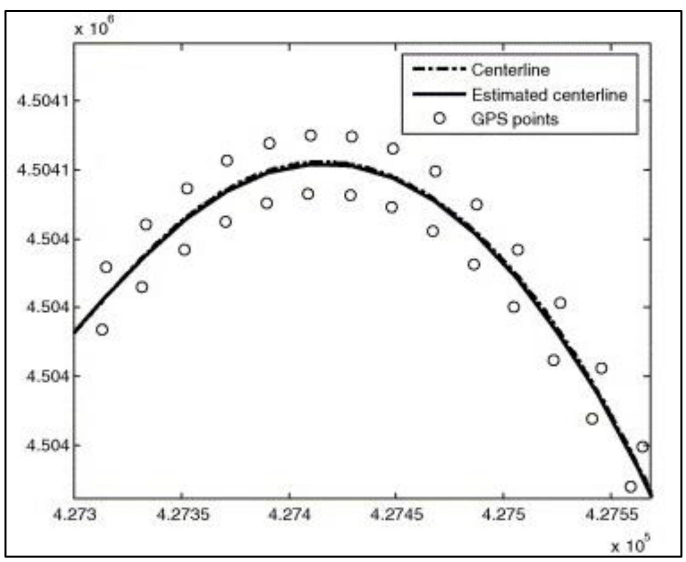

Figure 2.8 Comparison of Existing Horizontal Alignment with Spline Centerline (Castro et al. 2006)

The issue with spline functions, however, is that it becomes more difficult to extract curve parameters from them and it requires additional algorithms to do so. Garach et al. (2014)

performed a study in which curve parameters were determined from mapping done via a spline function. Spiral and circular curves were approximated using trapezoids, and the results returned an average error rate of less than 10 percent. Splines work well for mapping horizontal alignments, but not as well for separating curves from tangents and identifying curve geometry. Some studies have also been done to determine curve geometry from various fitting algorithms (Bassani et al. 2016).

2.3.3 Geometric Curve Parameters

Several studies have been done that differentiate curves from tangents based on geometric parameters. The study that is the basis for this research used this method to identify horizontal curves (Cook et al. 2015). It used a weighting system consisting of three different thresholds including segment length, radius, and a radius/length ratio to determine whether a particular segment was a curve or a tangent, as shown in a flowchart in Figure 2.9. This method worked with 84-93 percent accuracy on TLTW highways.

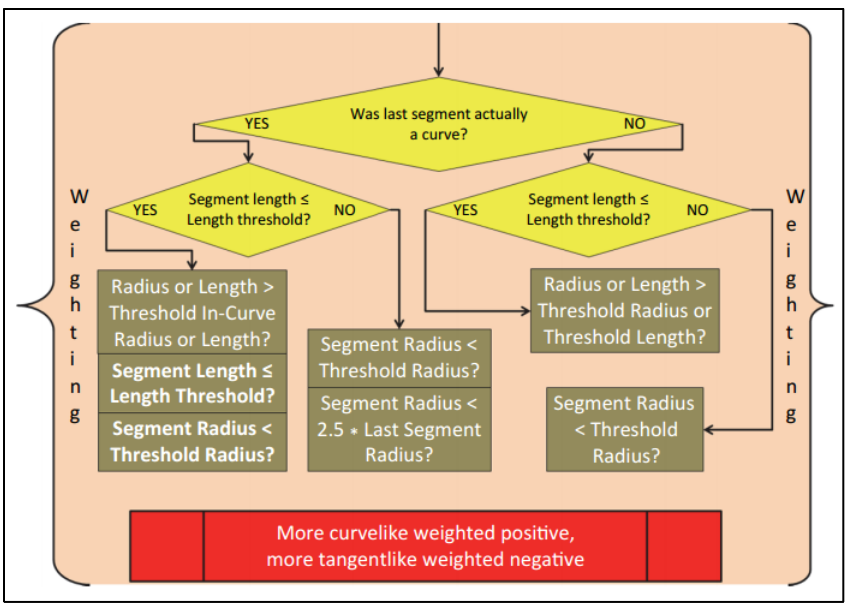

Figure 2.9 Curve Weighting Diagram (Cook et al. 2015)

Andrášik and Bíl (2014) used a simple radius threshold of 200 meters with an overall success rate of 90 percent in a study done in the Czech Republic. An illustration of this is shown in Figure 2.10. Ai and Tsai (2015) performed a similar study in the state of Georgia and produced the same identification accuracy rate. Geometric parameter calculation accuracy usually depends on the length of the curve (Bogenreif et al. 2012). The main issue with this method, however, is that it is difficult to differentiate intersections from mountain curves with small radius values. However, identifying curves from threshold values, according to these studies, seems to be a viable option. The advantage to this method is that thresholds can be adjusted easily to fit a given set of circumstances (Cook et al. 2015).

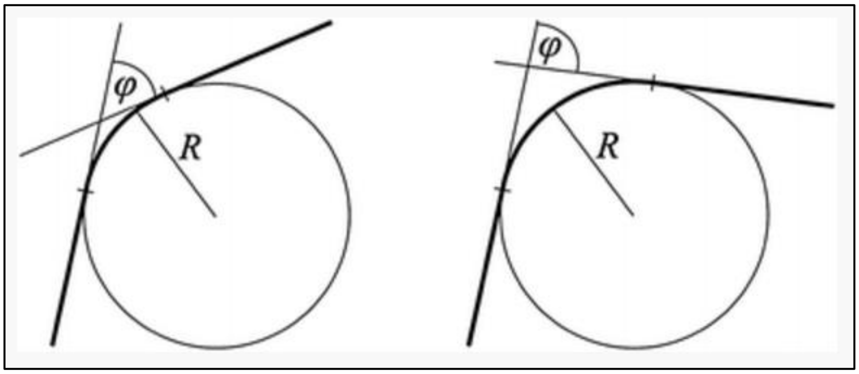

Figure 2.10 A Circular Curve Determined by its Radius and Angle (Andrášik and Bíl 2014)

2.4 Other Curve Parameters

Studies have been performed on methods to gather roadway parameters other than those associated with horizontal curvature. Some studies identified and measured vertical curves, while others measured road superelevation. These studies are summarized below.

2.4.1 Vertical Curves

Automatic extraction of vertical alignments can also be useful in safety research. Identifying vertical curves and their characteristics is necessary for determining sight distance (Figure 2.11). This is traditionally done through surveying, but improvements made in technology in recent years allow for faster, more efficient means to do so. Standards have changed in terms of passing sight distance requirements (Williams and Hawkins 2011), which means a method that can be implemented on a large scale is needed to determine which vertical curves do not meet the new requirements.

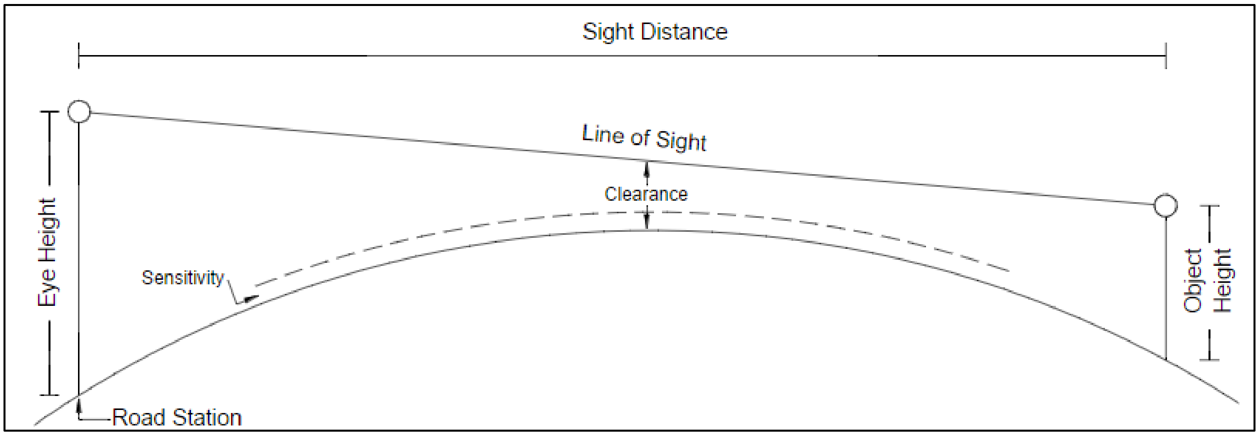

Figure 2.11 Vertical Sight Distance Diagram (Santiago-Chaparro et al. 2012)

Williams and Hawkins (2011) performed a study in which multiple passes were made in a GPS-equipped vehicle to gain elevation points and construct a vertical alignment using quadratic fitting. Santiago-Chaparro et al. (2012) performed a similar study using photologs as a data collection means. Photologs are similar in nature to Google Streetview, in that photos are taken at set intervals from a vehicle. The difficulty with determining vertical alignments, however, is that mapping them does not work as accurately as mapping horizontal alignments (Svenson et al. 2016). This suggests a need for further research.

2.4.2 Superelevation

Several studies have also been done on acquiring superelevation data. This is useful in safety-related research as it is important to know how a road has been designed. Luo et al. (2016) performed a study in which superelevation information was gathered by lasers mounted on the back of a vehicle while GPS and lateral acceleration data were collected simultaneously (Figure 2.12). This method works well for a large road network without using time-consuming traditional surveying methods.

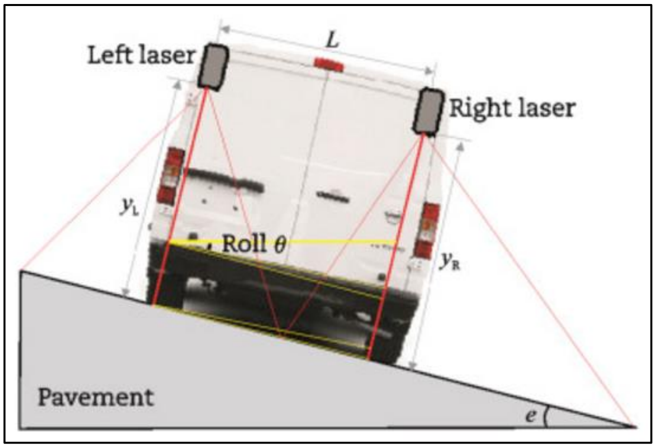

Figure 2.12 Measuring Superelevation (Luo et al. 2016).

The difficulty in measuring superelevation is that when traversing a curve, the chassis of the measuring vehicle is not always parallel to the road surface. This is particularly true in vehicles with softer suspension, and is often difficult to compensate for. Jiménez (2011) performed a study in which superelevation was measured using an inertial measurement device. An algorithm was developed to attempt to compensate for body roll. This was successful, and the data gathered were more accurate.

2.5 Chapter Summary

Identifying curve segments accurately is beneficial to safety research. Being able to identify what attributes of a road that contribute to crashes could save many lives. Various viable means of data collection and analysis are available for doing this. GPS, LiDAR, visual, and inertial measurement methods have been reviewed for this purpose. According to the studies included in this literature review, GPS and LiDAR data collection appear to be the best methods for use over a large road network because of their accuracy, widespread use, and convenience over other forms of gathering information.

Identifying curves through change in heading direction and through use of geometric threshold values are both valid methods. The advantage to the heading change method is that it is generally more accurate, while the geometric threshold method is more easily adjustable to fit specific needs. The original HAF Algorithm is based off this method, and provides a good foundation for further development.

Many studies have also been done to identify other road parameters, such as vertical curve characteristics and superelevation. These are good options for further research into road attributes that may contribute to crashes. From this literature review, it can be seen that valuable research has been done on the topic of horizontal curve identification and that it provides a solid basis from which more can be learned.

3.0 METHODOLOGY

3.1 Overview

This chapter contains an overview of the methodology behind the research in this report. The methodology consists of three parts, including (1) the calibration of the current HAF Algorithm to determine its errors and whether it works for all highway types, (2) a presentation of the sources of these errors and the improvements made to correct them, and (3) a summary of how the curve data were combined with crash data in a new program.

3.2 Calibration

The current HAF Algorithm was calibrated by comparing the calculated parameters of the output file against measured parameters found through overlaying arcs on satellite imagery in AutoCAD. Three primary performance measures were tested, including curve length calculation accuracy, radius calculation accuracy, and curve identification accuracy. A total of 100 segments were chosen at random to test from each highway type, including urban interstate, rural interstate, urban multilane, rural multilane, urban TLTW, and rural TLTW.

3.3 HAF Errors and Improvements

During the testing of the current HAF Algorithm, a total of six major errors were found, including curve length miscalculation, curve fragment identification, tangent identification, intersection identification, tangent-curve-tangent errors, and compound curve errors. The details of these errors will be described in Chapter 5. To reduce the number of tangents identified as curves, the code of the HAF Algorithm was altered to implement radius thresholds at a non-linear scale. To reduce large curve length calculation errors, changes were made to improve the accuracy at which the PC and PT of curves were selected. To reduce the number of intersections identified as curves, an existing ArcMap model was modified to eliminate curves from consideration below a certain radius value if the curves were within certain municipality boundaries.

3.4 Crash Data Combination

After the HAF Algorithm was improved, curve data were combined with roadway data and crash data through the use of a new tool. The combination took place by aligning common milepoints and route numbers. The roadway data included AADT, functional classifications, speed limits, urban codes, and the number of through lanes. Some additional measures had to be taken to compensate for segments where data were not available. Individual segments with abnormally high crash rates were then analyzed based on the characteristics of the curves and the types of crashes that occurred on them.

3.5 Chapter Summary

To summarize, there are three primary components to the methodology of this study: (1) calibrate the existing HAF Algorithm to see if it works for all highway types, (2) identify the errors of the existing HAF Algorithm and make improvements as necessary to increase overall accuracy, and (3) combine curve data with roadway and crash data to generate a list of curves with high crash occurrences. This is the basic outline of how the study was performed, and these components will be explored in depth in the coming chapters.

4.0 HAF ALGORITHM CALIBRATION PROCESS

4.1 Overview

This research tested the original HAF Algorithm to determine how well it identifies curves and estimates curve parameters for roadway types other than rural TLTW. Calibration of the algorithm for these other roadway types provided some understanding into how it could be improved. In this calibration process, approximately 100 curve segments were randomly selected for each of six highway categories – urban and rural interstates, urban and rural multilane highways, and urban and rural TLTW highways. 2013 and 2014 Mandli datasets were used in the calibration process. Included in this chapter is an overview of how the program works and the methodology detailing how curve segments were calibrated.

4.2 How the HAF Algorithm Works

In order to understand the calibration process of the HAF Algorithm, its workings must be understood first. LiDAR data in a shapefile format provide the algorithm input. The HAF Algorithm itself does not use image detection techniques common in LiDAR data analysis. Rather, it uses lines and curves that have already been post-processed by Mandli (the company performing the LiDAR survey for UDOT). The HAF Algorithm is necessary because the data are fragmented and several segments with slightly different parameters will often be contained within a single curve, making it not ideal for analyzing curves across a vast roadway network. These data contain curve length and radius information about each segment, and the HAF Algorithm's role is to combine and clean up the data to present them in the form of curves and tangents (Cook et al. 2015).

The HAF Algorithm accomplishes this task by analyzing each segment and weighting its parameters as more curve-like or more tangent-like. This means, for example, that segments with large radius values are more likely to be classified as a tangent rather than a curve. Additionally, adjacent curve segments that bend in the same direction are combined into a single curve. The starting point of the first curve segment and the ending point of the last curve segment are considered to be the PC and PT of the new curve, respectively. It is important to mention that while the algorithm is fully capable of combining segments together from the input data, it is not able to divide segments. This is because the algorithm analyzes data in table form, in which only the starting point and end point of each segment are available rather than continuous location information.

4.3 Calibration Procedures

This section contains a comprehensive description of the process involved in calibrating curve segments. It includes filtering the curve shapefile into separate road types, randomizing the samples used, and determining true curve parameters by drawing arcs across satellite imagery in AutoCAD.

4.3.1 Determination of Segments to be Used

The first step was to segment the list of curves into separate lists of curves from each highway type. The HAF Algorithm can determine curve parameters but is not able to distinguish between different types of highways. This task was accomplished by using ArcMap's Select by Attributes function. Interstates were filtered by selecting route names corresponding with known interstate routes, as shown in Figure 4.1. Other road types were filtered by using a lanes shapefile from UDOT that shows whether a facility is multilane or not.

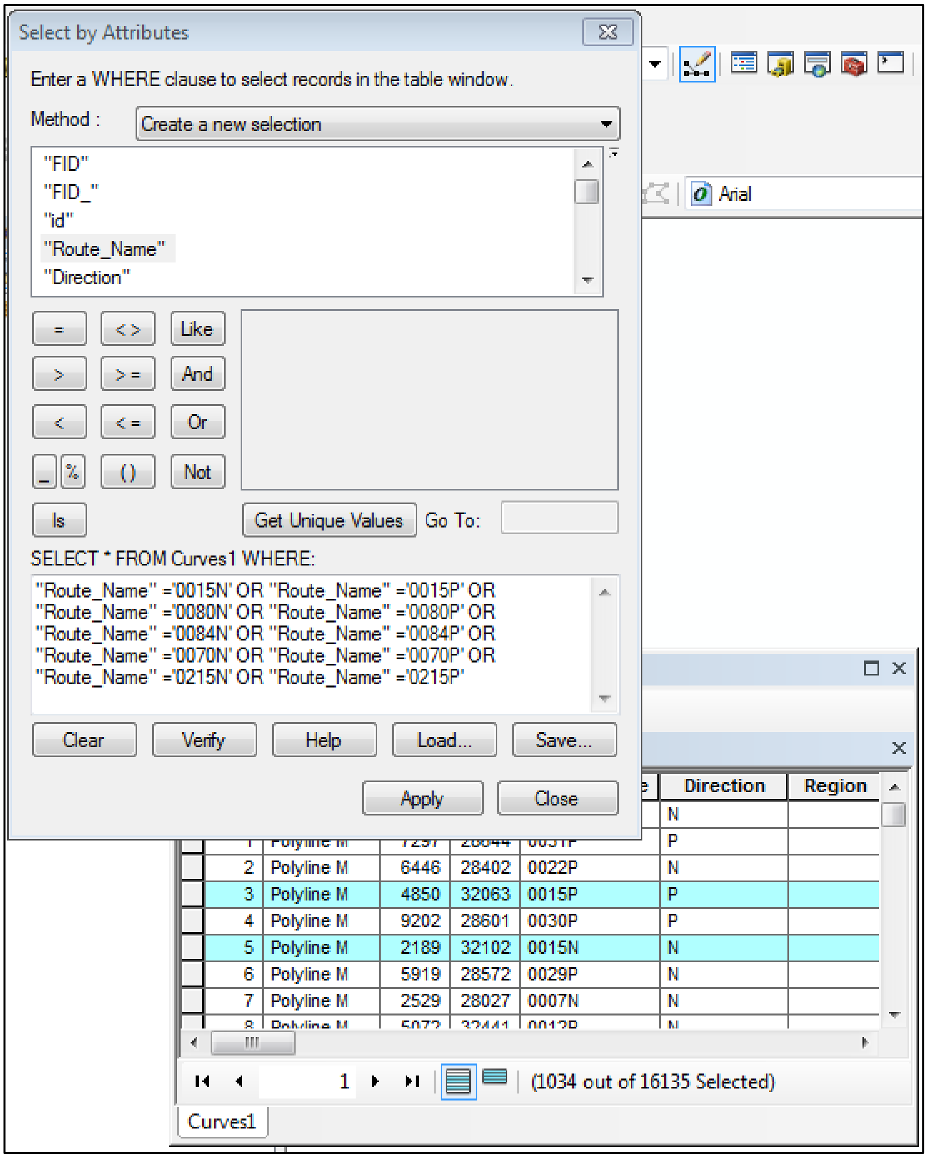

Figure 4.1 ArcMap Select by Attributes Function (Esri 2017)

Once this had been done, the selected segments were then exported to an Excel spreadsheet where each segment was assigned a random number through Excel's random number generator function. These segments were sorted in ascending order from the random number assigned to them, which then randomized the segments to get a more accurate representation of the population as a whole. Rural and urban areas were analyzed separately. Urban segments were defined as any highway inside the Salt Lake City (which includes Davis and Weber counties), Provo-Orem, Cedar City, and St. George metropolitan areas. A municipality shapefile downloaded from the Utah Automated Geographic Reference Center (AGRC) was used to determine which segments fall within those urban boundaries.

4.3.2 Comparing Satellite Imagery

After the curve segments were categorized, the next step was to calibrate them. A satellite imagery basemap was applied to the ArcMap file from which the location of a particular curve segment could be determined. The corresponding segment was then found in Google Earth through comparing the two images side-by-side, as shown in Figure 4.2. The Google Earth image is at the top and the ArcMap image is at the bottom. Two pins were then placed on opposite ends of the curve in Google Earth, forming a box from which to take a screenshot and import an image into AutoCAD.

4.3.3 Determining Actual Curve Parameters

This screenshot was used as the basis for recreating the curve (see Figure 4.3). A line was then drawn between the two pins in AutoCAD for scaling purposes. The distance between the two pins was measured on Google Earth to find the true distance across the image (see Figure 4.4). The distance obtained from Google Earth divided by the length of the line between the same two points in the pasted image in AutoCAD was used to determine the scale of the image, from which a scaling factor was obtained.

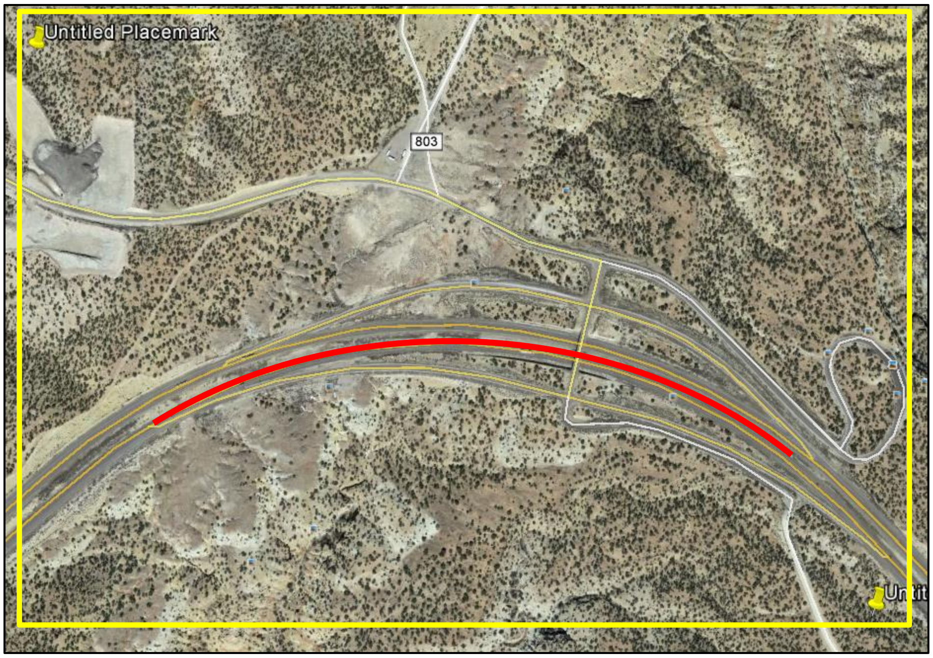

(a)

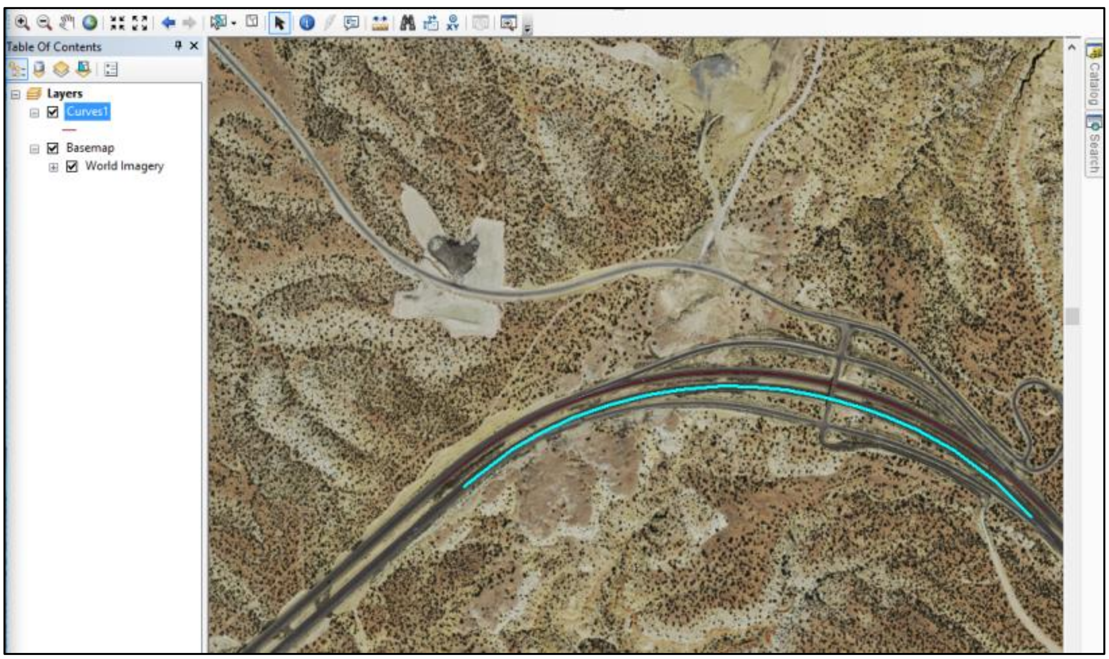

(b)

Figure 4.2 Google Earth (a) /ArcMap (b) Comparison (Google 2017, Esri 2017)

Figure 4.3 AutoCAD Image (Autodesk 2017)

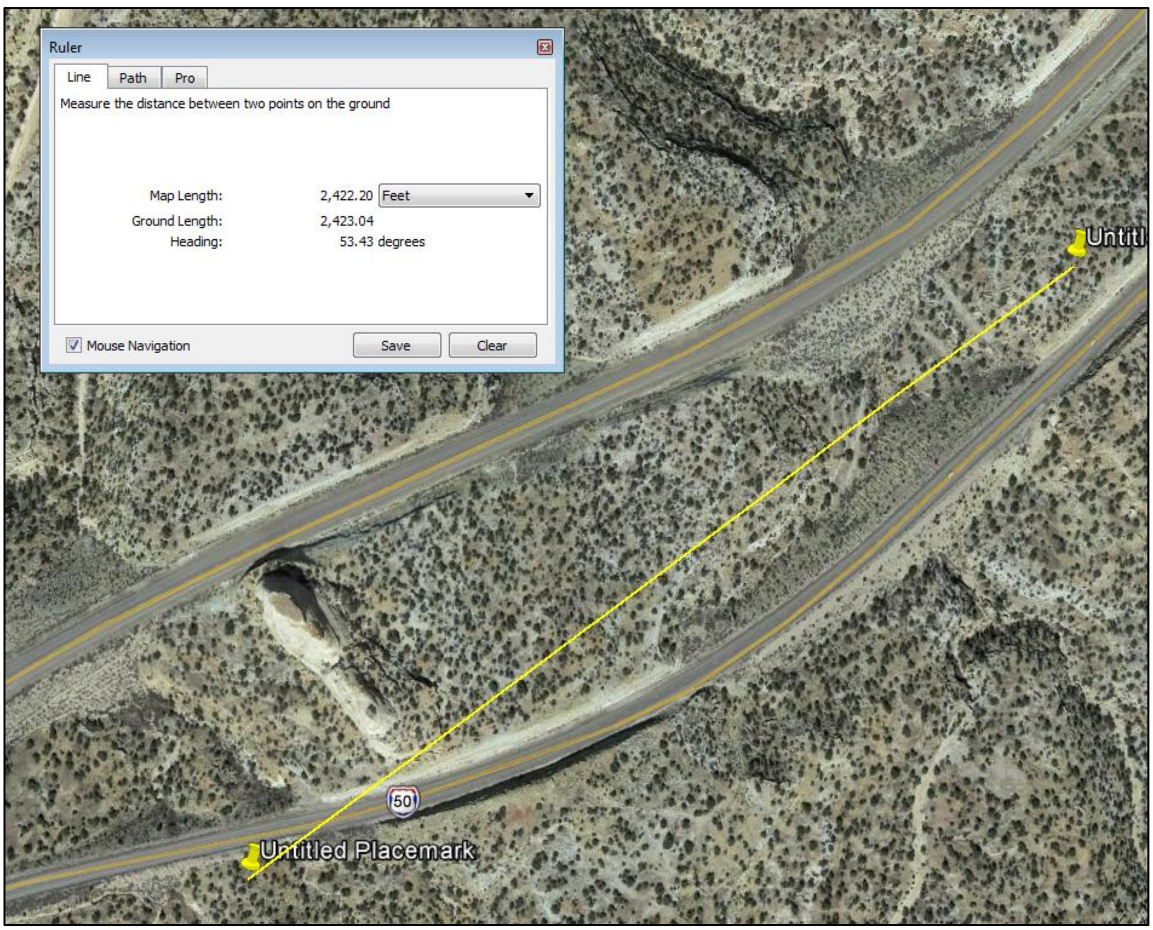

Figure 4.4 Google Earth Distance Measurement (Google 2017)

After the image had been scaled, a 3-point arc was drawn in AutoCAD. The PC and PT of the curve were matched as closely as possible to the ones identified in ArcMap (see Figure 4.5). Drawing this arc introduced a potential source of human error as it is difficult to match the exact road centerline. However, it is still a fairly accurate method of determining actual curve parameters.

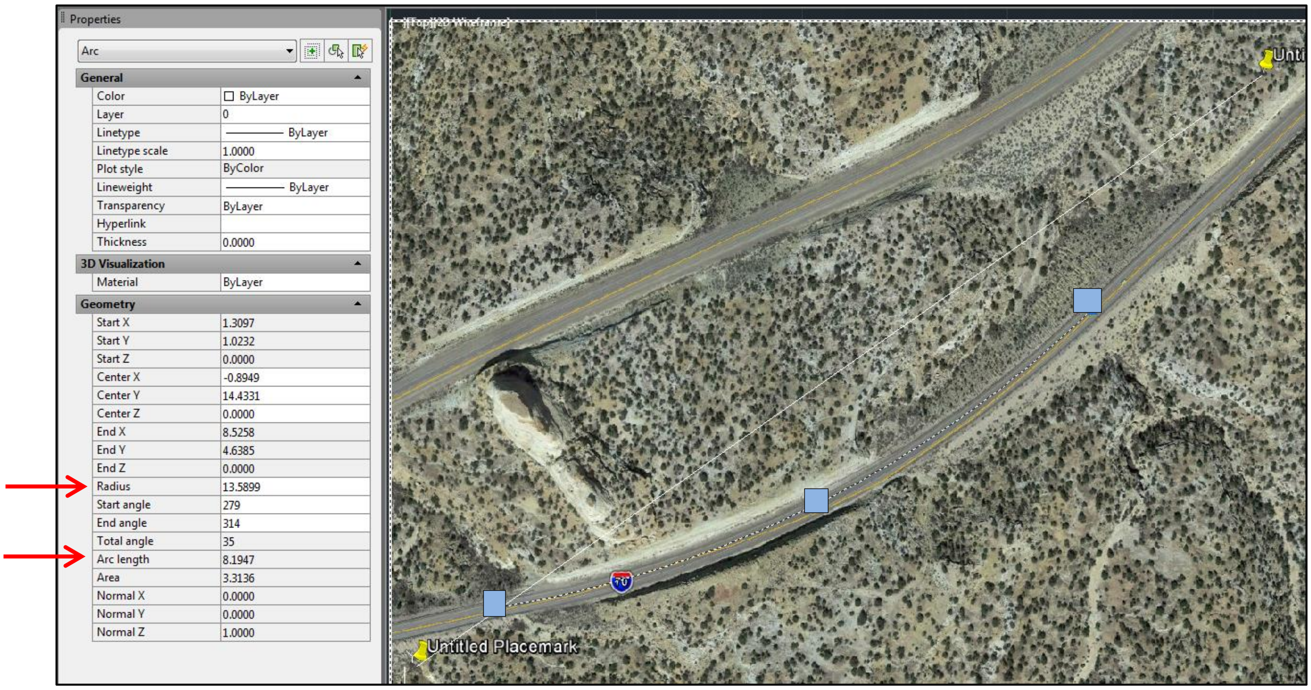

Figure 4.5 AutoCAD Arc Drawing (Autodesk 2017)

Once the arc was drawn, radius and curve length values were obtained from the properties table as shown on the left of Figure 4.5. These values were then multiplied by the scaling factor obtained earlier to reflect their true measurement. The measured radius and curve length were then compared with the radius and curve length that the HAF Algorithm had calculated to determine the accuracy.

4.4 Chapter Summary

In order for the capability of the existing HAF Algorithm to identify curves along all highway types to be evaluated, a calibration process had to be developed. This was done through matching curves determined by the HAF Algorithm to measurements taken from satellite imagery. Parameters such as radius and curve length were taken into consideration in determining the accuracy of the HAF Algorithm.

5.0 TYPES OF ERRORS IN THE ORIGINAL HAF ALGORITHM

5.1 Overview

This chapter includes a description of six problems with the existing HAF Algorithm. Some of these errors were known before this research was started, and others were discovered during the process of calibration. The first three errors deal with problems in calculating curve parameters, and the last three entail problems with identification of highway curves. Identifying these problems with the algorithm provided a starting point from which to improve it. These six errors include tangent-curve-tangent, compound curve, curve length calculation, intersection, tangent, and curve fragment errors. Curve length calculation, curve fragment, and intersection errors were reduced significantly, while the tangent error was also reduced to some degree. The improvements made to resolve these errors are detailed in Chapter 7.

5.2 Tangent-Curve-Tangent Error

Tangents and curves are often combined into single segment elements in the raw data. This is shown in Figure 5.1, and was found to be fairly common, especially along non-interstate highways. This particular curve segment exists along SR-115 in Spanish Fork. As can be seen, the PC and PT points do not line up where they should. The approximate PC and PT points as judged by the researcher have been marked. In this case, the data fed into the algorithm are flawed. As mentioned previously, the algorithm is not set up for dividing segments, nor can it be modified to do so. Due to this flaw, the actual radius value differs from the calculated values, both from the calibration and the algorithm itself. This shortcoming in the data is difficult to address, as the algorithm assumes all inputs are either a complete curve or a segment of a curve and therefore cannot address combined curve-tangent sections.

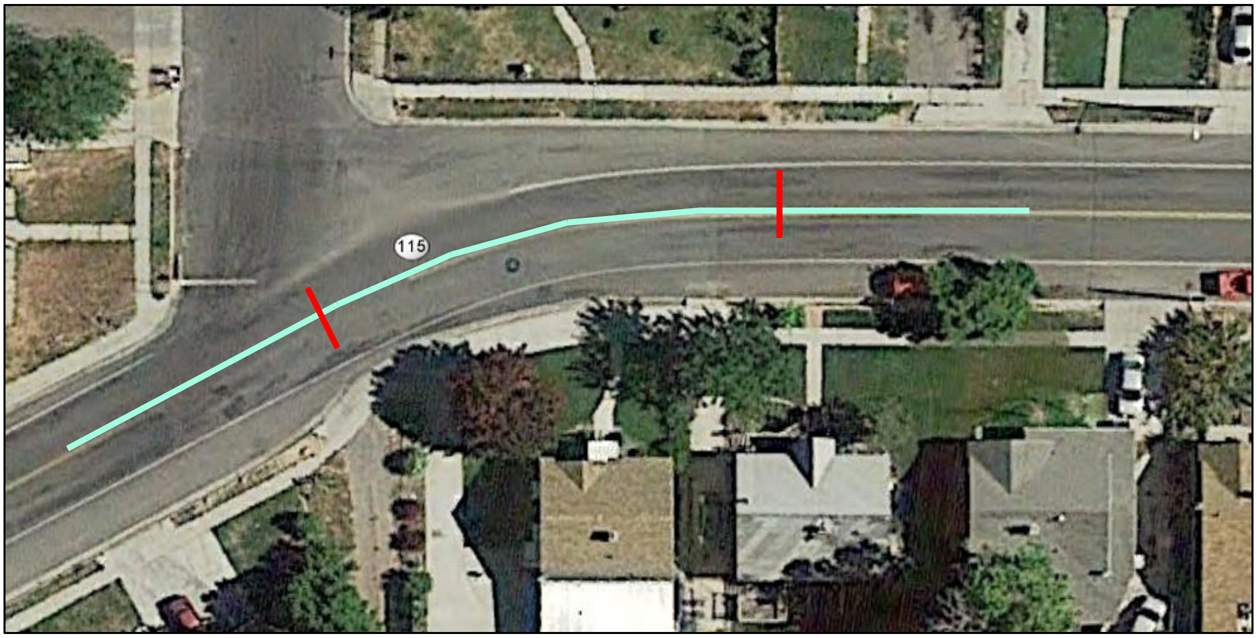

Figure 5.1 Tangent-Curve-Tangent Error (Esri 2017)

5.3 Compound Curve Error

A second type of error exists in attempting to calibrate compound curves, or multiple curves of different radius values combined together into a single segment. This type of error exists occasionally on mountain roads where broad curves will often be followed by sharp ones, as illustrated in Figure 5.2. This particular segment is on SR-153 near Beaver, UT. As can be seen, the issue is not that tangents are connected to the curve, but rather that there are two distinct curves adjacent to each other. The approximate PC and PT points have again been marked. This makes calibration difficult, as the algorithm is set up to produce simple circular curves, which cannot be fitted properly in a scenario such as this. The HAF Algorithm determines radius values on compound curves through a weighted average, which would be difficult to properly check for accuracy. Fortunately, this type of error is not common.

Figure 5.2 Compound Curve (Esri 2017)

5.4 Curve Length Calculation Error

A third type of error can occur when using the HAF Algorithm to calculate curve length. The HAF Algorithm calculates smoothed curve length by summing the individual curve lengths from the segments in the original data. This particular kind of error is not more common in one particular road type than in another. Human error was successfully ruled out in these situations through comparing the calibration's curve length to a rough approximation done by the path component of Google Earth's distance tool. Errors of this type often ranged from 100-500 percent. Table 5.1 contains four examples of this error and as can be seen, the HAF-calculated curve length is much larger than it should be. These errors occurred because the HAF Algorithm identified the wrong milepoints for the PC and PT locations, which is explained in Chapter 7.

Table 5.1 Curve Length Calculation Error

	Route Name	Actual (ft)	Calculated (ft)	Error
Rural Multilane	0091P	317.4	1348	325%
	0189P	265	1628	514%
Urban TLTW	0108P	227.3	525.4	131%
	0186P	198.7	744.5	274%

5.5 Intersection Error

A fourth error occurs because intersections are often included in the final output of the HAF Algorithm. In certain locations, route alignments often make a 90° turn at intersections that should not be classified as a curve. A process in the ArcMap model was added to compensate for this but it often fails to distinguish between intersections and sharp mountain curves. Figure 5.3 contains an illustration of the issue. This particular segment exists in front of the State Capitol building at the intersection of 300 North and State Street (SR-186), in Salt Lake City.

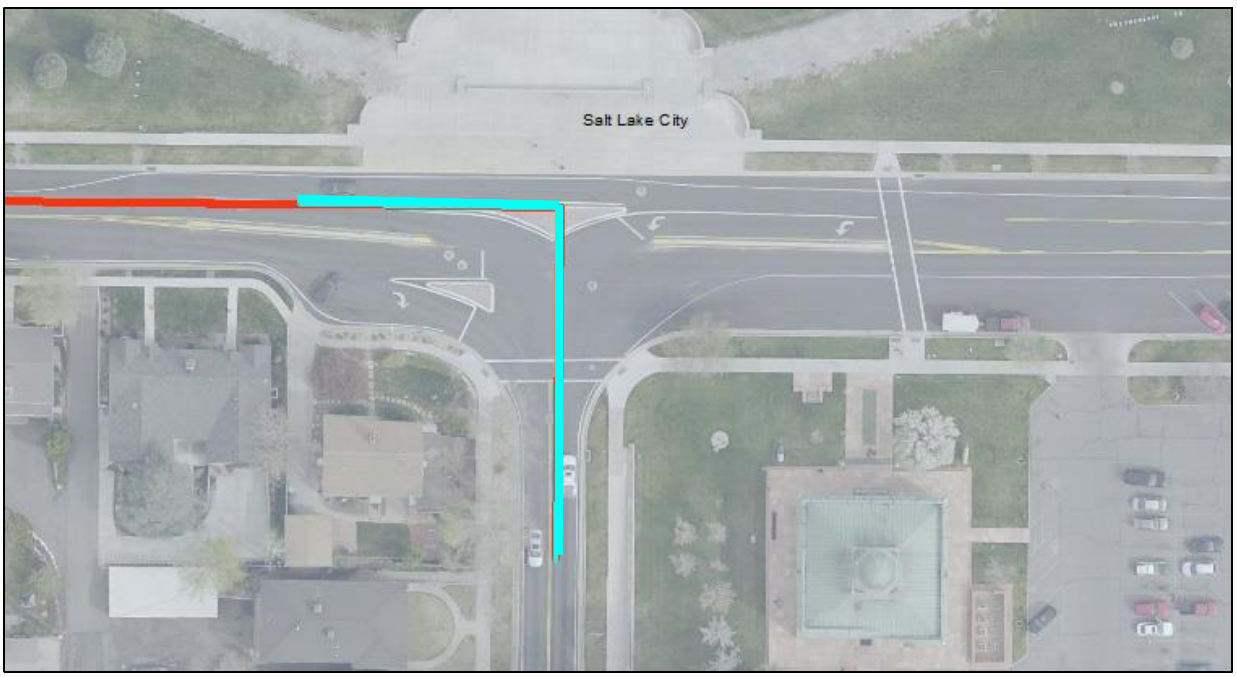

Figure 5.3 Intersection Error (Esri 2017)

5.6 Tangent Error

Tangent error is not unique to a particular type of road, with the exception of TLTW rural highways where it does not occur as often, and frequently involves a short segment that has been classified as a curve rather than a tangent. This error is demonstrated in Figure 5.4. This curve segment is along I-70 near Green River, UT. It is clearly a tangent, but it was assigned a radius value of 2770 feet, which is fairly typical for a freeway curve. Errors of this type were often due to small curve length values from the data. Additionally, this type of error often occurs on highway segments where the road widens to accommodate an additional lane. Because the centerline of the road changes, the HAF Algorithm classifies it as a curve and assigns it radius and curve length values.

Figure 5.4 Tangent Error (Esri 2017)

5.7 Curve Fragment Error

The sixth type of error to be addressed in this chapter is a problem with curve fragments. In many instances, a small segment of a curve will be identified rather than the whole. This issue is illustrated in Figure 5.5. The segment in question is highlighted in cyan on the left with an arrow pointing to it, and lies along I-15 near Nephi. The HAF Algorithm appropriately identified the curve to the right of it, but poorly estimated the PC and PT points on the left. This error was attributed to the same cause as the curve length calculation error, and occurred on between 3-5 percent of curves identified by the algorithm.

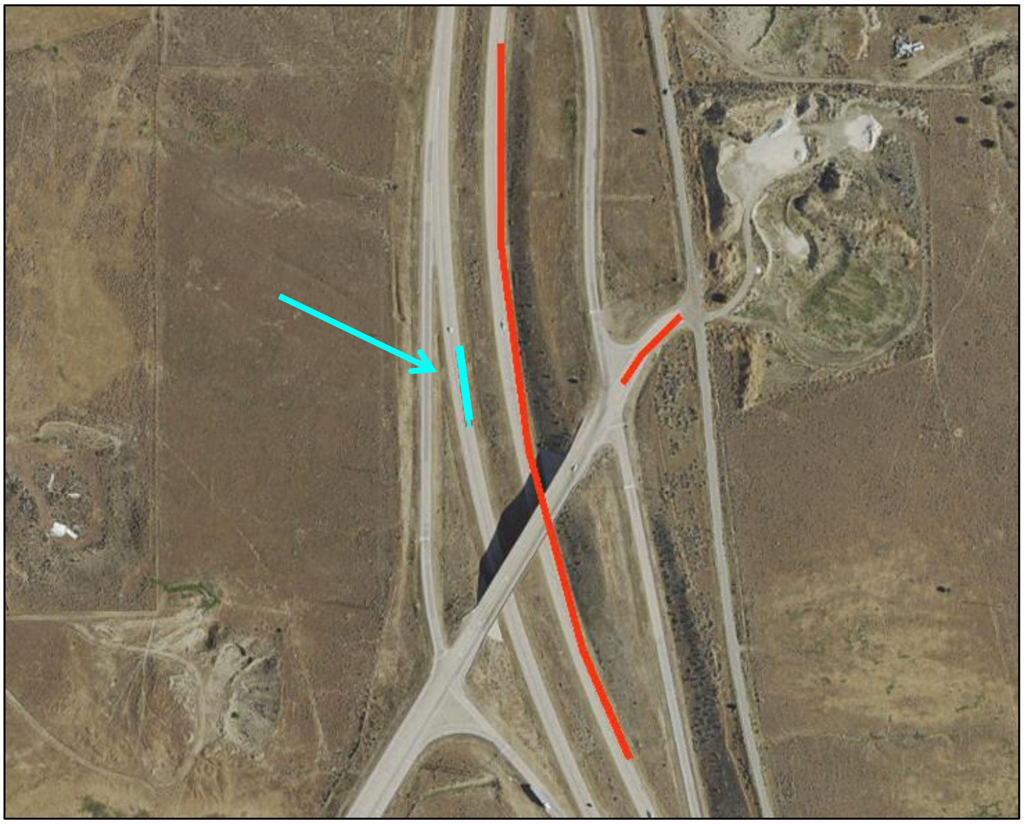

Figure 5.5 Curve Fragment Error (Esri 2017)

5.8 Chapter Summary

These six errors provided a basis upon which to improve the HAF Algorithm. While some errors were more difficult to correct than others due to problems with the data and limits of the program's ability, most of these errors were reduced to some degree. This process is explained further in Chapter 7.

6.0 HAF ALGORITHM CALIBRATION RESULTS

6.1 Overview

With the potential sources of larger error established, this chapter presents the results of the HAF Algorithm calibration process. It is important to note that there is some human error inherent in the outlined calibration process, particularly with fitting three-point arcs over satellite imagery. However, this error should not be large enough to have a significant impact on the final results. From these results, it was determined that the HAF Algorithm does not require modification to make it compatible with all highway types. This chapter contains a summary of the HAF Algorithm's accuracy in calculating radius and curve length, an overview of the curve identification accuracy, and a section on the analysis of the sample sizes used for the calibration.

6.2 Curve Parameter Calculation Accuracy

Table 6.1 contains a summary of the curve parameter error results obtained from comparing the different types of roads. Segments with intersection errors, tangent errors, or curve fragment errors were not included because these problems correspond more to the issue of curve identification rather than curve parameters. The other errors listed above, however, do affect the results of Table 6.1. Included in this table are basic averages for all errors in a particular road type, 95 percent confidence intervals, median error, and the percentage of segments that exceed an arbitrary 5 percent error threshold. The purpose behind this percent error threshold is to show a better representation of how well the segments meet a basic standard while simultaneously reducing the effect from data outliers. The percentage exceeding the threshold is presented rather than the percentage meeting it to keep some consistency with the other parts of the table (i.e. smaller percentages mean less error). The actual calibration data are contained in Table A.1 through Table A.6 in Appendix A, where increasing mileposts (to the north and east) indicate a positive direction while decreasing mileposts indicate a negative direction.

Table 6.1 Error Summary

	Interstate		Multilane Highway		Two-Way Two-Lane Highway		Total Average
Average	Urban	Rural	Urban	Rural	Urban	Rural	
Arc Length	5.3%	6.1%	8.2%	15.1%	7.0%	5.5%	7.9%
95% CI	2.8-7.8%	4.6-7.6%	3.7-12.7%	3.6-26.6%	3.2-10.8%	4.1-6.9%	**5.7-10.1%**
Standard Deviation	13.4%	7.8%	22.9%	59.9%	19.5%	7.2%	28.6%
Radius	13.8%	28.3%	59.6%	28.5%	25.3%	61.1%	36.1%
95% CI	10.7-16.9%	19.8-36.8%	45.8-73.4%	20.4-36.6%	7.1-45.3%	40.3-81.9%	**30.5-41.7%**
Standard Deviation	16.3%	43.2%	70.6%	42.4%	92.6%	106.0%	70.1%

	Interstate		Multilane Highway		Two-Way Two-Lane Highway		Total Average
Median	Urban	Rural	Urban	Rural	Urban	Rural	
Arc Length	1.8%	3.6%	2.6%	2.9%	2.1%	2.8%	**2.6%**
Radius	8.6%	12.6%	14.1%	15.2%	19.8%	25.3%	**15.9%**

	Interstate		Multilane Highway		Two-Way Two-Lane Highway		Total Average
>5% Threshold	Urban	Rural	Urban	Rural	Urban	Rural	
Arc Length	18.7%	37.0%	26.0%	35.2%	20.0%	31.0%	**28.0%**
Radius	65.4%	88.0%	80.0%	85.7%	86.0%	92.0%	**82.9%**

Table 6.1 provides some interesting results on errors across different road types. The HAF Algorithm produces the most accurate results for interstate curves, followed by TLTW highways and multilane highways. It is immediately apparent that curve length calculations are far more accurate than radius calculations, which could be due in part to the fact that radius values are more affected by the larger sources of error discussed in Chapter 5. Urban segments appear to be generally more accurate, while the average values are sometimes worse than rural averages. This would seem to suggest the presence of large outliers affecting the results, especially in urban settings. This could be due to tangent-curve-tangent errors, although more analysis would need to be done to provide a definitive answer as to the reason why. Another interesting point is that many of the larger errors occurred in rural TLTW highway segments despite the fact that the HAF Algorithm was designed specifically for that road type. In other words, the algorithm produced more accurate results for interstate highways than it did for other road types.

Table 6.2 contains a summary of errors not included in Table 6.1 and the total identification accuracy for each road type. These errors include misidentified intersections, misidentified tangent segments, and curve fragments. If a segment included any of these three errors, it was marked as misidentified. The error values were calculated by taking the number of errors for each type and dividing it by the number of segments used in the sample. It is important to acknowledge the fact that the errors mentioned in Table 6.2 were very infrequent, so the sample sizes may not have been large enough to be certain how common they were.

Table 6.2 Identification Accuracy

	Interstate		Multilane Highway		TLTW Highway	
	Urban	Rural	Urban	Rural	Urban	Rural
Intersection	0.0%	0.0%	10.3%	0.0%	8.6%	3.8%
Tangent	2.4%	0.0%	14.4%	5.3%	5.2%	0.0%
Curve Fragment	2.4%	3.9%	4.1%	1.8%	0.0%	1.9%
Total Accuracy	95.2%	96.1%	71.2%	92.9%	86.2%	94.3%

As can be seen from Table 6.2, interstate curve segments were found to be generally more accurately identified than other road types. This is likely due in part to a lack of complications associated with intersections. The most striking difference presented in these data is the gap between urban and rural segments. While the difference between the two is almost negligible in interstates, it is very large in other types of highways. This is especially true in intersection and tangent errors.

The required sample sizes for each road type for three different tolerance levels in accuracy are contained in Table 6.3. These different tolerances can be accepted by engineers at the 95 percent confidence level. Table 6.3 also contains the approximate number of usable segments for each road type, which is the limiting factor. One hundred segments were used for each road type. Instances where the requirement was not met are highlighted in blue.

Table 6.3 Adequacy Check of Required Sample Sizes

Curve Length				
Tolerance	**5%**	**7.5%**	**10%**	**Number of Usable Segments**
Urban Interstate	28	12	7	210
Rural Interstate	9	4	2	770
Urban Multilane	81	36	20	490
Rural Multilane	552	245	138	370
Urban TLTW	58	26	15	255
Rural TLTW	8	4	2	12000

Radius				
Tolerance	**5%**	**7.5%**	**10%**	**Number of Usable Segments**
Urban Interstate	41	18	10	210
Rural Interstate	287	127	72	770
Urban Multilane	766	340	191	490
Rural Multilane	277	123	69	370
Urban TLTW	1318	586	329	255
Rural TLTW	1725	767	431	12000

While the number of segments calibrated frequently fails to meet the requirement for radius data collection, it does meet the requirement in most road types for curve length data collection. The one exception, rural multilane, does not have enough usable segments in the state of Utah in order to meet the 5 percent tolerance level, so that one was left as is without calibrating more segments.

6.3 Chapter Summary

The HAF Algorithm is best suited for identifying curves and determining their parameters along interstates. While it generally does better in calculating curve parameters in urban settings across different road types, curve identification is stronger in rural ones, for which the HAF Algorithm was originally developed. Overall, the absence of large error percentages in the presented results confirms that the HAF Algorithm is suitable across all six highway types and that new algorithms for each highway type were not warranted.

7.0 HAF ALGORITHM IMPROVEMENTS

7.1 Overview

After calibrating the HAF Algorithm and discovering error sources, the next step was to make improvements to the algorithm. This chapter contains a summary of improvements designed to improve both curve identification and curve parameter determination. This includes solutions to errors that existed in the original algorithm, refinements made to the code to improve accuracy, and changes made to the ArcMap model to make final improvements on curve identification. The six primary errors that these improvements target were detailed in Chapter 5. The first three deal with curve identification, including curve fragment, tangent, and intersection errors. The last three errors pertain to curve parameter determination, and include tangent-curve-tangent, curve length calculation, and compound curve errors. These last three have an impact on the radius and length of a curve, which makes meaningful crash analysis difficult.

The curve fragment, tangent, intersection, and curve length errors were resolved to varying degrees. Their corrective measures are presented in this chapter. An examination of the remaining two errors – tangent-curve-tangent and compound curve – is also presented for future research consideration.

This chapter also includes an outline of the changes made to the code to be able to accept more recent LiDAR data as an input to the HAF Algorithm. Because the data fields contain changes in formatting of some sort every time the data are collected, the expectation is that the algorithm is prepared to deal with field omissions or symbol changes without the code needing to be changed further from year to year in order to adapt to new data setups. The HAF Algorithm is now able to run 2012, 2014, and 2015 data. The solutions are presented in the following sections.

7.2 Curve Fragment/Curve Length Calculation Fix

The curve fragment and curve length calculation errors stemmed from the same cause and had the same solution. These errors are caused by an error in the HAF Algorithm’s code.

The error affected 3-13 percent of segments, depending on highway type. The cause of this error was non-sequential milepost ordering, which disrupted the curve combination process.

This issue is illustrated in Table 7.1. The segments shown were all combined into a single curve that lies along I-80 near Park City. Originally, the algorithm was programmed with the expectation that each segment within a curve would be ordered with a string of increasing or decreasing mileposts. For instance, the end milepost of one segment would match the beginning milepost of the next and the pattern would continue. However, the example in Table 7.1 shows the beginning milepost of the first segment matching with the end milepost of the second. When combining the segments into a single curve, the algorithm would adopt the beginning milepost of the first segment and the end milepost of the last segment as the PC and PT, respectively, as highlighted in red in Table 7.1. This error leads to an incorrect overall curve length of 2,302 feet. The true curve length is 1.138 miles (6,009 feet), which is the difference in the green highlighted values. "N" in the third column indicates a negative direction, which in this case signifies that the direction of travel is to the west (for a road traveling north-south, "N" signifies a southerly direction).

Table 7.1 Curve Fragment Error Source

ID	Route	Direction	Beg. MP	End MP	Curve Length (ft)
322350	0080N	N	141.249	140.802	2358.14
322349	0080N	N	141.281	141.249	166.919
322348	0080N	N	141.368	141.281	462.944
322347	0080N	N	141.395	141.368	139.49
322346	0080N	N	141.441	141.395	244.689
322345	0080N	N	141.563	141.441	641.621
322344	0080N	N	141.604	141.563	219.504
322343	0080N	N	141.685	141.604	427.59
322342	0080N	N	141.94	141.685	1345.065

Because the wrong starting and ending points were used as inputs in ArcMap, measurements of several curves were much shorter than they should have been. The problem was compounded further by the fact that while the starting and ending points shortened the curve, the listed curve length was a value calculated by the algorithm rather than by ArcMap as a simple sum of each segment's length regardless of milepost order. This meant that the calculated curve length was often 50-300 percent larger than the measured value and while correct, produced a large error in calibration.

To solve this problem, an “if-then” conditional statement was coded into the HAF Algorithm to examine the order of the mileposts. If the segment mileposts increased from beginning to end individually while the curve mileposts decreased as a whole (or vice versa), the endpoint of the first segment was assigned as the PC and the beginning point of the last segment was assigned as the PT. **Error! Reference source not found.** shows a flowchart of how the logic works.

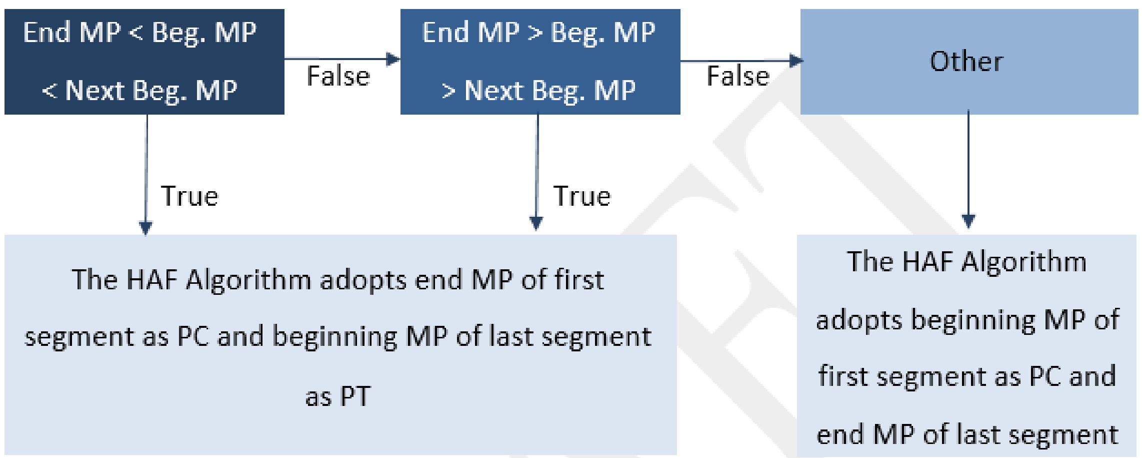

Figure 7.1 If/Then Curve Fix Diagram

The same conditional statement was also applied to the curve’s latitude, longitude, and elevation coordinates. This solution effectively eliminated the curve fragment and curve length calculation errors without affecting segments that did not experience a curve fragment error. A comparison of a curve near Park City along I-80 before and after the fix is shown in Figure 7.2 and Figure 7.3, respectively.

Figure 7.2 Before Curve Fragment Fix (Esri 2017)

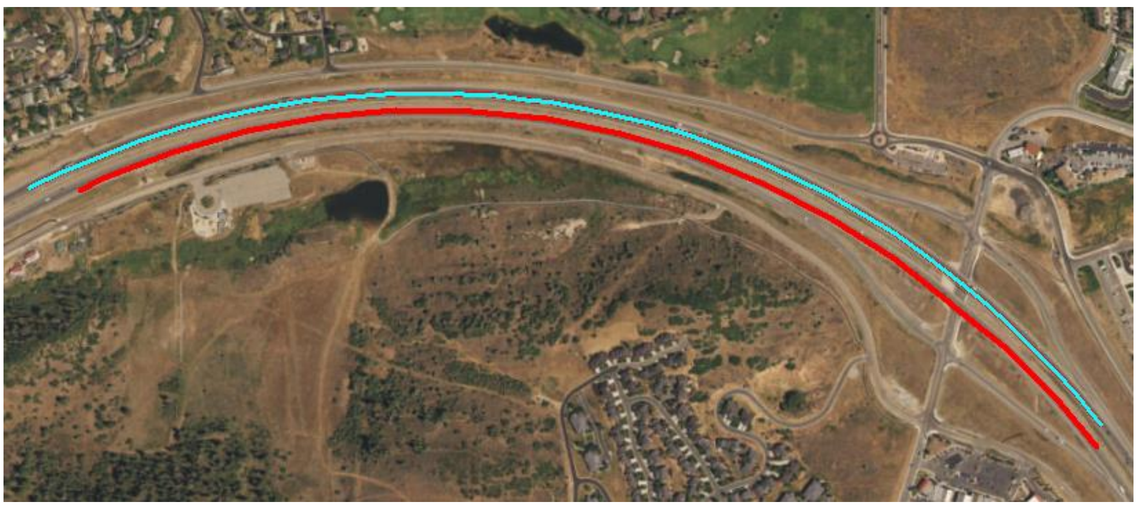

Figure 7.3 After Curve Fragment Fix (Esri 2017)

The curve segment in question is highlighted in cyan in both **Error! Reference source not found.** and

. The curve in **Error! Reference source not found.** covers only a small portion of the actual curve, especially when compared to the curve in the opposite direction that did not encounter this error. Additionally, the curve in the opposite direction remains unaffected by this change, which is a demonstration of the effectiveness of the fix.

An additional problem resolved with the fix was that on occasion, some curves would have no length at all. This problem pertains to the way segment mileposts are ordered in the LiDAR data. This situation was unique to curves that consisted of two segments. Since the beginning milepost of the first segment would occasionally be the same as the end milepost of the second, the starting and ending points of the curve would be exactly the same. **Error! Reference source not found.** shows an example of the error located along I-70, with the starting and ending points identified by the original HAF Algorithm highlighted in red and the starting and ending points identified by the improved HAF Algorithm highlighted in green. This error meant that because ArcMap was expecting a line feature with a length, nothing on the map would be created, as if the curve did not exist. This is also no longer an issue.

Table 7.2 Missing Segment Error

ID	Route	Direction	Beg. MP	End MP	Curve Length (ft)
321683	0070N	N	70.945	70.899	239.497
321682	0070N	N	70.984	70.945	206.118

7.3 Tangent Refinement

While the original HAF Algorithm is fairly accurate at identifying curves, there are occasions when tangent segments are identified as curves. To understand part of the cause of this error, a basic explanation of the curve weighting system in the algorithm is required. The user enters certain threshold values to assist in identifying curves, including radius, length, and the ratio between the two. A positive weight is assigned to segments that are more curve-like, and a negative weight is assigned to segments that are more tangent-like. For instance, in the original HAF Algorithm, a tangent would have its weight reduced by 1 for each multiple of the threshold that it exceeded. If the radius threshold were 6,000 and a segment had a radius of 6,001 feet, its weight would be -1. If the segment's radius was 12,001 feet, it would have a weight of -2, and so on.

While the threshold was acceptable and a few curve segments did have radii above 6,000 feet that were weighted positive due to them meeting other thresholds, tangent segments would slip through on occasion. **Error! Reference source not found.** contains a tangent segment identified as a curve along SR-173 in Taylorsville. This segment has a radius of 11,137 feet, which is well above the 6,000-foot threshold. After further examination, it was found that nearly all segments with a radius beyond 10,500 feet were tangents.

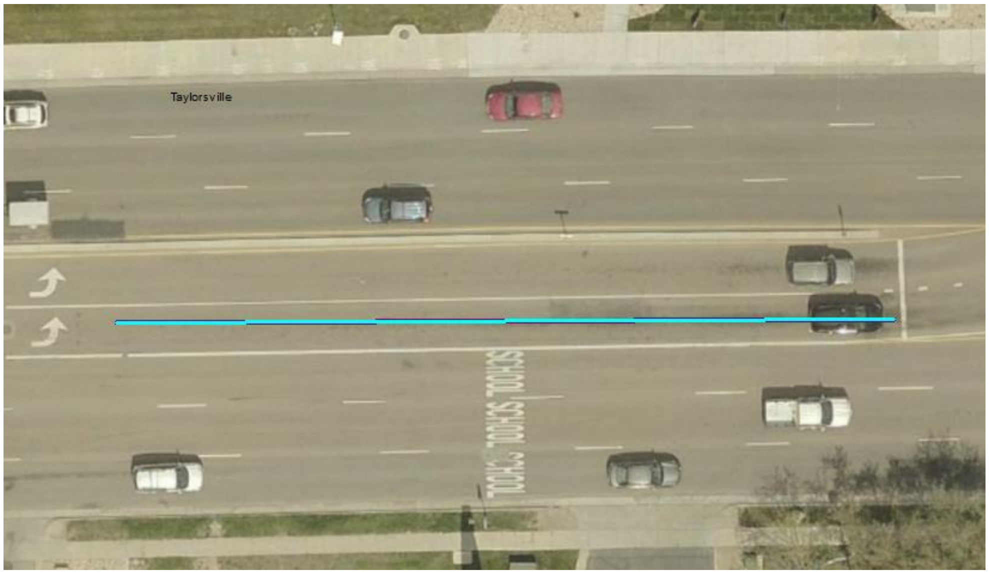

Figure 7.4 Large-Radius Tangent Error (Esri 2017)

This issue prompted the idea of introducing a non-linear weighting system with larger negative weights being imposed for each successive breach of a threshold. This way, segments with radii values fairly close to the threshold still had an opportunity to be considered a curve while segments with a radius that far exceeded the threshold would be removed from consideration entirely. For each successive threshold breached, a negative weight that exceeded the previous weight by one would be assigned. This was done using an arithmetic series. The scale at which each successive threshold (not the weight itself) was determined was 1.75^n, the reason being that 6,000 multiplied by 1.75 reached the 10,500 value beyond which nearly every segment was a tangent.

To clarify how this non-linear weighting system works, an example of ranges will be presented with an assumed initial radius threshold of 6,000 feet. For segments with a radius between 6,000 and 10,500 feet, a weight of -1 was assigned. For radius values between 10,500 and 18,375, a weight of -3 (-1 minus 2) was assigned. For radius values between 18,375 and 32,156 feet, a weight of -6 (-1 minus 2 minus 3) was assigned, and the pattern continues. The ranges for which the thresholds were adjusted were determined using a formula independent of the series used for the weights themselves.

This was found to reduce the number of tangent segments identified as curves. As an additional bonus, a few tangent-curve-tangent errors were resolved. The remaining tangents had parameters similar to those of curves in terms of radius and curve length, which made them much more difficult to isolate. However, this was an effective step in improving the performance of the algorithm.

7.4 Intersection Elimination

While steps were taken in the original HAF Algorithm to prevent the identification of intersections where highways changed direction as curves, it was not entirely successful and several intersections remained. An ArcMap model was developed to remove curves with a total length below a specified threshold, and it was effective to some degree. The issue with the remaining intersections, however, was that the ArcMap model and the HAF Algorithm were unable to differentiate between intersections and sharp curves on mountainous highways because the radii of the two are largely similar. Attempting to separate the two types of curves with a short radius (a true intersection and a sharp curve on a mountainous highway) by change in elevation was unsuccessful as many sharp mountain curves have small differences in elevation.

An alternative method was evaluated that involved isolating curves by location instead. Because urban areas lack sharp mountain curves, it seemed to be a feasible starting point from which to improve the model. A Utah municipality shapefile was downloaded from the Utah AGRC data portal. Upon closer inspection, it was found that very few sharp curves existed within urban municipalities and that many intersections were assigned a radius of less than 225 feet. This was further backed up by the AASHTO Greenbook in Table 3-9 (AASHTO 2011), which shows that such small radius values accompanied with a maximum design superelevation of 6 percent are rare and are only used with speeds of 25 mph or lower. UDOT uses a maximum superelevation of 6 percent for designing horizontal curves on state highways. With this information, a new addition to the ArcMap model was developed, as shown in **Error! Reference source not found.**.

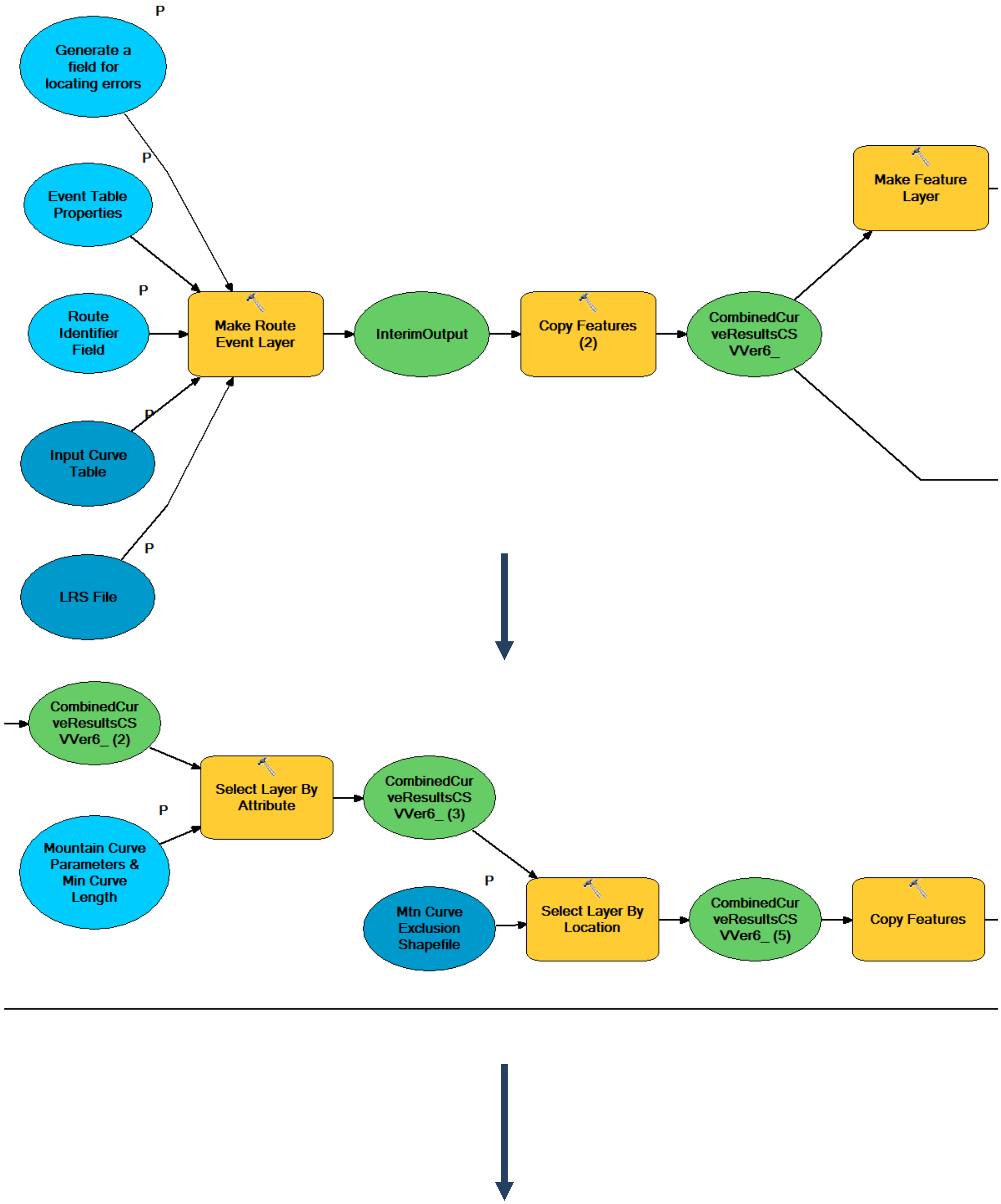

Figure 7.5 ArcMap Model (Esri 2017)

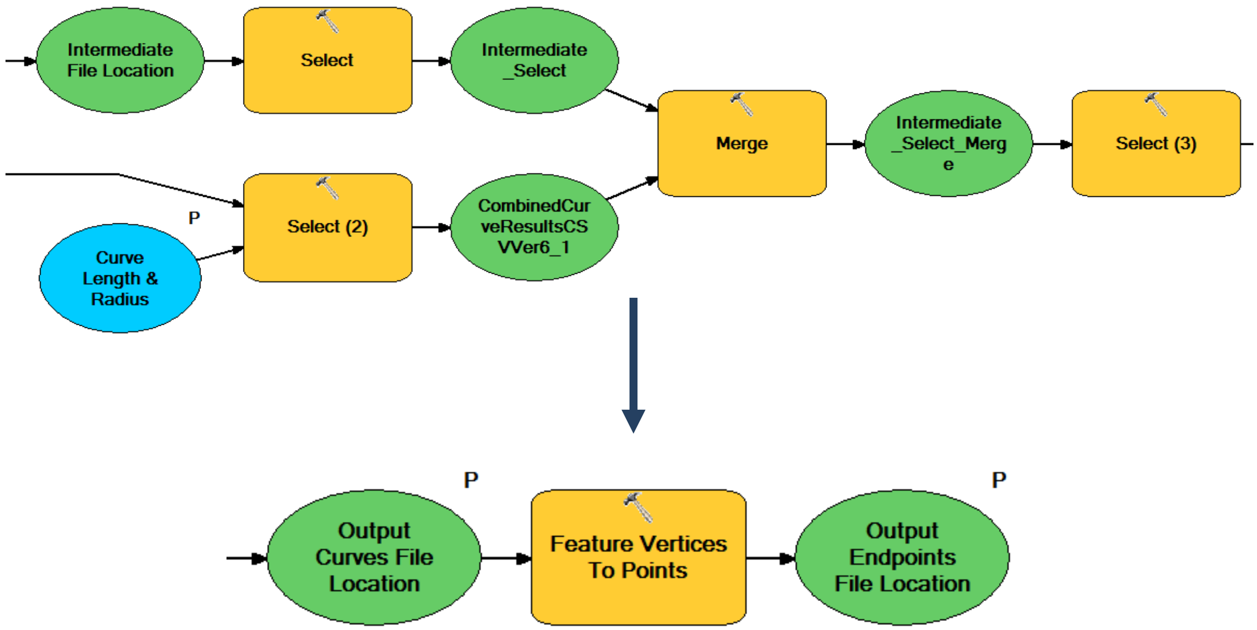

Figure 7.5 (Continued)

The complexity of the ArcMap model was increased significantly from the original one. A new shapefile was created as a modified version of the municipality file mentioned earlier that only included urban municipalities. This new shapefile was added to the ArcMap model and removed curves with a radius of less than 225 feet from urban areas. This reduced the number of intersections identified as curves in the final output, increasing the overall identification accuracy. However, many intersections remained, particularly in rural areas. The possibility of removing all highway segments identified as curves from within any city limits below a certain radius threshold was explored but it was found that several sharp mountain curves existed within rural municipality boundaries, especially in Park City and Brian Head.

To resolve this issue, a new shapefile was created that excluded all municipalities that contained sharp mountainous curves. This was done by selecting all curves within all municipalities with a radius of less than 225 feet and viewing which cities contained mountainous curves. With this new information, the radius thresholds and municipality boundaries were applied and the number of intersections identified as curves was reduced from

25 to 20. In checking the effectiveness of these changes, it was found that no actual curves were removed in the process.

7.5 Thoughts on Remaining Two Errors

The two remaining errors that did not appear to have an immediate solution are the tangent-curve-tangent and compound curve errors. In the vast majority of cases related to the tangent-curve-tangent error, the problem lies in the data themselves. In this case, small tangents are often attached to curves as part of a single segment. Because the HAF Algorithm is designed to combine data segments and not divide them, this is an issue that could not be resolved. Dividing segments would necessitate further research and would be extremely difficult due to the fact that the starting and ending points of each segment are the only points that are given in the LiDAR attribute table. Any solution to remedy this would likely need to be done through ArcMap and would require a complex procedure.

To resolve the compound curve problem, a change in the approach to calibration was made to reflect what the HAF Algorithm does. While compound curves are relatively rare, provisions were made to accommodate them. Rather than drawing a single circular arc over the road in AutoCAD, compound curves were overlaid with two or three simple circular arcs, depending on the needs of the situation. Each individual curve length was added as part of a sum, and each radius was included in part of a weighted average based on segment length, which is what the HAF Algorithm does. In further research, the HAF Algorithm could possibly be altered to separate compound curves and populate another sheet designed specifically for them.

7.6 New Data Adaptation

After the HAF Algorithm was improved, it needed to be modified to accept more recent data. The original HAF Algorithm was designed to run on 2012 LiDAR data. However, the order and names of the different columns included in the attribute table changed from the 2012 to 2014 data, which meant that the algorithm had to be revamped to include a new interface that required more user input. These changes meant that the algorithm was capable of running two years' worth of curve data despite the differences in format. However, the algorithm was not capable of running 2015 data due to further changes in formatting.

The new data omitted a segment ID column, which had been used previously to check if the segments had been ordered sequentially. This part of the code was removed from the algorithm as it was simply a redundancy designed to find errors and it was found to be unnecessary. The new 2015 data had "+" and "-" signs to indicate positive and negative milepost direction while 2012 and 2014 data had used "P" and "N" to indicate direction. This had been used in the original HAF Algorithm to confirm that directional errors did not exist in the data. To resolve the difference in route direction symbology, a VLookup function was added to the main interface to sort through the direction column in the data to find unique values of direction indication, which were then populated to a hidden sheet within the Excel file.

After the unique values had been found, the different options were made available for selection through the Data Validation function. **Error! Reference source not found.** shows the updated interface. In this updated interface, the user specifies the input and output file locations in addition to checking column headings as had been done in the original HAF Algorithm. After the "Apply" button has been pressed, the user then specifies what signs are used to indicate positive and negative milepost direction, the units in which the curve length is given, and the threshold parameters. After these have been filled, the HAF Algorithm is ready to be run.

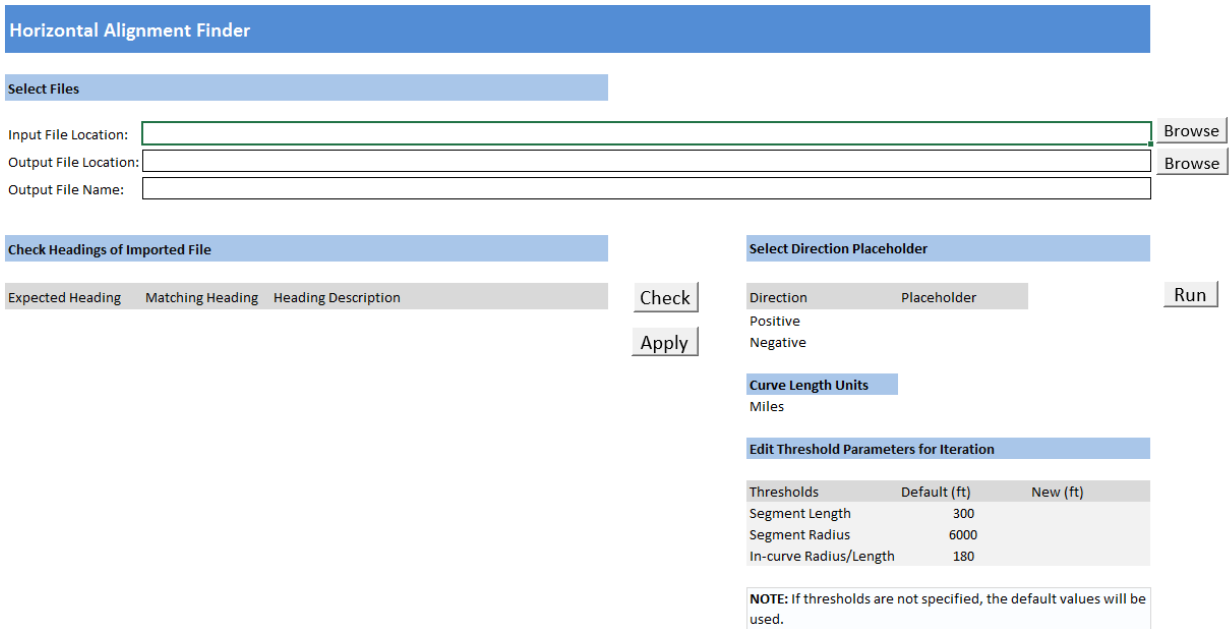

Figure 7.6 Updated HAF Algorithm Interface

The direction selection procedure is illustrated in **Error! Reference source not found.**. In this particular example, 2015 data are being run through the algorithm, which has a direction column filled with plus and minus signs. During the run of the program, the direction signs that the user had specified would be swapped with “P” for “+” and “N” for “-” in the output data for positive and negative directions, respectively.

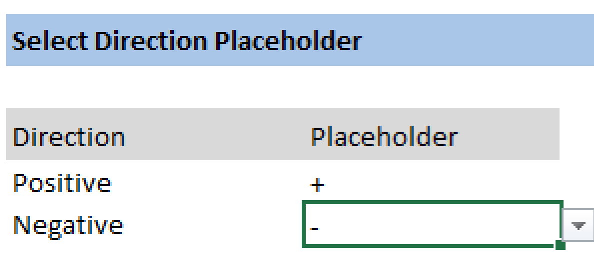

Figure 7.7 Direction Drop-Down Arrow

Another change in the 2015 data from previous years was that the units of segment length were different. In 2012 and 2014 data, every length measurement had been done in feet, while the 2015 data were in units of miles. The units were verified using a comparison of the ArcMap shapefile to Google Earth’s path measurement tool. To account for this change, a part of the program to convert miles into feet was written in the code and it would be activated should the user specify that the curve length units were in miles, as shown in **Error! Reference source not found.**.

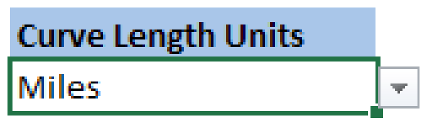

Figure 7.8 Units Drop-Down Arrow

These changes in the programming and the interface allowed the updated HAF Algorithm to run 2012, 2014, and 2015 data. The program now requires more user input, but contains easy-to-follow steps to ensure it runs smoothly.

An additional change that was made to the HAF Algorithm to allow for 2015 input data involved removing duplicate segments. These caused a problem on interstates in which two segments with the exact same parameters would overlap. The HAF Algorithm would identify them as two halves of the same curve and combine their respective curve lengths. This meant that the calculated curve length was exactly double what it was supposed to be. To resolve this issue, Excel's built-in "Remove Duplicates" function was implemented into the code and it searched for segments that had the exact same attributes as a previous one. Once these segments were identified, duplicates were removed, leaving the input data as they should have been.

The final change that was made to adapt to 2015 input data involved an isolated error that occurred along SR-201 in Salt Lake City. A situation in which two segments of the highway with the same direction ran parallel to each other disrupted the milepost order, which led to a 13-mile gap in the mileposts. One of the curves ended at an intersection and should have been classified as a tangent. This issue caused a large amount of the highway to be considered a single curve. This error was resolved through adding a stipulation that removed segments from curve consideration if there was more than a 5-mile gap between the PC and PT.

While the program is now able to run 2015 data effectively, the primary concern is that the data might change further in future years, which might prevent the algorithm from working properly. Unfortunately, it is not possible to predict what changes will occur. It was only after the directional issue was fixed that it was discovered that the 2015 segment lengths were in units of miles. This indicates that it is possible for large, unforeseen differences to appear in future datasets. This would require further alterations to the code and possible changes to the interface. A full list of what data the HAF Algorithm requires as well as the general formatting that is expected is detailed in the HAF Algorithm user's manual.

7.7 Chapter Summary

Six errors were targeted in order to make improvements to the existing HAF Algorithm, including curve fragment, curve length calculation, tangent, intersection, compound curve, and tangent-curve-tangent errors. Curve fragment and curve length calculation errors were both effectively reduced as they had the same cause. Intersection errors were also reduced due to new provisions being made in the updated ArcMap model. Tangent errors were reduced less effectively, although the new weighting system did eliminate some tangents from being identified as curves. The other two errors could not be resolved by making improvements to the HAF Algorithm. The results of the improvements to the HAF Algorithm are discussed in Chapter 8.

8.0 RESULTS OF HAF IMPROVEMENTS

8.1 Overview

Significant improvements were made to the HAF Algorithm. In addition to using newer data, errors were resolved to increase overall accuracy. Contained in this chapter is a summary of the curve length and radius calibration, an overview of the curve identification accuracy, and a review of the required sample sizes for each highway type. The results of the original algorithm do differ from those presented in the Chapter 5 due to the elimination of human error in the calibration process. Curves with larger errors were reviewed separately by a researcher who had not calibrated the segment the first time. This was done to verify that the calibration had been performed properly. Changes were made to both the original and improved algorithm results accordingly.

8.2 Curve Parameter Results

This section covers the results of curve parameter calculation and compares the outputs of both the original and improved algorithm. Table 8.1 contains a summary of the results for interstate calibration. Averages, 95 percent confidence intervals, standard deviations, and medians are included in these results. Additionally, a section was created that shows the percentage of segments that met a 5 percent error threshold. The average curve length error decreased in both urban and rural settings.

Rural interstate segments had an 18 percent improvement in the number of segments that now meet the 5 percent curve length error threshold. However, the median error remained relatively constant. This is because HAF Algorithm improvements for curve length specifically targeted larger errors that would be classified as outliers, which includes the curve length calculation error. The other improvements relate more to curve identification and adapting to more recent data. This also explains the lack of change in radius error.

Table 8.1 Interstate Calibration Result Comparison

	Urban		Rural	
Average	Original	Improved	Original	Improved
Curve Length	4.0%	3.0%	4.2%	2.4%
95% CI	2.4-5.6%	2.4-3.6%	3.1-5.3%	1.9-2.9%
Standard Deviation	8.34%	2.93%	5.57%	2.31%
Radius	12.3%	10.1%	13.1%	16.0%
95% CI	9.9-14.7%	8.0-12.2%	11.3-14.9%	13.1-18.9%
Standard Deviation	12.46%	10.57%	9.09%	14.61%

	Urban		Rural	
Median	Original	Improved	Original	Improved
Curve Length	1.7%	2.2%	2.7%	1.7%
Radius	8.6%	7.2%	10.2%	12.1%

	Urban		Rural	
<5% Threshold	Original	Improved	Original	Improved
Curve Length	84.1%	86.1%	73.0%	91.0%
Radius	36.6%	33.7%	14.0%	13.0%

Table 8.2 contains a summary of the calibration results for multilane highways. The reduction in average curve length error is 4.6 percent for urban areas and 7.0 percent for rural areas. This is again due to the targeting of outliers that the original HAF Algorithm produced on occasion. The median error values for both radius and curve length have remained consistent, adding credence to this explanation. The percentage of segment curve lengths that meet the 5 percent error threshold has increased by 16.0 percent for urban areas and 21.1 percent for rural areas. The radius averages have also improved, which could be due to the use of newer data. It is also worth pointing out that the standard deviations have decreased for all categories except for the 5 percent error threshold in rural areas, which generally suggests increased consistency.

Table 8.2 Multilane Highway Calibration Result Comparison

	Urban		Rural	
Average	Original	Improved	Original	Improved
Curve Length	6.6%	2.0%	8.8%	1.8%
95% CI	2.4-10.8%	1.7-2.3%	2.2-15.4%	1.4-2.2%
Standard Deviation	20.89%	1.75%	33.93%	1.91%
Radius	27.9%	17.0%	24.4%	12.7%
95% CI	16.1-39.7%	13.8-20.2%	16.7-32.1%	10.5-14.9%
Standard Deviation	58.86%	16.30%	39.67%	11.02%

	Urban		Rural	
Median	Original	Improved	Original	Improved
Curve Length	2.4%	1.6%	2.5%	1.1%
Radius	11.5%	11.4%	13.4%	9.7%

	Urban		Rural	
<5% Threshold	Original	Improved	Original	Improved
Curve Length	78.0%	94.0%	70.9%	92.0%
Radius	23.0%	15.0%	15.5%	31.0%

Table 8.3 contains a comparison of the improved HAF Algorithm with the original for TLTW highways. The results are similar to that of interstates and multilane highways, in that averages improved while medians remained fairly consistent for both radius and curve length. While there is some overlap in the 95 percent confidence intervals, the average curve length error decreased as a whole. The number of segment curve lengths that met the error threshold has improved in both cases, which means that all highway types with the exception of urban interstate have at least 90 percent of segments with an error of 5 percent or less.

Table 8.3 TLTW Highway Calibration Result Comparison

	Urban		Rural	
Average	Original	Improved	Original	Improved
Curve Length	6.2%	2.2%	4.6%	1.9%
95% CI	2.4-10.0%	1.8-2.6%	3.3-5.9%	1.5-2.3%
Standard Deviation	19.09%	1.90%	6.65%	2.06%
Radius	25.3%	21.9%	49.6%	27.0%
95% CI	13.6-37.0%	17.8-26.0%	30.4-68.8%	19.8-34.2%
Standard Deviation	59.34%	20.96%	96.86%	36.76%
	Urban		**Rural**	
Median	Original	Improved	Original	Improved
Curve Length	1.8%	1.7%	2.4%	1.2%
Radius	18.8%	18.9%	20.3%	19.1%
	Urban		**Rural**	
<5% Threshold	Original	Improved	Original	Improved
Curve Length	85.0%	92.0%	74.0%	93.0%
Radius	15.0%	15.0%	9.0%	12.0%

The curve length errors presented in Table 8.1, Table 8.2, and Table 8.3 are low, to the point that these percentages could be influenced by human error in the calibration process. This would suggest that no further improvements are warranted to improve the accuracy of curve length calculation. Additionally, these improvements have brought the accuracy of multilane and TLTW highways to a level similar to that of interstates, meaning that the HAF Algorithm is nearly equally effective across all highway types.

8.3 Curve Identification Results

This section focuses on the improved HAF Algorithm's ability to correctly identify curves. Table 8.4 presents errors that are associated with curve identification rather than curve parameters, specifically for interstate highways. As can be seen from the total accuracy row, there is a general trend toward improvement. The curve fragment fix was effective in eliminating those errors almost completely. While the number of tangents was reduced, tangent errors were uncommon for interstate highways to begin with, which means that more tests would need to be performed to determine whether the fix was effective.

Table 8.4 Interstate Identification Error Comparison

	Urban		Rural	
	Original	Improved	Original	Improved
Intersection	0.0%	0.0%	0.0%	0.0%
Tangent	2.4%	1.4%	0.0%	0.0%
Curve Fragment	2.4%	0.0%	3.9%	0.0%
Total Error	4.8%	1.4%	3.9%	0.0%
Total Accuracy	95.2%	98.6%	96.1%	100.0%

Table 8.5 contains a curve identification error comparison for multilane highways. While urban multilane segments showed a trend of improvement, rural segments remained relatively consistent as the number of errors was very low to begin with. While a 3.3 percent intersection error occurred in the improved algorithm results, it was found that these specific errors would have occurred under the original algorithm as well. The increase in error was a result of the randomness of the segments selected for comparison purposes. The most pronounced improvement came in the elimination of intersections identified as curves along urban multilane highways. This is because the revised ArcMap model targeted municipality areas, which make up the entirety of urban regions. This improvement brought the total accuracy of urban multilane segments to 87.3 percent from its original accuracy of 71.2 percent.

Table 8.5 Multilane Highway Identification Error Comparison

	Urban		Rural	
	Original	Improved	Original	Improved
Intersection	10.3%	1.8%	0.0%	3.3%
Tangent	14.4%	10.9%	5.3%	5.0%
Curve Fragment	4.1%	0.0%	1.8%	0.0%
Total Error	28.8%	12.7%	7.1%	8.3%
Total Accuracy	71.2%	87.3%	92.9%	91.7%

Table 8.6 contains an identification error comparison for TLTW highways. In both urban and rural settings, the number of intersections identified as curves has been reduced. However, the percentage of tangents identified as curves increased in urban TLTW highways. This could be due to the fact that the sample size of curves with this error was too small to provide a definitive conclusion. After further examination of this type of error, it was determined that the

segments that were identified as tangents in the improved HAF Algorithm would have likewise been identified as tangents in the original HAF Algorithm (with alterations made to adapt to 2015 data). Several of these errors occurred at locations where a highway was widened to accommodate a left-turn lane, which means that the centerline of a highway would have been adjusted at that point. Many of these tangents were assigned a radius of approximately 2,000 feet, which makes them virtually indistinguishable from curves from a data standpoint. Despite this, there is a general trend towards improvement.

Table 8.6 TLTW Highway Identification Error Comparison

	Urban		Rural	
	Original	Improved	Original	Improved
Intersection	8.6%	1.8%	3.8%	2.4%
Tangent	5.2%	10.5%	0.0%	0.0%
Curve Fragment	0.0%	0.0%	1.9%	0.0%
Total Error	13.8%	12.3%	5.7%	2.4%
Total Accuracy	86.2%	87.7%	94.3%	97.6%

In summary, it can be concluded that the curve fragment and intersection improvements were effective, while the tangent fix was less effective than expected.

8.4 Adequacy Check of Required Sample Sizes

When performing assessments of improvement efficacy, the data must be examined in order to determine if the minimum sample size was met. Table 8.7 provides an adequacy check of required sample sizes for curve length calculation for 5, 7.5, and 10 percent tolerance levels. The column on the very right shows the total number of useable curves listed for each highway type. The formula used to calculate the required sample size is outlined in Equation 8-1:

$$N = \frac{z^2\sigma^2}{E^2} \qquad (8\text{-}1)$$

Where:

N = the required sample size for a given confidence interval
z = 1.96 for a 95 percent confidence interval
σ = the standard deviation
E = the tolerance level expressed in decimal form

Approximately 100 curves were calibrated in each situation, and road types that did not meet the requirement are highlighted in blue. The original HAF Algorithm met the required number of segments for all highway types except for rural multilane in the 5 percent tolerance in accuracy at the 95 percent confidence level. The improved HAF Algorithm met the requirement for each highway type, due to small standard deviations in terms of error.

Table 8.7 Curve Length Adequacy Check of Required Sample Sizes

Tolerance	5 Percent		7.5 Percent		10 Percent		# of Segments
HAF Status	Original	Improved	Original	Improved	Original	Improved	
Urban Interstate	11	2	5	2	3	2	210
Rural Interstate	5	2	2	2	2	2	770
Urban Multilane	67	2	30	2	17	2	490
Rural Multilane	177	2	79	2	44	2	370
Urban TLTW	56	2	25	2	14	2	255
Rural TLTW	7	2	3	2	2	2	12000

Table 8.8 contains a similar adequacy check of required sample sizes for radius calculations in each road type. Radius errors varied far more, which meant that much larger sample sizes were required. In many cases, the required sample size for the original algorithm exceeded the number of usable segments available in a particular road type. However, the improved HAF Algorithm met the required sample size in every road type with the exception of rural TLTW, which means that average radius errors presented in Table 8.1, Table 8.2, and Table 8.3 are an accurate representation of the actual error percentage. It is worth mentioning that the LiDAR data seem to be more accurate in calculating curve length than they are at calculating radius values. At minimum 100 samples were again used for each highway type.

Table 8.8 Radius Adequacy Check of Required Sample Sizes

Tolerance	5 Percent		7.5 Percent		10 Percent		# of Segments
HAF Status	Original	Improved	Original	Improved	Original	Improved	
Urban Interstate	24	17	11	8	6	4	210
Rural Interstate	13	33	6	15	3	8	770
Urban Multilane	532	41	237	18	133	10	490
Rural Multilane	242	19	107	8	60	5	370
Urban TLTW	541	68	240	30	135	17	255
Rural TLTW	1442	208	641	92	360	52	12000

8.5 Chapter Summary

Overall, the new HAF Algorithm is an improvement over its predecessor. It shows a reduction of error both in terms of curve identification and curve parameter calculation. Of the six errors mentioned at the beginning of the chapter, four were effectively reduced or eliminated, including intersection, tangent, curve length calculation, and curve fragment errors. Compound curve errors require a change in calibration approach, and tangent-curve-tangent errors could not be reduced due to the way the LiDAR data is reported. While some tangents were eliminated, others remained due to issues with the data displaying an incorrect radius value. This may warrant further research, although it would be difficult to remedy because these tangents are virtually indistinguishable from curves when viewed in table form.

The new algorithm was also effective in adapting to 2015 data. Changes were made both to the interface and to the code itself, with more options for the user to specify in order to ensure that it runs properly. With these alterations, it should be prepared to accept future data.

Most significantly, the average curve length error was reduced across each road type. The improved HAF Algorithm is very accurate in determining curve length, and the presence of any curve length error is likely due in part to human error in the process of calibration. The improvements made to the algorithm, combined with newer data, have made curve identification and parameter calculation very accurate. With the improvements achieved, the next step was to combine curve, roadway, and crash data to identify curve segments with high crash occurrences.

9.0 HAF CRASH ANALYSIS

9.1 Overview

While the HAF Algorithm is effective at identifying curves and their attributes, it cannot process crash data and show the user crash hotspots. For this reason, a new program was needed to combine curve, roadway, and crash data. This chapter presents the process and results of that combination. It also includes several case study examples. Users of the program should be able to use output files to determine which highway curves warrant improvements to make them safer. Additionally, this program prepares the way for further crash analysis in the UCPM and UCSM so that curve parameters can be analyzed to determine if there is a correlation between those parameters and crash rates.

9.2 Excel VBA Program – Combining Road Data with Crash Data

This section contains an explanation of the VBA program designed to combine curve, roadway, and crash data. An overview of the program's function is included, as well as a look into the main interface and some of the features contained in it. A simplified explanation of how the code works in combining roadway and crash data is also included, as well as a discussion on how superelevation transition segments can be considered when determining the crash histories of each curve.

9.2.1 Overview of the Program's Function

The function of the VBA program is to format and clean up roadway data, and combine them with curve data and crash data in order to generate lists of curves with their parameters and crash histories. The algorithm loops through each dataset and identifies fields that are common between them, including route name, milepost, and direction, depending on the dataset. The first five input data files contain roadway data and were obtained from the UDOT Data Portal (UDOT 2017). The final four contain crash data that are not publicly available but also come from UDOT. All input files are listed as follows:

- AADT (Open Data)
- Functional Class

- Approximate Speed Limit (2015)
- Urban Code
- Lanes (2014)
- Crash_data_2010-2015
- Crash_Location_2010-2015
- Crash_Rollups_2010-2015
- Vehicle_2010-2015

The four crash data files were combined into a single file through the use of a program titled "Roadway and Crash Data Preparation" created earlier by a research team at BYU (Schultz et al. 2017).

9.2.2 Program Interface

The VBA program user interface is shown in Figure 9.1. The new program works similar to the HAF Algorithm in that there are areas at the top to specify the output file location. There are also places to match headings to ensure that the different data headings are picked up correctly. Additionally, several buttons are placed to allow the user to select input files for the various types of road data and crash data, with status indicators that signal when the data files have finished importing. The interface also allows the user to specify the minimum UDOT severity level for a crash to be considered severe, as well as choose whether superelevation transition segments will be considered in the total curve length.

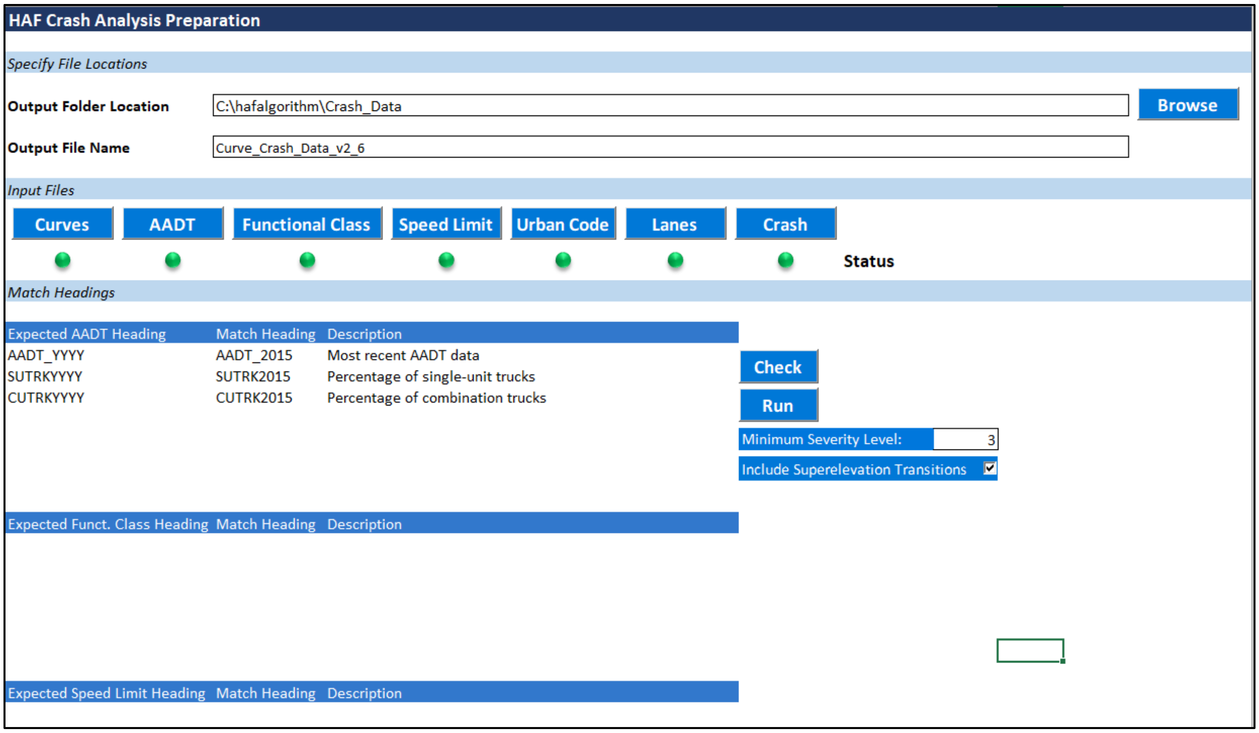

Figure 9.1 Excel Program User Interface

In this program, the user first specifies the folder directory in which the output file will be stored as well as the name of the output file. After this has been completed, the user selects the .csv files to be used as the input files. Seven total datasets are placed in separate sheets before the combination phase. The user will then press the “Check” button, which will initiate a program to check the headings of the input files. If an expected heading is not found, it will appear under the “Match Headings” section with a description of the proper heading. The user can then select the corresponding input heading from a drop-down list. Once the user clicks the “Run” button, the new headings are applied to the input sheet for the program to keep track of which columns correspond to their respective data fields. Like in the HAF Algorithm, the heading check section is necessary because data headings often change from year to year.

9.2.3 Roadway Data Combination

The program takes about two minutes using a Core2 processor to run through 16,000 curve segments, and copies necessary fields from the roadway data sheets to the Output Data sheet. The data are sorted first by route name, then by direction, and finally by beginning milepost. This puts the segments in consecutive order. The curve segments are the first to be copied to the output sheet because they are the main focus of the study. The program loops through each curve segment multiple times to place each road parameter with its respective curves. The data is combined through route name and milepoint. The program loops consecutively through each roadway sheet to determine which road parameter segment the curve segment lies within. If a curve segment is separated by two different road parameter segments, the data from the first segment is adopted and placed in the output sheet. Direction is also taken into consideration in some datasets. For instance, the speed limit for some segments varies depending on direction. The program takes this into account.

Some VLookup functions are required as county codes from station numbers are matched with their respective county names in a sheet entitled "Key." A similar process is done in looking up the description for each functional class to give a better idea of the type of highways being analyzed.

A correction is applied to the speed limits of certain segments. In some cases, the speed limit is listed as 0 or 10, which is an error with the data. Should this happen, the program obtains a speed limit based on the segment's functional class. In this case, a VLookup function is used in which to replace the erroneous speed limit with an average speed limit for each functional class from the Key sheet. After the data have been corrected, the program then calculates fields such as total truck percentage and VMT. These fields are necessary for full statistical analysis.

An additional correction is also applied to the Lanes sheet. Because of the nature of the file, this data is largely fragmented and contains several overlaps. A provision is made in the program to consolidate the data and organize it such that one segment starts where the previous one ends. The difficulty is that overlapping segments often have conflicting data. Because it is not possible to determine which segment is correct from the data alone, the number of through lanes from the first segment is adopted for the final output file.

9.2.4 Superelevation Transition Calculation

The final step the program takes before combining the crash data is to calculate superelevation according to recommended guidelines given in the Greenbook (AASHTO 2011).

Superelevation runoff is calculated using Equation 3-23 in the Greenbook, which is outlined in Equation 9-1.

$$L_r = \frac{(wn_1)e_d}{\Delta}(b_w) \tag{9-1}$$

Where:

L_r = superelevation runoff
w = width of one traffic lane (assumed to be 12 ft)
n_1 = number of lanes to be rotated
e_d = design superelevation
Δ = maximum relative gradient
b_w = lane adjustment factor

Because the number of lanes to be rotated is difficult to determine due to the existence of divided highways, n_1 is assumed to be 1 while b_w is given a conservative value of 1.0. This has been done because transition length does not need to be completely accurate as the PC and PT of identified curves often differ slightly from where they are actually located.

Design superelevation (e_d) is a value that is looked up from Table 3-9 in the Greenbook, assuming a maximum superelevation of 6 percent used by UDOT (UDOT 2012). This table has been replicated in the Superelevation Tables sheet, where superelevation is determined based on the speed limit and the radius of the curve. Figure 9.2 shows a screenshot of part of this table. Design superelevation is on the left, and is looked up based on design speed from the top row and an approximate radius value.

Design Superelevation, e_{max} = 6%								
	Speed Limit (MPH)							
e_d	15	20	25	30	35	40	45	50
2	868	1580	2290	3130	4100	5230	6480	7870
2	614	1120	1630	2240	2950	3770	4680	5700
2.2	543	991	1450	2000	2630	3370	4190	5100
2.4	482	884	1300	1790	2360	3030	3770	4600
2.6	430	791	1170	1610	2130	2740	3420	4170
2.8	384	709	1050	1460	1930	2490	3110	3800
3	341	635	944	1320	1760	2270	2840	3480
3.2	300	566	850	1200	1600	2080	2600	3200
3.4	256	498	761	1080	1460	1900	2390	2940
3.6	209	422	673	972	1320	1740	2190	2710
3.8	176	358	583	864	1190	1590	2010	2490
4	151	309	511	766	1070	1440	1840	2300
4.2	131	270	452	684	960	1310	1680	2110

Figure 9.2 Design Superelevation Table with e_{max} = 6 Percent

The program sorts through the table first by determining what column the speed limit matches. It then loops down the column to find the radius value that most closely matches the radius of the curve. After that, it finds the row this radius value is on, and determines the corresponding design superelevation. If the radius is greater than the value on the top row, a provision is made that sets the design superelevation as 2 percent. The maximum relative gradient (Δ) is determined by looking up a value in Table 3-15 from the Greenbook by correlating the speed limit with the maximum relative gradient. From these values, the superelevation runoff distance is calculated.

Tangent runout then is calculated by using equation 3-24 in the Greenbook, which is outlined in Equation 9-2.

$$L_t = \frac{e_{nc}}{e_d} L_r \qquad (9\text{-}2)$$

Where:

L_t = tangent runout
e_{nc}= normal crown superelevation

All other variables have been previously defined. Two thirds of the superelevation runoff and the whole tangent runout distance are then added together to produce a transition length, which can then be added to or subtracted from milepost values to have curves with transition segments included. New curve lengths are then calculated. The user is able to choose whether or not transition lengths are included by checking a box on the lower right-hand corner of the interface.

9.2.5 Crash Data Combination

The crash data are then combined with the roadway data by looping through each segment and determining the number of crashes that have occurred within the curve. This is done by comparing the mile point of a crash to the beginning and ending mile points of a curve. The number of crashes per segment is determined by counting the number of crashes with a mile point that is between the beginning and end of a curve. The number of severe crashes is determined by the user selecting a minimum UDOT crash severity level to be considered "severe."

After the number of total and severe crashes has been counted for each segment, the total and severe crash rates are calculated as the number of crashes/1 million VMT. This is done using the formula outlined in Equation 9-3.

$$R = \frac{C \times 10^6}{365VNL} \tag{9-3}$$

Where:

R = total or severe crash rate
C = number of total or severe crashes in a given segment
V = the average AADT for the six years' worth of data
N = the number of years included in the data (typically six)
L = the segment length in miles.

Because intersections have a tendency to skew results to some degree as crashes occur more frequently near intersections, code was added to the program to show the user the total and severe crash rates with and without intersection-related crashes. From here, the user can sort the data to eliminate crashes in intersections from consideration.

In the output file, the user is able to order the segments however they like and apply constraints such as looking at curves only in a particular region. This requires some knowledge of Excel and the ability to use Excel's sort and filter functions.

9.3 Crash Analysis

This section contains lists of curves with crash histories, as well as examples of a few curves of interest that had particularly high crash rates. Lists of curves ordered by the total crash rate and severe crash rate are included, as well as a list that includes superelevation transition segments in the total curve length and a list that applies a threshold to remove segments with low traffic volumes from consideration. In the examples of curves with high crash occurrences, the crash type and information about each curve are included in the analysis.

9.3.1 Segments Ordered by Severe Crash Rate

Lists of segments with the highest crash rates were generated following the creation of the output file. In this case, a severe crash is considered to be any crash with a level 3 or higher UDOT severity ranking. The UDOT severity ranking system is presented in **Error! Reference source not found.**. A rating of 1 is applied to crashes with no injury, while a rating of 5 is applied to crashes with at least one fatality.

Table 9.1 UDOT Severity Ranking

Severity Ranking	Description
1	Non-injury
2	Possible injury
3	Non-incapacitating evident injury
4	Incapacitating injury
5	Fatal

One of these lists is shown in Table 9.2, which contains details about the 20 curves with the highest severe crash rates in the state of Utah, including location information, VMT, and crash data. The presence of intersections does not affect the ranking. Segments highlighted in green will be analyzed further in this chapter on an individual basis. At least one segment of interest from each UDOT Region is included in this section. The severe crash rate is expressed in terms of the number of severe crashes per 1 million VMT. It is worth pointing out that several of these segments in Table 9.2 made this list due to extremely low AADT values paired with a single crash. This is particularly the case along SR-153, which is an unpaved mountain road in Beaver County.

Table 9.2 Curves Organized by Severe Crash Rate

Route	Beg MP	Length (mi)	County	Region	VMT (/day)	Total # of Crashes	# of Severe Crashes	Severe Rate (#/MVMT)	Segment #
0066	2.469	0.074	Morgan	1	33	3	3	45.9	1
0095	48.868	0.066	San Juan	4	11	1	1	45.4	
0066	4.944	0.082	Morgan	1	36	4	3	41.4	
0092	18.548	0.044	Utah	3	29	2	2	41.4	
0123	11.322	0.079	Carbon	4	13	1	1	38.5	
0153	3.645	0.059	Beaver	4	13	1	1	35.6	
0226	0.446	0.058	Weber	1	14	1	1	35.1	
0066	1.978	0.036	Morgan	1	16	1	1	31.5	
0153	10.046	0.07	Beaver	4	16	1	1	30.0	
0144	2.079	0.046	Utah	3	17	2	1	29.4	
0144	0.008	0.047	Utah	3	18	4	1	28.8	
0153	13.396	0.077	Beaver	4	17	1	1	27.3	
0072	31.03	0.166	Sevier	4	19	1	1	27.1	
0153	10.263	0.081	Beaver	4	18	1	1	25.9	
0012	40.771	0.157	Garfield	4	120	9	7	24.9	2
0072	10.002	0.182	Sevier	4	21	2	1	24.7	
0035	18.541	0.218	Wasatch	3	86	5	5	24.6	3
0022	4.432	0.092	Garfield	4	21	1	1	24.4	
0035	44.852	0.082	Duchesne	3	42	3	2	23.0	
0035	5.939	0.082	Summit	2	64	4	3	22.5	4

A discussion of applied constraints to eliminate segments like these is presented later in Section 9.3.4. For this reason, only segments with at least three severe crashes will be analyzed individually in this section. The vast majority of the curves listed are along TLTW rural highways. VMT numbers are low because of short segment lengths.

The following sections contain descriptions of the segments highlighted in green in Table 9.2. They include additional information about the types of crashes that were typical of the curve, as well as images of the curves and details about their properties and locations.

9.3.1.1 Segment 1: SR-66, MP 2.47, Morgan – Region 1

Figure 9.3 contains images of a curve located just above East Canyon Reservoir near Morgan. The curve in question is highlighted in yellow. Three crashes occurred on this curve between the years of 2010 and 2015, and all of them were severe. The image on the top right-hand corner shows that it is a blind curve with a steep cut on one side and a steep drop-off with a guardrail on the other. Overturn/rollover crashes accounted for two out of the three crashes. There are presently no curve advisory signs warning drivers of the curve. As illustrated by the red dots in the lower left-hand corner of Figure 9.3, all crashes on this segment occurred in the middle of the curve at approximately the same location.

9.3.1.2 Segment 2: SR-12, MP 40.77, Escalante – Region 4

Figure 9.4 contains images of a compound curve located along SR-12 between Henrieville and Escalante. This particular curve had nine crashes between the years of 2010 and 2015, seven of which were classified as severe. While there were no fatalities, five crashes involved incapacitating injuries, most of which were motorcycle-related. This location has two sharp, blind curves directly adjacent to each other. A steep, tall cut exists on one side with a steep drop off on the other, partially protected by a guardrail. There is also a grade on this curve. While there are chevron signs along the outside of the curve, there are no advanced warning or advisory speed signs. Roadway departure was the most common type of crash.

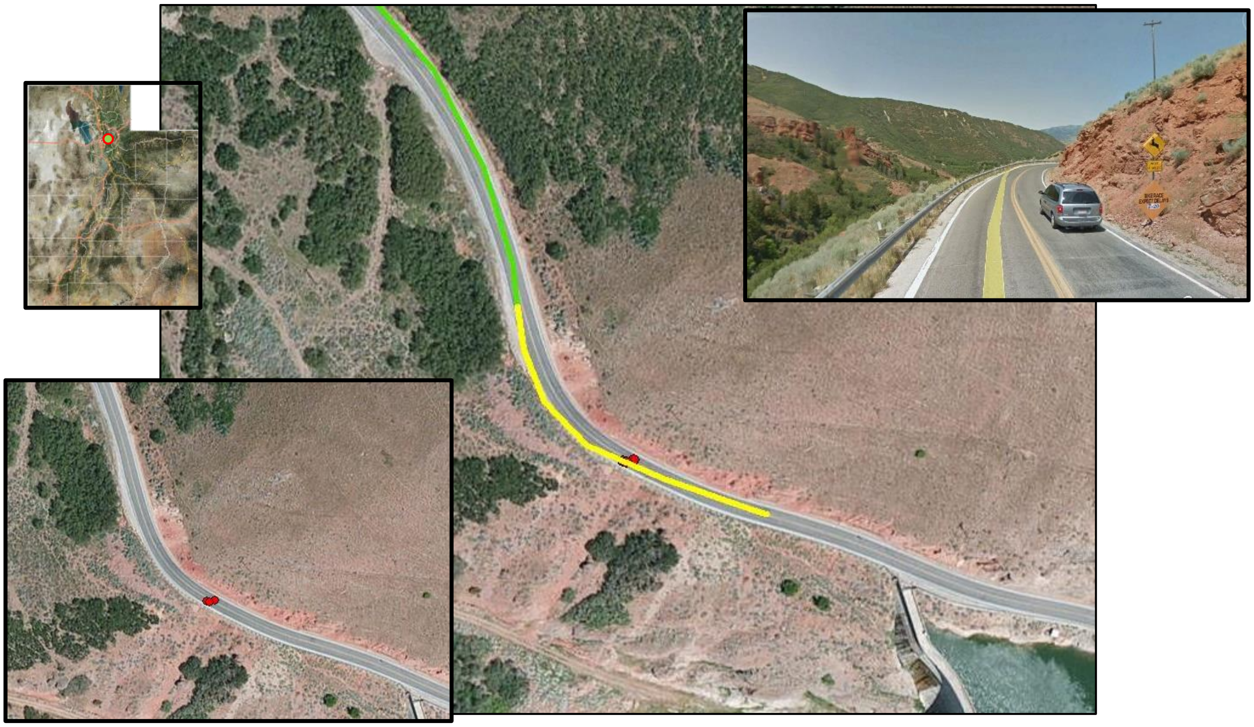

Figure 9.3 Segment 1: SR-66, MP 2.47, Morgan – Region 1 (Esri 2017, Google 2017, and UDOT 2017)

Figure 9.4 Segment 2: SR-12, MP 40.77, Escalante – Region 4 (Esri 2017, Google 2017, and UDOT 2017)

9.3.1.3 Segment 3: SR-35, MP 18.54, Wolf Creek Pass – Region 3

Figure 9.5 contains images of a curve near Wolf Creek Pass, just south of the Uinta mountain range. This particular curve lies in Region 3. Five severe crashes (also five total) crashes have occurred at this location between the years of 2010 and 2015. As can be seen, this is a horseshoe curve with chevron signs marking the outer edge. Curve advisory speed signs indicating a curve were present as of 2015. A noticeable grade is also present. Driving under the influence (DUI) and high speed were involved in some crashes, and many of the crashes were also motorcycle-related.

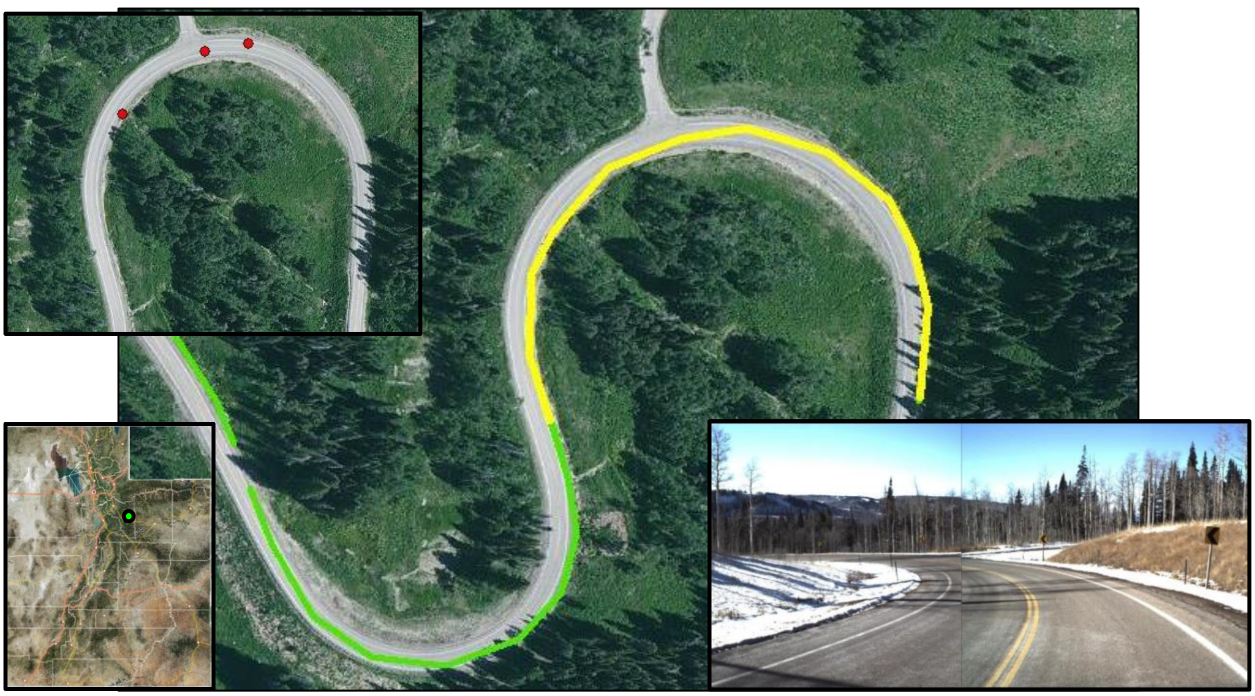

Figure 9.5 Segment 3: SR-35, MP 18.54, Hanna – Region 3 (Esri 2017, UDOT 2015, and UDOT 2017)

9.3.1.4 Segment 4: SR-35, MP 5.939, Francis – Region 2

Figure 9.6 shows a curve located near Francis, in Region 2. Out of four total crashes between 2010 and 2015, three were considered to be severe. While this is a gradual curve, the steep cut on the inside makes it a blind curve. Trees line the outside of the curve close to the roadway. According to AGRC crash data (crashmapping.utah.gov), some crashes involved trees or shrubbery (UDOT 2015). DUI, high speed, and adverse road conditions were also common contributing factors.

Figure 9.6 Segment 4: SR-35, MP 5.939, Francis – Region 2 (Esri 2017, UDOT 2015, and UDOT 2017)

9.3.1.5 Segment 5: SR-171, MP 8.728, West Valley City

Figure 9.7 contains images of a gradual curve at the intersection of 3300 South and Cultural Center Drive, West Valley City. This segment was not listed in Table 9.2 because it did not have a high enough crash rate to be listed in the top 20 curves. However, it was deemed worthy of further analysis because it is the curve with the highest severe crash rate out of any urban area. The crash rate is 11.2 severe crashes/1 million VMT, with a total of 25 severe crashes between 2010 and 2015. The vast majority of crashes were intersection-related.

Figure 9.7 Segment 5: SR-171, MP 8.728, West Valley City (Esri 2017, Google 2017, and UDOT 2017)

9.3.2 Segments Ordered by Total Crash Rate

Table 9.3 contains a list of the top 20 segments organized by total crash rate, expressed in terms of total crashes per 1 million VMT. This list includes curves affected by intersections. There is some overlap between segments listed in Table 9.2 and Table 9.3. However, most curves are unique to their respective tables. The segments highlighted in green will again be analyzed. Table 9.3 is more affected by intersections than Table 9.2 and it also contains curves located in urban areas. SR-153 in Beaver is a particular standout in this list again, primarily because it experiences very little traffic and its low AADT values have a tendency to exaggerate the total crash rate. For this reason, it will not be examined further in this report.

Table 8.9 Curves Organized by Total Crash Rate

Route	Beg MP	Length (mi)	County	Region	VMT (/day)	Total # of Crashes	# of Severe Crashes	Total Rate (#/MVMT)	Segment #
0153	22.894	0.043	Piute	4	1	1	0	490.1	
0153	21.953	0.121	Piute	4	3	1	0	174.2	
0144	0.008	0.047	Utah	3	18	4	1	115.1	
0153	37.891	0.204	Piute	4	5	1	0	103.3	
0057	2.982	0.091	Emery	4	13	2	0	74.3	
0030	121.383	0.122	Rich	1	99	13	4	62.7	6
0102	10.449	0.048	Box Elder	1	18	3	1	61.7	
0029	9.589	0.035	Emery	4	9	1	0	59.5	
0092	21.956	0.046	Utah	3	30	3	0	59.4	
0144	2.079	0.046	Utah	3	17	2	1	58.8	
0066	4.944	0.082	Morgan	1	36	4	3	55.2	
0161	2.79	0.039	Millard	4	4	1	0	55.1	
0029	5.848	0.04	Emery	4	11	1	0	52.1	
0072	10.002	0.182	Sevier	4	21	2	1	49.4	
0101	14.093	0.044	Cache	1	18	2	0	48.2	
0153	7.258	0.044	Beaver	4	10	1	0	47.7	
0065	14.396	0.043	Morgan	1	17	2	0	47.6	
0066	2.469	0.074	Morgan	1	33	3	3	45.9	
0095	48.868	0.066	San Juan	4	11	1	1	45.4	
0022	3.994	0.051	Garfield	4	11	1	0	44.0	

9.3.2.1 Segment 6: SR-30, MP 121.38, Laketown

Figure 9.8 shows a curve located near Bear Lake in Region 1. This is a 90-degree blind curve with steep cuts on both sides and a runaway truck ramp tangent to it. A 7 percent grade exists south of the curve. Thirteen crashes occurred along this curve between 2010 and 2015, primarily at the beginning and end points. Roadway departure and overturn/rollover were the most common crash types. Many were motorcycle-related and speed-related and some occurred in adverse weather conditions. Chevron and curve advisory speed signs are present. The advisory speed is 30 mph for traffic going east and south (uphill), while the advisory speed is 20 mph for traffic going north and west (downhill).

Figure 9.8 Segment 6: SR-30, MP 121.38, Laketown (Esri 2017, Google 2017, and UDOT 2017)

9.3.3 Segments Ordered by Severe Crash Rate with Superelevation Transition

Table 9.4 is similar to Table 9.2 in that it contains a list of the curves with the highest severe crash rates. The difference is that the curves listed in Table 9.4 add superelevation transition segments to the total curve length, increasing the potential for more crashes to be included within the curves. Segments highlighted in blue match those listed in Table 9.2, so as to provide an idea of how much including superelevation transition segments alters the ranking.

Three of the curves in Table 9.4 are not listed in Table 9.2. The segment highlighted in green will be examined further in this section.

9.3.3.1 Segment 7: SR-68, MP 11.74, Elberta

Figure 9.9 shows a curve on the southwest side of Utah Lake near Elberta, in Region 3. Eight severe crashes occurred either on the curve or in the superelevation transition segments between 2010 and 2015. As shown in the lower right-hand corner of the figure, many of the crashes occurred at the beginning and end of the curve. This is why this particular segment was not ranked in the 20 curves with the highest severe crash rate. The most common crash types were road departure and overturn/rollover. This curve is located after a particularly long straight segment, possibly catching drivers unaware. There are curve advisory speed signs located on both ends of the curve. Speed-related crashes were common, and many involved either motorcycles or commercial vehicles. Adverse weather conditions were also a factor.

Table 9.4 Curves Organized by Severe Crash Rate with Superelevation Transition

Route	Beg MP	Length (mi)	County	Region	VMT (/day)	Total # of Crashes	# of Severe Crashes	Severe Rate (#/MVMT)	Segment #
0095	48.855	0.091	San Juan	4	11	1	1	32.9	
0066	2.45	0.113	Morgan	1	33	3	3	30.2	
0153	3.624	0.084	Beaver	4	11	1	1	25.5	
0066	4.918	0.134	Morgan	1	36	4	3	25.3	
0092	18.533	0.073	Utah	3	29	3	2	24.8	
0123	11.198	0.126	Carbon	4	13	1	1	24.2	
0144	2.07	0.063	Utah	3	17	2	1	21.4	
0072	31.006	0.213	Sevier	4	19	1	1	21.1	
0057	3.487	0.161	Emery	4	18	1	1	21.0	
0153	10.031	0.1	Beaver	4	16	1	1	20.9	
0035	18.517	0.267	Wasatch	3	86	5	5	20.2	
0153	10.251	0.106	Beaver	4	18	1	1	19.8	
0012	40.74	0.198	Garfield	4	120	9	7	19.7	
0153	13.381	0.107	Beaver	4	17	1	1	19.6	
0068	11.74	0.163	Utah	3	127	13	8	19.4	7
0226	0.422	0.105	Weber	1	14	1	1	19.4	
0072	9.977	0.233	Sevier	4	21	2	1	19.3	
0144	0.0	0.076	Utah	3	18	4	1	17.8	
0226	0.485	0.119	Weber	1	18	1	1	17.2	
0066	1.999	0.123	Morgan	1	16	1	1	17.1	

Figure 9.9 Segment 7: SR-68, MP 11.74, Elberta (Esri 2017, Google 2017, and UDOT 2017)

9.3.4 Example of Using Filtering Constraints

A problem with these lists is that curves with very little traffic sometimes pair with a single severe crash that causes their crash rate to rank highly. One possible solution to this problem would be to apply constraints to eliminate segments with very few crashes from consideration. This would be up to the user's discretion. This technique is effective in filtering out curves that are ranked highly due to low VMT values. Table 9.5 contains a list of segments organized by severe crash rate with a minimum number of three severe crashes per segment. This was done using Microsoft Excel's Filter tool by unchecking boxes next to 0, 1, and 2 for the severe crash column. Segments highlighted in blue are also included in Table 9.2, which does not apply the constraint. Segments highlighted in green are discussed further.

Table 9.5 Curves Organized by Severe Crash Rate with Constraint

Route	Beg MP	Length (mi)	County	Region	VMT (/day)	Total # of Crashes	# of Severe Crashes	Severe Rate (#/MVMT)	Segment #
0066	2.469	0.074	Morgan	1	33	3	3	45.9	
0066	4.944	0.082	Morgan	1	36	4	3	41.4	
0012	40.771	0.157	Garfield	4	120	9	7	24.9	
0035	18.541	0.218	Wasatch	3	86	5	5	24.6	
0035	5.939	0.082	Summit	2	64	4	3	22.5	
0068	11.876	0.089	Utah	3	110	9	5	22.2	
0039	42.992	0.143	Weber	1	68	3	3	21.8	
0030	121.383	0.122	Rich	1	99	13	4	19.3	
0092	13.911	0.217	Utah	3	142	4	4	16.8	
0171	8.728	0.035	Salt Lake	2	1065	73	25	11.2	
0006	143.657	0.093	Utah	3	129	4	3	11.1	8
0313	18.965	0.137	Grand	4	177	4	3	9.0	
0068	21.487	0.186	Utah	3	230	5	4	8.5	
0006	143.358	0.13	Utah	3	180	4	3	7.9	9
0006	143.122	0.233	Utah	3	323	11	5	7.4	10
0224	4.638	0.052	Summit	2	246	28	5	7.2	
0014	12.988	0.186	Iron	4	304	6	4	6.9	
0190	6.124	0.082	Salt Lake	2	276	10	3	6.0	
0039	24.987	0.217	Weber	1	339	5	4	5.9	
0190	3.948	0.057	Salt Lake	2	294	14	3	5.6	

Only the top five segments in Table 9.5 are listed in Table 9.2. A few urban segments make the list in Table 9.5 now that there is a minimum crash number criterion. Curves from Region 3 now account for 35 percent of the segments listed in Table 9.5 and curves from Region 4 now make up 15 percent. In Table 9.2, curves from Region 3 make up 25 percent and Region 4 makes up 50 percent. This illustrates that different constraints yield quite different results.

9.3.4.1 Segments 8, 9, and 10: US-6, MP 143.12-143.75, Eureka

Figure 9.10 contains images of three curves; all of them lie within close proximity of each other along US-6 between Eureka and Goshen. These curves warranted a closer look because all of them separately make the list of segments in Table 9.5. This section of road contains sharp, winding curves with a steep grade. While some advisory signs do exist, a total of 11 severe crashes occurred between the years of 2010 and 2015. The crash types were most commonly overturn/rollover or roadway departure. Eastbound drivers encounter a steep downgrade and must slow down carefully while navigating consecutive curves.

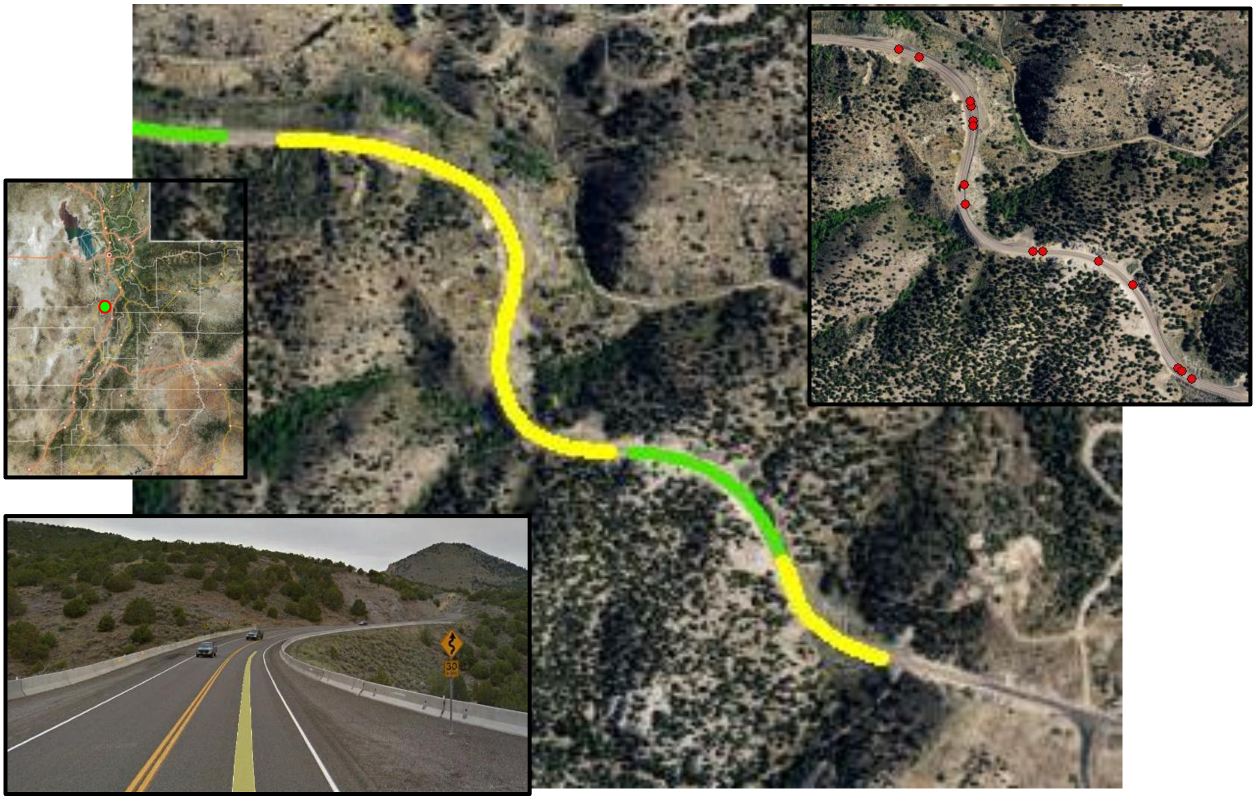

Figure 9.10 Segments 8, 9, and 10: US-6, MP 143.12-143.75, Eureka (Esri 2017, Google 2017, and UDOT 2017)

9.4 Chapter Summary

Table 9.2 through Table 9.5 show that TLTW rural highway curves frequently show up in lists of curves organized by crash rates. The analysis presented in this chapter shows that many severe injuries stem from motorcycle-related crashes. Additionally, the most common types of crashes for curves with high crash rates without intersections appear to be roadway departure and overturn/rollover. Blind curves were also present in many of the curves analyzed. Interestingly, no interstates made the lists of curves with the highest crash rate, likely due to high traffic volumes. While curves with intersections were included in these lists, the user could also order segments by crash rate without intersections if they wished.

The program to combine crash data with curve data works well. Curves with high crash occurrences can be identified in order to make improvements to them. Additionally, particular attributes of different curves can be analyzed to identify correlations between a certain property and crashes. Curves with the highest severe crash rates often had several motorcycle-related crashes, which is something that could be explored further. The program provides flexible filtering options and choices for analyzing curves.

10.0 CONCLUSIONS AND RECOMMENDATIONS

10.1 Summary

This research was effective in testing and improving the original HAF Algorithm, as well as combining curve data with crash data. The study objectives were met, including testing the HAF Algorithm's ability to cover types of highways other than rural TLTW, improving its accuracy, combining curve data with crash data to identify highway curves with high crash occurrences, and combining curve data with roadway parameters such as radius, curve length, AADT, and other fields to aid in future analysis. The HAF Algorithm was tested for other (i.e. non-TLTW) highway types by comparing the calculated results to results obtained by measuring curve parameters using satellite imagery. The algorithm was improved by making changes to the code that targeted a few specific errors and updating the code to make it compatible with more recent data. Finally, a VBA program was developed to combine curve data with crash data and other roadway parameters like AADT, functional class, speed limit, urban code, and the number of lanes.

Included in this chapter are a summary of the findings and some limitations inherent with the raw LiDAR data and the HAF Algorithm.

10.2 Findings

This section contains research findings, separated into three parts: (1) results of the HAF Algorithm calibration to determine whether it works across all highway types, (2) results of the improved HAF Algorithm accuracy compared to the original algorithm, and (3) an outline of the findings from the curve and crash data combination.

10.2.1 Results of HAF Algorithm Tests for Other Highway Types

After an initial calibration phase, it was determined that the HAF Algorithm did not need to be modified to accommodate types of highways other than rural TLTW. Curve identification accuracy ranged from 71-96 percent, depending on highway type. Additionally, curve length calculation accuracy ranged from 91-96 percent.

10.2.2 Results of HAF Algorithm Improvements

Six specific errors were targeted to improve the HAF Algorithm – tangent-curve-tangent, tangent identification, curve fragment, curve length calculation, intersection identification, and compound curve errors. The details of these errors are explained in depth in Chapter 5. Intersection, curve fragment, and curve length calculation errors were reduced significantly, while the tangent fix was less effective. The compound curve error was reduced by changing the calibration process to allow for compound curves, and the tangent-curve-tangent error could not be resolved due to problems with the raw LiDAR data.

Curve identification accuracy now ranges from 87 to near 100 percent, depending on highway type. These improvements are due primarily to resolving curve fragment and intersection identification errors. Curve length calculation accuracy now lies within 97-98 percent. At this point, human error in the calibration process has the potential to affect these results, so no further improvement to curve length calculation is warranted. The elimination of the arc length calculation error was one of the primary causes of this improvement. Radius accuracy could not be improved due to the limitations of the input data. Additionally, as part of the process of improving the HAF Algorithm, changes were made to the code and interface to allow the program to run 2015 data.

10.2.3 Curve Data/Crash Data Combination

The new VBA program written to combine curve data with crash data was successful. Each curve segment lists the total number of crashes and the number of crashes in each severity type that occurred within a specified time span as well as their respective crash rates. Additionally, roadway data such as AADT, functional class, speed limit, urban code, and lanes have been effectively combined in order to display the roadway parameters associated with each curve. Superelevation transition segments can also be accounted for in the new algorithm.

10.3 Limitations and Challenges

There are still some limitations to the accuracy of the HAF Algorithm despite the improvements made in this research. The algorithm itself can only be as accurate as the data inputs. While the provided LiDAR data are very accurate, there are occasional issues that surface, particularly in determining the start and end points of each segment. This was primarily responsible for the tangent-curve-tangent error, which the algorithm was not able to overcome because it cannot divide individual segments. Additionally, improving radius calculation accuracy is difficult due to errors in the data. These types of errors are likely to be reduced best by trying to obtain more accurate input data in the future.

10.4 Recommendations

Possibilities exist for this research to be furthered. For example, the radius calculation has room for improvement. While improving the radius calculation accuracy in the HAF Algorithm itself may not be possible, further research could be done into developing a tool in ArcMap that automatically calculates curve radius. This would likely require advanced Python scripting, but it may be possible.

Further research could also be done into motorcycle related crashes. Many of the segments listed in Chapter 9 had high numbers of severe motorcycle related crashes. This type of research could provide a basis on which to identify motorcycle safety improvements.

Additionally, further research could be done into common causes of crashes along Utah highway curves. While curves with worse crash histories have been identified, no statistical analysis has been done to determine which curve parameters correlate with higher crash rates. This would certainly be worthy of a study of its own as it has the potential to aid UDOT in constructing and maintaining safer highway curves. Because several parameters are affixed to each curve in the output of the new VBA program, this research provides a good starting point from which to do further analysis of crashes on curves.

REFERENCES

AASHTO (American Association of State Highway and Transportation Officials). (2011). "A Policy on Geometric Design of Highways and Streets." *GDHS-6*, Washington, D.C.

Ai, C., and Tsai, Y. (2015). "Automatic Horizontal Curve Identification and Measurement Method Using GPS Data." *Journal of Transportation Engineering*, 10.1061/(ASCE)TE.1943-5436.0000740.

Andrášik, R., and Bíl, M. (2016). "Efficient Road Geometry Identification from Digital Vector Data." *Journal of Geographical Systems*, 18(3), 249-264.

Andrášik, R., Bíl, M., Janoška, Z., and Valentová, V. (2013). "Identification of Curves and Straight Sections on Road Networks from Digital Vector Data." *Transactions on Transport Sciences*, 6, 73-80.

AutoCAD 2017. (2017). "AutoCAD 2017 Display." Autodesk.

Bassani, M., Marinelli, G., and Piras, M. (2016). "Identification of Horizontal Circular Arc from Spatial Data Sources." *Journal of Surveying Engineering*, 10.1061/(ASCE)SU.1943-5428.0000186.

Ben-Arieh, D., Chang, S., Rys, M., and Zhang, G. (2004). "Geometric Modeling of Highways Using Global Positioning System Data and B-Spline Approximation." *Journal of Transportation Engineering*, 10.1061/(ASCE)0733-947X(2004)130:5(632).

Bogenreif, C., Souleyrette, R. R., and Hans, Z. (2012). "Identifying and Measuring Horizontal Curves and Related Effects on Highway Safety." *Journal of Transportation Safety & Security*, 4(3), 179-192.

Camacho-Torregrosa, F. J., Perez-Zuriaga A. M, Campoy-Ungria, J. M., Garcia, A., and Tarko, A. P. (2015). "Use of Heading Direction for Recreating the Horizontal Alignment of an Existing Road." *Computer-Aided Civil and Infrastructure Engineering*, 30, 282-299.

Carlson, P. J., Burris, M., Black, K., and Rose, E. R. (2005). "Comparison of Radius-Estimating Techniques for Horizontal Curves." *Transportation Research Record,* 1918, 76-83.

Castro, M., Iglesias, L., Rodriguez-Solano, R., and Sanchez, J. A. (2006). "Geometric Modelling of Highways Using Global Positioning System (GPS) Data and Spline Approximation." *Transportation Research Part C: Emerging Technologies,* 14(4), 233-243.

Cook, A. A., Saito, M., and Schultz, G. G. (2015). "A Heuristic Approach for Identifying Horizontal Curves and their Parameters Given LiDAR Point Cloud Data." *Transportation Research Record,* 2521, 22-30.

Dong, H., Easa, S., and Li, J. (2007). "Approximated Extraction of Spiraled Horizontal Curves from Satellite Imagery." *Journal of Surveying Engineering,* 10.1061/(ASCE)0733-9453(2007)133:1(36).

Easa, S. M., Dong, H., and Li, J. (2007). "Use of Satellite Imagery for Establishing Road Horizontal Alignments." *Journal of Surveying Engineering,* 10.1061/(ASCE)0733-9453(2007)133:1(29)

Ellsworth, P. (2013). "Utah DOT Leveraging LiDAR for Asset Management Leap." In the *UDOT Transportation Blog.* <https:// udot.utah.gov/public/ucon/uconowner.gf?n=8336606666333974>

Esri ArcMap 10.5. (2017). “World Imagery.” *Esri.*

Garach, L., De Oña, J., and Pasadas, M. (2014). "Mathematical Formulation and Preliminary Testing of a Spline Approximation Algorithm for the Extraction of Road Alignments." *Automation in Construction,* 47, 1-9.

Google Earth. (2017). “Utah.” *Google.*

Green, E. R., Agent, K. R., and Lammers, E. (2017). "Development of an Improved Method for Determining Advisory Speeds on Horizontal Curves." In *Compendium of the 2017 Annual Meetings,* Transportation Research Board, Washington, D.C.

Higuera de Frutos, S. and Castro, M. (2014). "Using Smartphones as a Very Low-Cost Tool for Road Inventories." *Transportation Research Part C: Emerging Technologies,* 38, 136-145.

Imran, M., Hassan, Y., and Patterson, D. (2006). "GPS--GIS-Based Procedure for Tracking Vehicle Path on Horizontal Alignments." *Computer-Aided Civil and Infrastructure Engineering*, 21, 383-394.

Jiménez, F. (2011). "Improvements in Road Geometry Measurement Using Inertial Measurement Systems in Datalog Vehicles." *Measurement,* 44(1), 102-112.

Jiménez, F., Aparcio, F., and Estrada, G. (2009). "Measurement Uncertainty Determination and Curve-Fitting Algorithms for Development of Accurate Digital Maps for Advanced Driver Assistance Systems." *Transportation Research Part C: Emerging Technologies,* 17(3), 225-239.

Kim, J., Lee, J., Kang, I., Cha, S., Choi, H., and Lee, T. (2008). "Extraction of Geometric Information on Highway Using Terrestrial Laser Scanning Technology*." Beijing: The International Archives of the Photogrammetry, Remote Sensing and Spatial Information Sciences*, 539-544.

Li, Z., Chitturi, M., Bill, A., and Noyce, D. (2012). "Automated Identification and Extraction of Horizontal Curve Information from GIS Roadway Maps." *Transportation Research Record*, 2291, 80-92.

Li, Z., Chitturi, M. V., Bill, A. R., Zheng, D., and Noyce, D. A. (2015). "Automated Extraction of Horizontal Curve Information for Low-Volume Roads." *Transportation Research Record*, 2472, 172-184.

Luo, W., Li, L., and Wang, K. C. (2016). "Automated Pavement Horizontal Curve Measurement Methods Based on Inertial Measurement Unit and 3D profiling Data." *Journal of Traffic and Transportation Engineering (English Edition),* 3(2), 137-145.

Osei-Asamoah, A. and Jackson, E. (2015). "Automated Horizontal Curve Classification and Parameter Calculation Methods Using Vehicle Collected Road Inventory Data." In *Compendium of the 2015 Annual Meeting*, Transportation Research Board, Washington, D.C.

Santiago-Chaparro, K. R., Chitturi, M. V., Bill, A. R., Noyce, D. A. (2012). "Using Existing Datasets to Automate Identification of No-Passing Zones on Vertical Curves." In *Compendium of the 2012 Annual Meeting*, Transportation Research Board, Washington, D.C.

Schultz, G. G., Seat, M. L., Saito, M., and Clegg, W. (2017). "Using LiDAR Data to Analyze Access Management Criteria in Utah." Utah Department of Transportation, Report No. UT-17.09.

Svenson, G., Flisberg, P., and Rönnqvist, M. (2016). "Using Analytics in the Implementation of Vertical and Horizontal Curvature in Route Calculation." *IEEE Transactions on Intelligent Transportation Systems*, 17(6), 1772-1785.

Tong, X., Meng, X., and Ding, K. (2010). "Estimating Geometric Parameters of Highways and Railways Using Least-Squares Adjustment." *Survery Review*, 42(318), 359-374.

Tsai, Y. J., Wu, J., Wang, Z., and Hu, Z. (2010). "Horizontal Roadway Curvature Computation Algorithm Using Vision Technology." *Computer-Aided Civil and Infrastructure Engineering*, 25(2), 78-88.

UDOT (Utah Department of Transportation). (2017). “Functional Classification Maps.” <https://udot.utah.gov/main/f?p=100:pg:0::::V,T:,1224>

UDOT (Utah Department of Transportation). (2017). “UDOT Data Portal.” <http://data-uplan.opendata.arcgis.com>

UDOT (Utah Department of Transportation). (2015). “Utah Vehicle Collisions.” <http://crashmapping.utah.gov/>

UDOT (Utah Department of Transportation). (2012). “Project Design Criteria Form.” <https://udot.utah.gov/main/f?p=100:pg:0:::1:T,V:1560,>

Williams, C. and Hawkins, H. G. (2011). "Field Location and Marking of No-Passing Zones Due to Vertical Alignments Using the Global Positioning System." In *Compendium of the 2011 Annual Meeting*, Transportation Research Board, Washington, D.C.

Xu, H., and Wei, D. (2016). Improved Identification and Calculation of Horizontal Curves with GIS Road Layers. *Transportation Research Record*, 2595, 50-58.

APPENDIX A: HAF CALIBRATION DATA

This appendix includes data that were used for the HAF calibration portion of the project. This table includes comparisons of the measured and HAF-calculated results for each highway type. The results include curve length, radius, and percent error for the original algorithm, and the data used were obtained from 2012 Mandli data.

Table A.1 contains the calibration results for urban interstates, Table A.2 contains results for rural interstates, Table A.3 contains results for urban multilane highways, Table A.4 contains results for rural multilane highways, Table A.5 contains results for urban TLTW highways, and Table A.6 contains results for rural TLTW highways.

Table A.1 Urban Interstate Calibration.

					RADIUS			CURVE LENGTH		
#	ID	Route Name	PC	PT	AutoCAD	ArcMap	Error %	AutoCAD	ArcMap	Error %
1	320696	0015P	258.0	258.5	2940	-3089	5.1%	2900	2916	0.6%
2	320710	0015P	267.3	267.6	1794	-2148	19.7%	1460	1521	4.1%
3	316369	0215N	7.6	7.4	1922	2802	45.8%	877	808	7.8%
4	296796	0084N	81.8	81.6	2308	2997	29.9%	1041	1086	4.3%
5	321167	0015N	267.5	267.2	1740	2226	27.9%	1531	1560	1.9%
6	316402	0215N	0.6	0.3	2454	-2440	0.6%	1645	1727	4.9%
7	316323	0215N	22.8	22.7	2547	4806	88.7%	691	711	2.9%
8	320716	0015P	270.0	270.4	3055	4182	36.9%	1841	1775	3.6%
9	320508	0015P	0.0	0.1	3173	5005	57.7%	631	674	6.8%
10	316352	0215N	11.4	11.3	3124	2247	28.1%	527	535	1.4%
11	321068	0015N	307.1	306.8	1878	2040	8.7%	1627	1649	1.4%
12	295990	0080P	124.6	124.7	4380	5034	14.9%	519	497	4.2%
13	316284	0215P	13.7	14.6	3213	3236	0.7%	4857	4859	0.1%
14	316311	0215P	28.3	28.9	1545	-2312	49.7%	3405	3296	3.2%
15	321031	0015N	318.7	318.5	1854	2730	47.2%	881	951	7.9%
16	320518	0015P	5.8	6.8	5341	5082	4.8%	4941	4897	0.9%
17	320707	0015P	266.8	267.2	2400	2485	3.6%	1704	1664	2.4%
18	320510	0015P	2.9	3.0	3916	-935	76.1%	757	1598	111.1%
19	322474	0080N	119.6	119.3	854	-935	9.4%	1684	1598	5.1%
20	316404	0215N	0.3	0.2	2028	2541	25.3%	714	672	5.9%
21	320748	0015P	286.0	286.4	2533	3600	42.2%	2121	2044	3.6%
22	296526	0084P	88.9	89.1	1639	-2079	26.8%	969	1006	3.8%

					RADIUS			CURVE LENGTH		
#	**ID**	**Route Name**	**PC**	**PT**	**AutoCAD**	**ArcMap**	**Error %**	**AutoCAD**	**ArcMap**	**Error %**
23	321063	0015N	307.8	307.7	1467	2514	71.4%	547	498	8.9%
24	296798	0084N	81.2	80.9	2652	2847	7.3%	1724	1751	1.6%
25	321000	0015N	340.2	339.9	2801	-2955	5.5%	1890	1918	1.5%
26	295963	0080P	106.7	107.1	2252	2994	33.0%	2391	2299	3.8%
27	316321	0215N	26.5	26.3	3623	-4725	30.4%	1002	954	4.8%
28	320990	0015N	343.5	343.3	1712	2050	19.7%	982	918	6.4%
29	316252	0215P	3.9	4.1	1688	-2058	21.9%	1024	928	9.3%
30	320521	0015P	7.6	7.9	5103	-5120	0.3%	1321	1353	2.5%
31	321007	0015N	335.9	335.7	5480	4739	13.5%	645	644	0.2%
32	320694	0015P	257.6	257.6	5536	5231	5.5%	400	323	19.3%
33	316274	0215P	11.4	11.7	2833	2917	3.0%	1253	1261	0.6%
34	320998	0015N	340.7	340.6	2877	2908	1.1%	485	453	6.6%
35	316398	0215N	1.1	0.8	2299	2547	10.8%	1391	1390	0.1%
36	316317	0215N	27.4	27.2	1219	1309	7.4%	1327	1319	0.6%
37	296781	0084N	86.0	85.9	5379	4902	8.9%	780	705	9.6%
38	320778	0015P	299.2	299.6	3351	3213	4.1%	1928	1886	2.2%
39	320798	0015P	306.9	307.2	2208	2228	0.9%	1822	1799	1.3%
40	316340	0215N	13.3	12.9	2317	2371	2.3%	2224	2076	6.7%
41	320739	0015P	280.4	280.7	3358	3454	2.9%	2026	2002	1.2%
42	321145	0015N	272.5	272.9	3818	3686	3.5%	1867	2982	59.7%
43	296801	0084N	80.6	80.5	2166	2283	5.4%	485	496.5	2.4%
44	320880	0015P	340.7	340.8	2993	3464	15.7%	576	548	4.9%
45	316307	0215P	26.8	27.4	2922	3036	3.9%	3473	3454	0.5%
46	320516	0015P	4.5	4.9	2383	2476	3.9%	1731	1704	1.6%
47	296522	0084P	85.9	86.4	2922	3086	5.6%	2399	2420	0.9%
48	321015	0015N	329.6	329.3	4894	4652	4.9%	1555	1574	1.2%
49	320775	0015P	298.6	299.0	4638	4622	0.3%	2150	2183	1.5%
50	320853	0015P	326.6	326.6	5457	4015	26.4%	272	268	1.5%
51	316338	0215N	14.0	14.6	3317	3447	3.9%	3352	5056	50.8%
52	295979	0080P	119.6	119.8	1820	1946	6.9%	935	927	0.9%
53	321116	0015N	286.2	285.8	2769	2977	7.5%	1866	1889	1.2%
54	321080	0015N	303.3	303.1	3010	2964	1.5%	1022	997	2.4%
55	320994	0015N	342.5	341.8	2822	2819	0.1%	3558	3560	0.1%
56	320984	0015N	346.0	345.7	3772	4717	25.1%	1464	1426	2.6%
57	316278	0215P	12.1	12.7	3822	4321	13.1%	2850	2852	0.1%
58	316258	0215P	7.4	7.5	3047	2931	3.8%	877	862	1.7%
59	320893	0015P	346.4	346.7	3802	4306	13.3%	1284	1291	0.5%
60	321196	0015N	249.0	248.5	5975	5051	15.5%	2644	2616	1.1%
61	320864	0015P	329.5	329.7	5123	4631	9.6%	1472	1468	0.3%

					RADIUS			CURVE LENGTH		
#	**ID**	**Route Name**	**PC**	**PT**	**AutoCAD**	**ArcMap**	**Error %**	**AutoCAD**	**ArcMap**	**Error %**
62	316375	0215N	4.1	4.0	1943	1999	2.9%	1073	1041	3.0%
63	320977	0015N	350.6	350.4	5860	4892	16.5%	1264	1278	1.1%
64	296786	0084N	85.1	85.6	2870	3556	23.9%	2545	3202	25.8%
65	321011	0015N	330.7	330.4	2112	2174	2.9%	1688	1681	0.4%
66	296524	0084P	88.2	88.3	2850	2954	3.6%	813	790	2.8%
67	320523	0015P	8.7	9.3	3734	4055	8.6%	2778	2746	1.2%
68	316269	0215P	10.9	11.2	2051	2110	2.9%	1205	1183	1.8%
69	321378	0015N	6.8	5.9	5570	4954	11.1%	4457	4408	1.1%
70	316247	0215P	3.0	3.4	3969	4316	8.7%	1978	1953	1.3%
71	322476	0080N	118.8	118.7	3330	3011	9.6%	475	466	1.9%
72	321369	0015N	13.7	13.3	5603	5047	9.9%	2482	2499	0.7%
73	295999	0080P	127.1	127.4	1098	1267	15.4%	1284	1272	0.9%
74	316229	0215P	0.0	0.2	2166	2411	11.3%	888	1142	28.6%
75	320878	0015P	340.0	340.4	2745	2813	2.5%	1824	1833	0.5%
76	320861	0015P	328.9	329.3	2941	3095	5.2%	2481	2467	0.6%
77	322470	0080N	122.6	122.2	1052	1092	3.8%	1654	1760	6.4%
78	295971	0080P	118.1	118.3	3756	4720	25.7%	950	961	1.2%
79	316348	0215N	11.9	11.8	2786	3088	10.8%	750	732	2.4%
80	321181	0015N	264.5	264.4	4611	3511	23.9%	609	618	1.5%
81	320988	0015N	343.9	343.6	2056	2176	5.8%	1822	1796	1.4%
82	316315	0215N	28.8	28.4	1460	1452	0.5%	2011	2058	2.3%
83	320982	0015N	346.6	346.3	3872	4097	5.8%	1340	1341	0.1%
84	320703	0015P	264.5	264.6	3884	3930	1.2%	666	683	2.6%
85	316357	0215N	10.9	10.7	1933	2135	10.5%	1173	1159	1.2%
86	320824	0015P	312.4	312.8	2208	2390	8.2%	1824	1844	1.1%
87	321192	0015N	257.5	257.4	5999	4925	17.9%	479	456	4.8%
88	320792	0015P	304.2	304.3	2902	2847	1.9%	604	596	1.3%
89	320839	0015P	318.6	318.7	1644	1831	11.4%	977	996	1.9%
90	320813	0015P	310.4	310.5	5172	4624	10.6%	581	561	3.4%
91	320859	0015P	328.5	328.7	4646	4543	2.2%	1200	1197	0.3%
92	320770	0015P	297.9	298.0	5832	5244	10.1%	1001	979	2.2%
93	320512	0015P	3.6	3.9	5781	5398	6.6%	1102	1379	25.2%
94	322472	0080N	119.8	119.7	1169	1276	9.2%	668	666	0.3%
95	321021	0015N	327.2	327.0	3732	4362	16.9%	1341	1333	0.6%
96	316355	0215N	11.2	11.0	1831	1915	4.6%	1072	1084	1.2%
97	320735	0015P	279.8	280.1	3126	3273	4.7%	1779	1724	3.1%
98	320895	0015P	347.1	347.2	3797	4412	16.2%	744	696	6.4%
99	320811	0015P	309.7	310.0	2825	2838	0.4%	1310	1317	0.6%
100	321119	0015N	285.1	285.0	5144	5350	4.0%	578	561	3.0%

					RADIUS			CURVE LENGTH		
#	**ID**	**Route Name**	**PC**	**PT**	**AutoCAD**	**ArcMap**	**Error %**	**AutoCAD**	**ArcMap**	**Error %**
101	320730	0015P	278.1	278.3	5942	4600	22.6%	1227	1219	0.7%
102	321013	0015N	330.3	330.1	2106	2243	6.5%	1047	1067	1.9%
103	296003	0080P	127.9	128.1	2678	3258	21.7%	1280	1268	0.9%
104	322466	0080N	124.0	123.9	5120	5257	2.7%	397	404	1.7%
105	322460	0080N	126.1	125.9	2429	2473	1.8%	665	634	4.6%
106	316245	0215P	2.6	2.7	5226	4842	7.4%	502	493	1.8%
107	295975	0080P	118.7	118.8	2897	2934	1.3%	485	483	0.3%

Table A.2: Rural Interstate Calibration

					RADIUS			CURVE LENGTH		
#	**ID**	**Route Name**	**PC**	**PT**	**AutoCAD**	**ArcMap**	**Error %**	**AutoCAD**	**ArcMap**	**Error %**
1	294673	0070P	7.1	7.3	1313	1394	6.1%	1062	1091	2.7%
2	294683	0070P	11.5	11.9	1702	1908	12.1%	1484	1964	32.4%
3	294697	0070P	14.8	15.2	2100	2217	5.6%	2384	2370	0.6%
4	294727	0070P	24.2	24.7	2801	3036	8.4%	2722	2718	0.1%
5	294734	0070P	28.6	28.8	2889	3105	7.5%	1434	1351	5.8%
6	294747	0070P	32.6	32.8	2562	3024	18.0%	1247	1195	4.1%
7	294759	0070P	37.9	38.2	2405	2957	22.9%	1444	1382	4.3%
8	294772	0070P	47.6	47.7	1924	4674	143.0%	891	833	6.6%
9	294774	0070P	48.7	48.9	3632	4953	36.4%	1117	1324	18.6%
10	294799	0070P	60.9	61.2	2101	3079	46.5%	1554	1705	9.7%
11	294812	0070P	64.1	64.2	2969	3097	4.3%	607	606	0.2%
12	294834	0070P	67.7	67.9	3427	4444	29.7%	1171	1311	11.9%
13	294863	0070P	71.8	71.9	1715	3837	123.7%	546	363	33.6%
14	294871	0070P	72.7	72.9	2842	2991	5.2%	1546	1380	10.8%
15	294887	0070P	76.2	76.5	2064	2339	13.3%	1281	1294	1.0%
16	294896	0070P	79.0	79.2	2545	3209	26.1%	721	760	5.4%
17	294906	0070P	80.4	80.5	1957	1625	16.9%	516	515	0.1%
18	294918	0070P	82.6	83.0	2266	2450	8.1%	1699	1739	2.3%
19	294927	0070P	84.1	84.4	2791	3051	9.3%	1364	1483	8.7%
20	294932	0070P	84.7	84.8	1666	3211	92.8%	691	660	4.6%
21	294962	0070P	96.0	96.5	1548	1884	21.7%	2038	2252	10.5%
22	294968	0070P	99.9	100.0	5234	4770	8.9%	687	684	0.5%
23	294982	0070P	106.1	106.8	3832	4292	12.0%	3698	3689	0.3%
24	294998	0070P	113.1	113.2	2407	4536	88.4%	695	510	26.6%
25	295029	0070P	118.6	118.9	2638	2892	9.6%	1318	1434	8.8%
26	295031	0070P	119.0	119.3	2823	2920	3.4%	1540	1495	2.9%

					RADIUS			CURVE LENGTH		
#	**ID**	**Route Name**	**PC**	**PT**	**AutoCAD**	**ArcMap**	**Error %**	**AutoCAD**	**ArcMap**	**Error %**
27	295044	0070P	123.7	124.1	2754	2892	5.0%	1832	1866	1.8%
28	295050	0070P	131.1	131.4	5826	4938	15.2%	1674	1643	1.9%
29	295053	0070P	132.5	132.9	4772	5125	7.4%	2294	2317	1.0%
30	295066	0070P	140.3	141.0	1753	1860	6.1%	3240	3263	0.7%
31	295085	0070P	144.1	144.6	1135	1224	7.9%	2461	2562	4.1%
32	295087	0070P	144.7	145.0	1355	1660	22.6%	1525	1571	3.0%
33	295094	0070P	145.6	145.7	1585	1845	16.4%	542	546	0.7%
34	295106	0070P	162.6	163.1	2857	2971	4.0%	2904	2914	0.3%
35	295110	0070P	167.9	168.2	5743	4967	13.5%	1600	1654	3.4%
36	295116	0070P	181.9	182.0	5641	5031	10.8%	912	891	2.3%
37	295118	0070P	187.7	188.2	2835	3023	6.7%	2976	2930	1.6%
38	295953	0080P	62.2	62.9	4556	4804	5.4%	3361	3320	1.2%
39	296048	0080P	132.9	133.0	1048	2415	130.4%	448	439	1.8%
40	296057	0080P	133.7	134.1	1267	1339	5.7%	2207	2221	0.6%
41	296080	0080P	136.3	136.7	1760	1861	5.7%	2453	2515	2.6%
42	296167	0080P	150.2	150.3	1065	1309	22.9%	758	783	3.3%
43	296192	0080P	153.6	153.7	1110	1324	19.3%	585	557	4.8%
44	296196	0080P	155.2	155.7	2324	2459	5.8%	2864	2868	0.1%
45	296477	0084P	14.8	15.1	2136	2829	32.4%	1949	1810	7.2%
46	296487	0084P	26.0	26.2	2045	4836	136.4%	622	634	1.9%
47	296497	0084P	29.3	29.4	3469	4975	43.4%	923	892	3.4%
48	296499	0084P	29.9	30.1	5188	4632	10.7%	732	728	0.5%
49	296505	0084P	31.4	31.5	5566	5079	8.7%	804	865	7.6%
50	296540	0084P	90.5	90.6	1921	2050	6.7%	661	685	3.6%
51	296553	0084P	91.5	91.6	1673	1790	7.0%	553	548	0.8%
52	296618	0084P	111.9	112.3	1434	1480	3.2%	1714	1774	3.5%
53	296620	0084P	112.3	112.4	1108	3713	235.2%	251	257	2.6%
54	296665	0084N	111.4	111.0	1323	1545	16.8%	1647	1844	11.9%
55	296684	0084N	107.1	106.8	1072	1319	23.0%	1689	1620	4.1%
56	296686	0084N	106.8	106.4	1257	1371	9.0%	2121	2129	0.4%
57	296716	0084N	96.9	96.6	1907	2038	6.9%	1558	1489	4.4%
58	296724	0084N	94.0	93.8	1718	2196	27.8%	1066	1046	1.9%
59	296760	0084N	89.5	89.5	1414	1633	15.4%	391	401	2.7%
60	320533	0015P	14.3	14.6	2272	2452	7.9%	1433	1404	2.0%
61	320556	0015P	35.4	35.4	4130	4310	4.4%	317	240	24.4%
62	320603	0015P	138.9	139.5	2856	2877	0.7%	3119	3274	5.0%
63	320605	0015P	139.8	139.9	3559	3773	6.0%	700	737	5.3%
64	320609	0015P	140.0	140.3	1915	2345	22.5%	1189	1175	1.2%
65	320611	0015P	140.3	140.8	1796	1964	9.3%	2392	2390	0.1%

					RADIUS			CURVE LENGTH		
#	**ID**	**Route Name**	**PC**	**PT**	**AutoCAD**	**ArcMap**	**Error %**	**AutoCAD**	**ArcMap**	**Error %**
66	320900	0015P	352.1	352.2	1335	3158	136.6%	578	612	6.0%
67	320911	0015P	357.9	358.1	7255	5093	29.8%	1261	1325	5.1%
68	320974	0015N	352.1	352.0	1246	2915	134.0%	564	559	0.9%
69	321224	0015N	224.5	224.2	2356	2961	25.7%	1358	1430	5.3%
70	321252	0015N	184.5	185.0	4639	4858	4.7%	2721	3924	44.2%
71	321269	0015N	140.1	139.9	2083	2540	22.0%	1165	1268	8.8%
72	321318	0015N	105.3	104.8	3594	4627	28.7%	2842	2879	1.3%
73	321351	0015N	34.9	34.8	3085	2960	4.0%	1071	974	9.0%
74	321414	0070N	182.0	181.9	1513	4782	216.0%	464	374	19.4%
75	321416	0070N	172.4	171.9	4911	5085	3.5%	2991	2957	1.1%
76	321449	0070N	145.0	144.7	1483	1654	11.5%	1492	1540	3.2%
77	321459	0070N	143.0	142.5	1492	1579	5.8%	2852	2691	5.7%
78	321461	0070N	142.3	142.0	1760	1911	8.6%	1367	1375	0.6%
79	321535	0070N	112.4	112.2	6137	5337	13.0%	882	868	1.6%
80	321550	0070N	107.5	108.0	4592	4653	1.3%	2837	3235	14.0%
81	321582	0070N	95.6	95.2	4267	5142	20.5%	1920	1891	1.5%
82	321624	0070N	83.1	82.7	2233	2388	6.9%	1650	1738	5.3%
83	321638	0070N	80.9	80.7	1669	2011	20.5%	1402	1272	9.2%
84	321648	0070N	78.8	78.6	2278	2690	18.1%	1136	1162	2.3%
85	321658	0070N	75.6	75.4	1561	2576	65.1%	1090	1039	4.7%
86	321668	0070N	73.0	72.8	3066	2992	2.4%	1831	1357	25.9%
87	321674	0070N	72.2	72.0	1573	1683	7.0%	879	818	7.0%
88	321705	0070N	68.0	67.7	3851	4402	14.3%	1347	1323	1.8%
89	321752	0070N	55.0	54.8	3643	4877	33.9%	1191	1216	2.1%
90	321775	0070N	45.0	44.8	3904	4872	24.8%	832	791	5.0%
91	321815	0070N	23.1	22.8	2617	3003	14.7%	1651	1524	7.7%
92	321850	0070N	12.6	12.2	1702	1861	9.3%	2022	2098	3.8%
93	322221	0080N	186.2	185.8	3800	4440	16.8%	1839	2063	12.1%
94	322231	0080N	180.6	180.4	2686	2787	3.8%	956	977	2.1%
95	322260	0080N	171.5	171.3	1317	2121	61.0%	889	1051	18.2%
96	322293	0080N	153.2	153.1	1229	1425	15.9%	647	601	7.1%
97	322313	0080N	150.4	150.2	977	1226	25.5%	1031	1122	8.8%
98	322410	0080N	132.5	132.3	1415	1580	11.7%	996	984	1.2%
99	322432	0080N	129.9	129.8	999	1750	75.2%	676	742	9.8%
100	322434	0080N	129.5	129.3	2413	2607	8.1%	1185	1138	3.9%

Table A.3: Urban Multilane Calibration

#	ID	Route Name	PC	PT	RADIUS AutoCAD	RADIUS ArcMap	RADIUS Error %	CURVE LENGTH AutoCAD	CURVE LENGTH ArcMap	CURVE LENGTH Error %
1	294237	0068P	27.4	27.5	966	-1369	41.6%	486	484	0.4%
2	299372	0089P	348.9	348.8	166	597	260.6%	213	196	7.9%
3	310457	0154P	4.6	4.5	2192	3356	53.1%	570	553	3.1%
4	303448	0106P	7.0	7.0	1637	-536	67.3%	1953	370	81.1%
5	304147	0115P	6.9	6.8	661	-922	39.4%	650	717	10.3%
6	310359	0154P	20.5	20.7	2060	2929	42.2%	1325	1276	3.7%
7	298239	0089P	383.1	383.3	1759	1861	5.8%	893	983	10.0%
8	303910	0114P	0.5	0.6	822	-1536	86.8%	698	793	13.6%
9	314758	0198P	8.6	8.7	1507	2449	62.4%	314	310	1.2%
10	294612	0068P	25.1	25.0	1114	1777	59.6%	368	384	4.4%
11	314787	0198P	13.4	13.5	3836	-2521	34.3%	488	670	37.3%
12	292084	0051P	0.1	0.0	621	-698	12.5%	514	512	0.4%
13	303743	0111P	6.1	6.4	4602	-4850	5.4%	1622	1568	3.3%
14	310408	0154P	18.8	18.7	1987	-2136	7.5%	471	495	5.0%
15	306982	0140P	0.0	0.1	166	-218	31.8%	389	362	7.0%
16	291767	0048P	11.6	11.4	1390	1376	1.0%	1209	1174	2.9%
17	305075	0126P	0.4	0.3	966	4300	345.2%	215	217	0.8%
18	294114	0067P	5.4	5.6	2497	4496	80.0%	840	815	2.9%
19	295656	0073P	36.8	36.9	164	-260	58.2%	272	268	1.4%
20	315454	0209P	11.5	11.8	2039	2874	40.9%	1654	1679	1.5%
21	323823	0201N	15.1	15.0	2014	4817	139.2%	534	519	2.8%
22	295310	0071P	3.2	3.0	1346	1603	19.1%	1011	984	2.7%
23	292746	0060P	6.5	6.4	809	764	5.6%	677	625	7.7%
24	292729	0060P	7.1	7.2	1466	2696	83.9%	483	513	6.2%
25	285334	0026P	1.8	1.9	2124	-3062	44.1%	251	265	5.5%
26	294206	0068P	24.7	24.7	1217	2946	142.0%	140	256	82.4%
27	303674	0109P	1.1	1.2	746	903	21.1%	245	254	4.0%
28	305081	0126P	0.1	0.0	887	-553	37.7%	239	231	3.2%
29	310468	0154P	2.0	1.6	2400	-2378	0.9%	1912	1810	5.4%
30	299505	0089N	327.8	327.7	368	-1681	356.8%	618	604	2.2%
31	292691	0060P	3.6	3.7	1168	-2955	153.1%	510	516	1.2%
32	311973	0168P	0.4	0.2	1213	1647	35.7%	752	787	4.7%
33	312504	0186P	4.0	4.0	256	250	2.2%	467	381	18.3%
34	295140	0071P	3.5	3.8	2262	2255	0.3%	1318	1304	1.1%
35	315418	0209P	6.9	6.9	3439	4599	33.7%	444	445	0.1%
36	298152	0089P	349.2	349.5	1439	1614	12.2%	1319	1354	2.6%
37	308112	0145P	3.0	3.1	2000	2461	23.1%	922	911	1.2%

					RADIUS			CURVE LENGTH		
#	**ID**	**Route Name**	**PC**	**PT**	**AutoCAD**	**ArcMap**	**Error %**	**AutoCAD**	**ArcMap**	**Error %**
38	299482	0089P	331.7	331.6	3272	2817	13.9%	565	535	5.3%
39	295158	0071P	5.8	5.8	1545	1620	4.9%	301	296	1.7%
40	323751	0201P	8.9	8.9	6042	3409	43.6%	279	265	5.0%
41	318284	0265P	2.4	2.5	3318	3583	8.0%	698	687	1.6%
42	294376	0068P	64.6	64.8	6135	5257	14.3%	1012	969	4.3%
43	298247	0089P	384.6	384.7	3705	3150	15.0%	463	416	10.1%
44	294122	0067P	7.7	7.9	2090	2313	10.6%	1141	1132	0.8%
45	323838	0201N	8.9	9.1	4360	5106	17.1%	1123	1667	48.4%
46	303745	0111P	6.6	7.2	3397	3757	10.6%	3413	3470	1.7%
47	312676	0189P	6.9	7.2	5400	5607	3.8%	1400	1436	2.6%
48	310300	0154P	0.1	0.4	1018	759	25.4%	1305	1332	2.1%
49	304967	0126P	2.9	3.0	5523	5452	1.3%	545	548	0.5%
50	308123	0145P	4.6	4.8	1081	1149	6.3%	883	850	3.8%
51	292098	0052P	1.6	1.7	4108	4891	19.1%	329	332	1.0%
52	298091	0089P	336.1	336.1	1222	1144	6.4%	436	450	3.3%
53	310324	0154P	8.3	8.6	2632	2639	0.3%	1807	1774	1.8%
54	292327	0056P	56.1	55.9	1565	1754	12.1%	945	934	1.1%
55	323753	0201P	9.0	9.4	5646	5138	9.0%	1864	1851	0.7%
56	298089	0089P	336.0	336.0	1427	1425	0.1%	321	316	1.5%
57	310354	0154P	19.1	19.2	2438	2381	2.3%	521	523	0.4%
58	283030	0018P	6.8	7.0	1450	1584	9.3%	1082	1067	1.4%
59	299238	0089N	397.7	397.4	2345	2386	1.7%	1693	1673	1.2%
60	310440	0154P	9.2	8.9	2892	2866	0.9%	1894	1867	1.4%
61	295665	0073P	35.7	35.6	4429	4357	1.6%	406	396	2.4%
62	310381	0154P	23.9	23.9	4462	3435	23.0%	258	252	2.3%
63	308159	0145P	3.3	3.3	2792	3305	18.4%	196	188	4.0%
64	283028	0018P	6.2	6.4	3119	2909	6.7%	814	796	2.2%
65	318461	0266P	2.7	2.7	2143	1342	37.4%	190	192	1.1%
66	294120	0067P	7.0	7.4	2086	2253	8.0%	1990	2052	3.1%
67	313062	0190P	0.5	0.7	855	911	6.5%	1247	1238	0.7%
68	295138	0071P	3.0	3.2	1580	1733	9.7%	1020	1031	1.1%
69	282991	0018P	1.6	1.8	1904	1892	0.6%	1347	1345	0.2%
70	310404	0154P	19.9	19.7	2845	2682	5.7%	1105	1099	0.5%
71	310470	0154P	1.3	0.9	2294	2310	0.7%	1813	1765	2.7%
72	299233	0089P	405.7	405.8	2496	3261	30.7%	520	1492	187.0%
73	299240	0089N	396.1	396.0	2694	2950	9.5%	484	481	0.6%
74	295294	0071P	5.9	5.9	1986	2661	34.0%	313	303	3.1%
75	310314	0154P	3.8	3.9	3184	3340	4.9%	423	423	0.1%
76	309267	0151P	2.6	2.6	1864	2027	8.7%	449	445	1.0%

					RADIUS			CURVE LENGTH		
#	ID	Route Name	PC	PT	AutoCAD	ArcMap	Error %	AutoCAD	ArcMap	Error %
77	299217	0089P	410.4	410.3	2434	1789	26.5%	766	763	0.4%
78	294132	0067P	8.4	8.1	2117	2132	0.7%	1453	1418	2.4%
79	298236	0089P	382.5	382.8	2126	2152	1.2%	1465	1399	4.5%
80	310453	0154P	5.7	6.0	3056	3678	20.4%	1644	2055	25.0%
81	324739	0079P	0.1	0.0	814	1025	25.9%	477	510	7.0%
82	292115	0052P	4.0	3.8	1174	1172	0.2%	728	730	0.3%
83	312666	0189P	5.4	5.7	7919	7225	8.8%	1313	1316	0.2%
84	280301	0008P	1.2	1.0	1280	1550	21.1%	930	920	1.1%
85	303352	0104P	2.6	2.7	1947	1780	8.6%	738	856	16.0%
86	315336	0204P	0.1	0.0	718	602	16.1%	291	291	0.0%
87	294567	0068P	32.8	32.9	3274	4267	30.3%	372	614	65.2%
88	303781	0111P	6.4	6.1	5329	4918	7.7%	1198	1192	0.5%
89	310391	0154N	21.3	21.2	5667	5081	10.3%	484	469	3.0%
90	279269	0006P	174.0	174.2	4319	3838	11.1%	832	782	6.1%
91	304962	0126P	1.9	2.1	6503	4683	28.0%	934	924	1.1%
92	316791	0225P	0.1	0.3	1244	1245	0.1%	1024	995	2.9%
93	294142	0067P	5.5	5.3	12601	5035	60.0%	578	610	5.5%
94	294126	0067P	10.4	10.6	4969	4621	7.0%	1059	1059	0.0%
95	299351	0089P	362.7	362.6	728	2484	241.2%	643	607	5.6%
96	304954	0126P	0.6	0.7	3160	2827	10.5%	295	284	3.6%
97	279277	0006P	177.6	177.8	1120	-1218	8.7%	1201	1228	2.2%
98	319511	0284P	1.3	1.3	271	336	23.7%	254	263	3.5%
99	299383	0089P	347.8	347.7	541	-659	21.7%	415	425	2.5%
100	292679	0060P	2.8	2.9	1114	5142	361.5%	409	404	1.2%

Table A.4: Rural Multilane Calibration

					RADIUS			CURVE LENGTH		
#	ID	Route Name	PC	PT	AutoCAD	ArcMap	Error %	AutoCAD	ArcMap	Error %
1	316644	0224P	8.6	8.8	1244	1173	5.7%	1294	1212	6.4%
2	280938	0010P	47.6	48.1	1602	1635	2.0%	2636	2600	1.3%
3	288417	0036P	65.8	66.1	1256	-2326	85.2%	1276	1312	2.9%
4	290172	0040P	139.0	139.3	2860	4511	57.7%	1338	1371	2.5%
5	311764	0165P	6.7	6.6	1422	2904	104.2%	463	490	6.0%
6	313887	0191P	128.9	129.0	1915	-2928	52.9%	386	318	17.7%
7	297857	0089P	256.1	256.2	897	-866	3.5%	442	435	1.6%
8	317072	0248P	4.2	4.3	82983	-5049	93.9%	428	394	8.0%

					RADIUS			CURVE LENGTH		
#	**ID**	**Route Name**	**PC**	**PT**	**AutoCAD**	**ArcMap**	**Error %**	**AutoCAD**	**ArcMap**	**Error %**
9	280786	0009P	6.7	6.5	2428	2766	13.9%	1128	1051	6.8%
10	300517	0091P	37.6	37.9	4521	-4312	4.6%	1552	1557	0.4%
11	312748	0189P	14.2	14.4	1198	-1570	31.0%	1292	1346	4.2%
12	280794	0009P	3.6	3.5	1445	1517	5.0%	645	596	7.6%
13	300432	0091P	7.8	7.9	2075	2796	34.7%	696	632	9.3%
14	312961	0189P	12.2	12.0	782	1060	35.5%	591	668	13.1%
15	312715	0189P	11.1	11.3	3218	-1535	52.3%	1996	771	61.4%
16	312778	0189P	17.4	17.5	1470	-1562	6.2%	693	626	9.6%
17	312701	0189P	9.2	9.4	1053	-1214	15.2%	897	969	8.0%
18	312893	0189P	18.3	18.2	886	-1085	22.4%	656	623	5.1%
19	280321	0009P	2.0	2.5	4472	4904	9.7%	2744	2642	3.7%
20	280790	0009P	4.4	4.2	2722	-2903	6.6%	1296	1263	2.5%
21	312901	0189P	17.5	17.4	1388	1465	5.5%	701	625	10.9%
22	312776	0189P	17.1	17.2	1375	-1707	24.2%	492	550	11.8%
23	312915	0189P	15.7	15.6	840	-968	15.2%	808	805	0.4%
24	323277	0191P	128.7	128.5	983	1102	12.1%	1056	1039	1.7%
25	312783	0189P	18.0	18.1	1422	-976	31.3%	1531	831	45.7%
26	299166	0089P	426.3	426.0	2472	3079	24.6%	1229	1194	2.8%
27	312720	0189P	11.8	11.9	1993	1636	18.0%	442	479	8.2%
28	304366	0118P	5.7	5.5	1753	-2121	21.0%	733	769	4.9%
29	300437	0091P	8.7	8.9	1397	1613	15.4%	1365	1367	0.2%
30	280796	0009P	3.4	3.0	1877	-2030	8.1%	2284	2204	3.5%
31	304486	0120P	3.3	3.4	1162	1207	3.9%	607	399	34.2%
32	290256	0040P	145.3	145.1	964	-1243	29.0%	936	958	2.3%
33	312965	0189P	11.6	11.3	2663	-3278	23.1%	1276	1383	8.4%
34	300578	0091P	6.7	6.8	1160	-4057	249.8%	317	1348	324.6%
35	312779	0189P	17.5	17.8	1283	3159	146.2%	265	1628	514.1%
36	312916	0189P	15.6	15.3	938	106	88.7%	1327	1350	1.8%
37	290275	0040P	140.7	140.8	1962	-3484	77.6%	756	1154	52.7%
38	300588	0091P	4.8	4.7	1749	-2519	44.0%	494	543	10.0%
39	279558	0006P	232.6	233.2	2245	2483	10.6%	3426	3459	1.0%
40	323271	0191P	131.0	130.5	1830	1974	7.9%	2455	2495	1.6%
41	312897	0189P	17.9	17.8	760	988	29.9%	529	511	3.4%
42	279949	0006P	188.1	187.9	2000	-2384	19.2%	920	813	11.6%
43	300593	0091P	4.2	4.0	2642	-2902	9.9%	1054	1162	10.3%
44	317141	0248P	5.5	5.3	2252	2875	27.7%	1148	1252	9.1%
45	316694	0224P	5.0	5.1	910	-2523	177.4%	418	798	91.1%
46	310998	0160P	1.7	1.8	895	-1154	28.8%	650	642	1.3%

					RADIUS			CURVE LENGTH		
#	**ID**	**Route Name**	**PC**	**PT**	**AutoCAD**	**ArcMap**	**Error %**	**AutoCAD**	**ArcMap**	**Error %**
47	313788	0191P	104.8	105.5	5253	5568	6.0%	3624	3548	2.1%
48	312973	0189P	10.2	10.1	791	-1155	46.1%	471	536	13.6%
49	317243	0252P	0.7	0.7	1207	-4209	248.9%	247	230	7.0%
50	311731	0165P	6.6	6.7	1939	-3216	65.8%	629	594	5.6%
51	290137	0040P	113.9	114.1	575	-716	24.6%	804	754	6.2%
52	280792	0009P	4.1	3.7	1425	1469	3.1%	2070	2011	2.8%
53	279672	0006P	243.4	243.2	5650	4178	26.0%	764	754	1.3%
54	312768	0189P	16.0	16.1	874	1111	27.1%	500	501	0.2%
55	298356	0089P	426.0	426.3	3046	3441	13.0%	1349	1343	0.5%
56	317064	0248P	2.9	3.1	860	970	12.8%	719	717	0.3%
57	284368	0024P	60.1	60.2	555	763	37.4%	645	624	3.2%
58	300443	0091P	9.8	10.1	1981	2030	2.5%	1315	1430	8.7%
59	297855	0089P	256.0	256.1	481	591	23.0%	588	582	1.1%
60	299638	0089P	277.3	276.9	1664	1633	1.9%	1700	1660	2.4%
61	299163	0089P	426.7	426.5	2841	3078	8.3%	984	996	1.2%
62	288412	0036P	62.0	62.2	2992	3150	5.3%	851	865	1.7%
63	316650	0224P	10.4	10.5	2962	2893	2.3%	747	732	2.0%
64	312944	0189P	13.6	13.5	1632	1748	7.1%	334	327	2.1%
65	280765	0009P	11.9	11.8	1886	2059	9.2%	763	739	3.2%
66	316667	0224P	10.2	9.9	2721	2892	6.3%	1679	1675	0.3%
67	312955	0189P	12.6	12.5	984	1240	26.0%	399	385	3.4%
68	300389	0091P	3.4	3.8	1456	1432	1.7%	1891	1816	3.9%
69	300572	0091P	7.6	7.2	1423	1594	12.0%	2085	2081	0.2%
70	312711	0189P	10.3	10.5	1311	1470	12.1%	805	809	0.5%
71	323580	0191P	51.5	51.3	962	1018	5.9%	949	936	1.4%
72	290316	0040P	114.1	114.0	589	634	7.6%	703	672	4.4%
73	312703	0189P	9.5	9.6	1430	1568	9.6%	410	434	5.8%
74	298378	0089P	433.3	433.5	2984	2865	4.0%	1166	1177	0.9%
75	289797	0040P	14.9	15.2	2877	2942	2.3%	1727	1681	2.7%
76	300429	0091P	7.2	7.6	1397	1660	18.8%	1938	2018	4.1%
77	300498	0091P	25.3	25.7	3084	5371	74.1%	1955	1970	0.7%
78	304305	0118P	5.4	5.5	1439	1287	10.5%	510	546	7.1%
79	297852	0089P	254.8	255.0	944	1031	9.2%	774	769	0.7%
80	300580	0091P	6.4	5.9	1958	2048	4.6%	2489	2431	2.3%
81	300270	0089P	64.2	64.1	304	354	16.5%	583	564	3.2%
82	312742	0189P	13.8	13.8	1579	1986	25.8%	325	324	0.3%
83	298389	0089P	459.9	459.9	700	1210	72.8%	212	212	0.2%
84	290176	0040P	140.6	140.9	2744	3225	17.5%	1203	1197	0.5%
85	312724	0189P	12.2	12.3	933	1115	19.5%	573	567	1.0%

					RADIUS			CURVE LENGTH		
#	ID	Route Name	PC	PT	AutoCAD	ArcMap	Error %	AutoCAD	ArcMap	Error %
86	312837	0189P	28.8	28.9	590	594	0.6%	217	222	2.1%
87	311762	0165P	6.9	6.8	2767	2928	5.8%	533	526	1.4%
88	311023	0160P	1.8	1.7	1046	1263	20.7%	727	697	4.1%
89	299136	0089P	460.5	460.4	1382	1497	8.3%	578	557	3.6%
90	300453	0091P	14.8	14.9	5504	5010	9.0%	471	508	7.9%
91	290607	0040P	16.5	16.4	908	1188	30.9%	327	325	0.6%
92	300284	0089P	63.1	63.3	2748	3842	39.8%	840	1518	80.6%
93	298359	0089P	426.5	426.7	2988	3145	5.2%	1004	1008	0.4%
94	299134	0089P	460.8	460.7	1513	1616	6.8%	953	967	1.4%
95	300385	0091P	2.3	2.6	1881	2044	8.7%	1379	1384	0.4%
96	312738	0189P	13.5	13.6	1526	1867	22.3%	371	359	3.2%
97	288435	0036P	55.8	55.7	3197	2862	10.5%	190	189	0.7%
98	312707	0189P	9.9	10.1	973	1130	16.1%	920	944	2.6%
99	300411	0091P	5.0	5.1	1655	2029	22.6%	317	336	5.8%
100	312983	0189P	9.1	9.0	912	1088	19.3%	658	655	0.5%
101	300399	0091P	4.3	4.6	2793	3191	14.3%	1538	1640	6.6%
102	324399	0012P	59.8	59.7	748	773	3.4%	664	679	2.3%
103	289795	0040P	13.8	14.0	5390	4670	13.4%	859	860	0.1%
104	280332	0009P	4.2	4.4	3030	2928	3.4%	1171	1157	1.2%
105	300418	0091P	5.9	6.4	1922	2103	9.4%	2357	2389	1.3%

Table A.5: Urban TLTW Calibration

					RADIUS			CURVE LENGTH		
#	ID	Route Name	PC	PT	AutoCAD	ArcMap	Error %	AutoCAD	ArcMap	Error %
1	308369	0147P	11.8	11.8	386	-741	92.0%	309	303	1.9%
2	313515	0190P	2.2	2.1	800	1161	45.2%	453	437	3.7%
3	315505	0209P	12.1	11.9	1136	1286	13.2%	973	963	1.0%
4	292717	0060P	5.3	5.4	1849	1419	23.3%	790	379	52.0%
5	303450	0106P	7.1	7.2	287	-985	242.8%	366	361	1.5%
6	308263	0146P	2.6	2.4	1476	-1657	12.3%	956	929	2.9%
7	304135	0115P	8.0	8.0	493	-543	10.1%	271	265	2.2%
8	295746	0074P	1.3	1.5	3109	2362	24.0%	962	947	1.6%
9	314852	0198P	4.1	3.9	1461	-2107	44.2%	803	783	2.5%
10	312450	0186P	0.7	0.7	1423	-2892	103.3%	441	490	11.1%
11	308278	0146P	0.9	0.9	1345	-1005	25.3%	396	406	2.5%
12	294126	0067P	10.4	10.6	2768	-4621	66.9%	1095	1059	3.3%

#	ID	Route Name	PC	PT	RADIUS AutoCAD	RADIUS ArcMap	RADIUS Error %	CURVE LENGTH AutoCAD	CURVE LENGTH ArcMap	CURVE LENGTH Error %
13	315935	0210P	2.9	2.8	1152	1106	4.0%	976	772	21.0%
14	294151	0067P	0.8	0.4	2188	2163	1.1%	2023	1994	1.4%
15	304143	0115P	8.0	8.0	665	537	19.3%	280	270	3.5%
16	309331	0152N	1.1	0.8	16529	-5261	68.2%	1273	1246	2.1%
17	315944	0210P	1.6	1.5	1212	1064	12.2%	868	844	2.7%
18	294584	0068P	27.5	27.4	1050	1218	15.9%	445	438	1.6%
19	312623	0186P	0.9	1.0	1043	-3167	203.7%	227	525	131.1%
20	292725	0060P	6.6	6.8	1497	-1465	2.2%	1271	1095	13.8%
21	312995	0189P	7.6	7.5	794	-899	13.2%	723	706	2.4%
22	313076	0190P	2.1	2.2	672	-1017	51.4%	386	371	3.7%
23	315937	0210P	2.5	2.4	1562	-2070	32.5%	868	824	5.0%
24	308368	0147P	11.9	11.8	197	345	74.9%	218	205	5.9%
25	294206	0068P	24.7	24.7	1171	2946	151.7%	248	256	3.3%
26	307031	0140P	0.5	0.5	993	-2194	120.9%	198	187	5.5%
27	295755	0074P	4.9	4.7	1176	-1282	9.0%	1134	1121	1.1%
28	315458	0209P	11.9	12.1	1087	-1317	21.2%	987	984	0.3%
29	292719	0060P	5.5	5.7	1623	-1930	19.0%	789	794	0.6%
30	303690	0109P	2.7	2.7	1644	-2569	56.3%	495	485	2.0%
31	294251	0068P	29.1	29.2	1003	1196	19.3%	934	897	4.0%
32	312340	0173P	0.5	0.3	912	1114	22.1%	725	733	1.0%
33	303677	0109P	1.3	1.5	2833	2904	2.5%	1035	1029	0.6%
34	292668	0060P	2.3	2.4	477	-3672	669.4%	525	535	1.9%
35	292746	0060P	6.5	6.4	711	764	7.4%	653	625	4.2%
36	294223	0068P	26.4	26.6	4103	-4006	2.4%	1256	1290	2.7%
37	298016	0089P	322.4	322.7	2548	3226	26.6%	1523	1507	1.0%
38	304046	0114P	3.3	3.2	12712	3162	75.1%	619	593	4.2%
39	308280	0146P	0.8	0.7	808	1024	26.7%	391	400	2.3%
40	311695	0164P	2.7	2.7	342	422	23.2%	365	344	5.8%
41	294448	0068P	65.9	66.0	1742	7662	339.8%	487	428	12.0%
42	292666	0060P	2.1	2.2	400	-481	20.4%	450	456	1.3%
43	306985	0140P	0.2	0.2	931	567	39.1%	254	256	1.1%
44	292742	0060P	7.1	7.0	1165	1503	29.0%	605	558	7.8%
45	292721	0060P	6.1	6.4	679	747	10.0%	1172	1175	0.3%
46	306982	0140P	0.0	0.1	178	-218	23.0%	385	362	6.0%
47	323838	0201N	8.9	9.1	3856	5106	32.4%	1072	1667	55.5%
48	299270	0089N	383.7	383.6	1047	1466	40.1%	789	792	0.4%
49	292695	0060P	3.7	3.9	806	2096	159.9%	702	737	5.0%
50	315572	0210P	1.5	1.7	1234	-1269	2.8%	980	1027	4.8%
51	294610	0068P	25.2	25.2	747	-1541	106.3%	355	421	18.6%

					RADIUS			CURVE LENGTH		
#	ID	Route Name	PC	PT	AutoCAD	ArcMap	Error %	AutoCAD	ArcMap	Error %
52	308207	0146P	2.2	2.3	706	-838	18.7%	731	747	2.1%
53	303408	0106P	0.1	0.2	668	-2195	228.7%	293	299	1.9%
54	314741	0198P	4.5	4.6	2625	-3435	30.9%	849	938	10.5%
55	295782	0075P	1.7	1.7	870	-3261	274.7%	197	198	0.3%
56	311975	0168P	0.1	0.0	2235	2281	2.1%	215	219	1.7%
57	308327	0147P	13.2	13.2	2140	3137	46.6%	199	190	4.7%
58	279994	0006P	178.1	177.9	1130	1281	13.4%	834	857	2.7%
59	279277	0006P	177.6	177.8	1185	1218	2.8%	1238	1228	0.8%
60	312617	0186P	1.3	1.2	735	791	7.6%	244	245	0.5%
61	304137	0115P	8.1	8.1	330	540	63.9%	268	283	5.4%
62	303707	0109P	0.8	0.8	584	775	32.7%	279	278	0.2%
63	292059	0051P	0.0	0.1	695	659	5.2%	608	615	1.1%
64	292679	0060P	2.8	2.9	1087	5142	373.0%	419	404	3.5%
65	292707	0060P	4.4	4.5	646	765	18.4%	445	459	3.2%
66	302640	0097P	2.8	2.7	923	1117	21.0%	771	756	1.9%
67	303724	0110P	1.2	1.2	1035	1586	53.2%	279	266	4.5%
68	295748	0074P	2.2	2.3	2455	2513	2.3%	642	631	1.7%
69	308240	0146P	5.0	5.0	4739	3144	33.7%	176	180	2.1%
70	308198	0146P	0.7	0.8	868	943	8.6%	368	363	1.5%
71	294595	0068P	26.4	26.6	3315	4188	26.3%	470	1041	121.5%
72	303469	0106P	8.7	8.7	1501	1558	3.8%	263	256	2.5%
73	312191	0173P	0.0	0.3	955	977	2.3%	1354	1334	1.5%
74	306761	0134P	7.1	7.0	1331	1481	11.3%	380	360	5.3%
75	318414	0266P	7.0	6.9	1291	1318	2.1%	553	544	1.6%
76	292787	0060P	3.3	3.2	1023	1249	22.0%	319	304	4.7%
77	292744	0060P	6.8	6.6	1308	1386	6.0%	1002	1031	2.9%
78	294215	0068P	25.5	25.6	2890	3433	18.8%	573	578	0.9%
79	314838	0198P	7.9	7.8	1577	1697	7.6%	666	674	1.3%
80	299516	0089P	326.5	326.2	2350	2461	4.7%	1382	1372	0.7%
81	312193	0173P	0.4	0.5	927	1061	14.4%	671	680	1.3%
82	295777	0075P	0.7	0.8	6724	5121	23.8%	827	824	0.4%
83	303625	0108P	12.8	12.6	1337	1470	10.0%	738	739	0.2%
84	292067	0051P	2.2	2.4	1403	1454	3.6%	920	923	0.3%
85	303497	0106P	8.0	7.9	329	382	16.3%	663	644	2.9%
86	294586	0068P	27.3	27.2	1995	1860	6.8%	448	442	1.3%
87	314850	0198P	4.6	4.5	1153	1309	13.6%	843	846	0.4%
88	315491	0209P	13.9	13.8	1818	2007	10.4%	505	512	1.4%
89	308238	0146P	5.3	5.2	534	751	40.6%	465	462	0.6%
90	303940	0114P	2.0	2.2	2584	2271	12.1%	1226	1209	1.4%

					RADIUS			CURVE LENGTH		
#	**ID**	**Route Name**	**PC**	**PT**	**AutoCAD**	**ArcMap**	**Error %**	**AutoCAD**	**ArcMap**	**Error %**
91	314787	0198P	13.4	13.5	2744	2521	8.1%	667	670	0.5%
92	295853	0077P	6.4	6.6	959	1046	9.1%	944	937	0.7%
93	298023	0089P	323.0	323.2	5847	5284	9.6%	1126	1100	2.3%
94	306765	0134P	6.3	6.3	1912	2486	30.0%	280	278	0.6%
95	303701	0109P	1.3	1.5	2735	3194	16.8%	778	1171	50.5%
96	308246	0146P	4.3	4.2	2037	1822	10.5%	321	319	0.8%
97	319586	0287P	0.3	0.2	1172	1306	11.4%	652	664	1.9%
98	314734	0198P	3.6	3.7	2442	2088	14.5%	199	193	3.2%
99	292757	0060P	4.9	4.8	1035	1405	35.8%	357	351	1.5%
100	312455	0186P	1.2	1.3	1034	-309	70.1%	226	224	1.1%

Table A.6: Rural TLTW Calibration

					RADIUS			CURVE LENGTH		
#	**ID**	**Route Name**	**PC**	**PT**	**AutoCAD**	**ArcMap**	**Error %**	**AutoCAD**	**ArcMap**	**Error %**
1	307903	0143P	12.5	12.5	500	2019	303.5%	441	418	5.1%
2	314495	0191P	390.8	390.9	518	588	13.6%	790	794	0.6%
3	291499	0046P	11.7	11.8	4259	2992	29.7%	797	629	21.0%
4	305015	0126P	21.6	21.4	860	1044	21.4%	855	973	13.9%
5	294623	0068P	22.3	22.3	1387	2402	73.2%	277	218	21.3%
6	292936	0062P	34.8	35.0	2684	4118	53.5%	1498	1459	2.6%
7	306384	0132P	29.8	30.0	1821	3003	65.0%	973	1103	13.4%
8	281841	0012P	110.0	110.1	2535	-504	80.1%	683	556	18.6%
9	288050	0035P	25.9	25.9	735	1187	61.6%	374	359	4.1%
10	282967	0017P	1.5	1.4	718	907	26.5%	514	506	1.7%
11	291642	0046P	8.4	8.2	2240	2827	26.2%	1035	995	3.9%
12	321951	0072P	11.2	11.3	807	-983	21.7%	1023	980	4.1%
13	302580	0096P	3.3	3.0	1187	1000	15.8%	1336	1442	7.9%
14	287441	0035P	20.4	20.5	720	-3956	449.1%	739	739	0.1%
15	305233	0128P	10.6	10.6	862	-3956	358.7%	584	739	26.5%
16	307635	0143P	47.7	47.5	1388	1654	19.2%	864	731	15.4%
17	282691	0014P	6.2	6.1	1272	1654	30.0%	623	731	17.3%
18	281536	0012P	74.2	74.3	255	-107	58.1%	358	387	8.0%
19	291486	0046P	10.4	10.5	974	-1619	66.3%	623	633	1.6%
20	319741	0302P	2.3	2.3	785	643	18.1%	232	256	10.2%
21	304390	0119P	0.0	0.0	136	-150	9.8%	212	224	5.5%
22	301154	0092P	21.7	21.7	57	-221	284.5%	186	189	1.7%

					RADIUS			CURVE LENGTH		
#	**ID**	**Route Name**	**PC**	**PT**	**AutoCAD**	**ArcMap**	**Error %**	**AutoCAD**	**ArcMap**	**Error %**
23	324672	0012P	6.5	6.3	1729	-1400	19.1%	1301	1316	1.1%
24	281252	0012P	25.3	25.6	1406	-1526	8.5%	1627	1597	1.9%
25	307948	0143P	9.0	8.9	1087	-2520	131.9%	355	370	4.3%
26	289234	0039P	62.7	62.8	979	-4584	368.1%	865	844	2.4%
27	296378	0083P	19.7	19.8	975	-1382	41.7%	681	680	0.2%
28	309033	0150P	23.4	23.3	1438	2038	41.7%	720	710	1.4%
29	324255	0012P	79.2	79.1	556	1289	131.8%	366	408	11.5%
30	310589	0157P	2.4	2.5	1375	2335	69.7%	316	272	13.9%
31	309924	0153P	31.9	31.8	148	205	38.5%	260	236	9.3%
32	317769	0261P	5.8	5.7	914	1270	38.9%	721	691	4.1%
33	306944	0138P	3.0	2.6	1826	2035	11.5%	2460	2454	0.2%
34	306290	0132P	0.5	0.6	975	1386	42.1%	496	501	0.9%
35	308916	0150P	38.9	38.8	1376	-2498	81.6%	773	722	6.6%
36	308910	0150P	40.6	40.4	1771	1977	11.6%	1212	1182	2.5%
37	323907	0012P	120.0	119.9	845	1251	48.0%	509	582	14.2%
38	289091	0039P	43.0	43.1	997	1245	24.9%	779	794	1.9%
39	282221	0014P	8.5	8.7	1324	1184	10.6%	834	851	2.1%
40	285906	0030P	18.9	19.1	2611	-2872	10.0%	832	797	4.2%
41	305980	0128P	7.5	7.2	1324	1497	13.1%	1351	1282	5.1%
42	307402	0143P	18.6	18.9	1891	-2579	36.3%	1426	1522	6.7%
43	318809	0276P	60.6	60.8	3570	-5262	47.4%	961	966	0.5%
44	322877	0191P	294.3	294.2	902	-1263	39.9%	542	483	10.9%
45	290948	0044P	26.3	26.6	1862	-2037	9.4%	1594	1584	0.7%
46	305574	0128P	41.3	41.4	2355	-1556	33.9%	301	275	8.7%
47	324252	0012P	79.4	79.3	866	1024	18.3%	736	702	4.7%
48	296952	0087P	14.5	14.7	595	-648	8.8%	1022	1036	1.4%
49	304115	0115P	2.2	2.2	1789	-2682	49.9%	378	318	16.0%
50	314163	0191P	284.0	284.4	3375	-3366	0.3%	2171	2136	1.6%
51	279219	0006P	143.6	143.7	470	3670	680.3%	495	511	3.2%
52	306020	0128P	3.0	3.0	1427	1808	26.7%	296	295	0.4%
53	319358	0279P	2.0	1.7	1239	1320	6.6%	1252	1205	3.7%
54	287422	0035P	18.9	19.0	857	2297	168.0%	577	601	4.2%
55	299740	0089P	242.5	242.4	2682	2883	7.5%	637	635	0.3%
56	307980	0143P	4.1	4.0	1146	1387	21.0%	476	478	0.3%
57	302528	0096P	10.7	10.5	683	767	12.3%	1318	1319	0.1%
58	311115	0162P	7.6	7.9	2828	2904	2.7%	1372	1694	23.5%
59	319979	0313P	6.0	6.2	1243	1071	13.8%	666	648	2.7%
60	303281	0102P	9.5	9.4	315	385	22.1%	573	602	5.0%
61	323064	0191P	268.7	268.6	2814	4160	47.8%	255	248	2.9%

					RADIUS			CURVE LENGTH		
#	ID	Route Name	PC	PT	AutoCAD	ArcMap	Error %	AutoCAD	ArcMap	Error %
62	287731	0035P	55.6	55.7	841	1149	36.7%	234	318	35.7%
63	308007	0144P	0.3	0.4	936	3477	271.5%	253	251	0.6%
64	311235	0162P	31.2	31.4	1030	1197	16.2%	930	915	1.7%
65	287669	0035P	50.2	50.3	2492	2538	1.9%	293	288	1.5%
66	323174	0191P	254.9	254.8	1923	2313	20.3%	437	460	5.3%
67	279854	0006P	206.6	206.4	964	1081	12.1%	892	887	0.6%
68	305391	0128P	25.6	25.7	1966	2263	15.1%	268	265	1.3%
69	317700	0261P	10.6	10.5	1033	1326	28.4%	497	496	0.2%
70	299533	0089P	312.6	312.5	1012	1154	14.0%	445	456	2.4%
71	284838	0024P	89.4	89.2	524	629	20.1%	850	861	1.3%
72	293248	0065P	8.2	8.3	384	224	41.7%	393	406	3.4%
73	323644	0191P	26.5	26.3	1419	1527	7.6%	721	680	5.6%
74	317640	0261P	29.9	29.9	2168	2792	28.8%	328	326	0.5%
75	285680	0029P	17.9	18.0	1033	1233	19.4%	634	632	0.3%
76	282335	0014P	20.1	20.4	2890	2945	1.9%	1140	1141	0.1%
77	292847	0062P	0.6	0.7	2127	2290	7.7%	783	786	0.4%
78	314666	0196P	17.7	17.9	5642	5482	2.8%	1147	1143	0.4%
79	300038	0089P	103.0	103.5	5883	5293	10.0%	2887	3918	35.7%
80	300071	0089P	97.5	97.5	2132	2566	20.4%	259	253	2.3%
81	314963	0199P	12.7	12.7	565	1544	173.5%	234	225	4.0%
82	309804	0153P	33.8	33.9	419	855	104.1%	536	539	0.6%
83	309880	0153P	34.0	33.9	173	634	266.9%	378	432	14.3%
84	285923	0030P	50.0	50.2	2844	2820	0.8%	1151	1146	0.4%
85	292344	0056P	43.6	43.5	1305	1430	9.6%	918	877	4.5%
86	305969	0128P	8.7	8.6	1000	1311	31.1%	544	536	1.4%
87	290571	0040P	25.5	25.4	1284	1469	14.4%	777	744	4.3%
88	314343	0191P	370.6	370.7	659	828	25.7%	582	592	1.7%
89	303876	0113P	6.7	6.7	979	1248	27.5%	282	278	1.3%
90	300357	0089P	5.5	5.2	5892	4783	18.8%	1833	1837	0.2%
91	295491	0072P	15.0	14.9	1689	1910	13.1%	659	638	3.2%
92	281706	0012P	96.1	96.2	546	868	58.9%	558	555	0.5%
93	289966	0040P	52.4	52.8	3827	4528	18.3%	1731	1733	0.1%
94	283081	0018P	23.4	23.6	2276	2329	2.3%	1065	1110	4.3%
95	295849	0077P	3.7	3.7	537	717	33.6%	358	355	0.9%
96	310850	0158P	10.3	10.2	772	2408	211.7%	326	293	10.1%
97	297364	0089P	86.4	86.7	2301	2435	5.8%	1250	1225	2.0%
98	312882	0189P	21.0	20.5	1042	1077	3.4%	2635	2647	0.5%
99	290978	0044P	22.8	22.7	1344	1748	30.1%	318	306	3.7%
100	284609	0024P	106.1	106.4	1125	1197	6.4%	1901	1787	6.0%